

1           **Tropospheric ozone maxima observed over the Arabian Sea during the**  
2                                                           **pre-monsoon**  
3                                                           **by J. Jia et al.**

4                                           **Answers to referee comments, Referee #2**

5     The authors would like to thank Referee #2 for reviewing the manuscript.

7     **Comments:**

8     *The authors provide a detailed analysis for the variation of tropospheric ozone over Arabian*  
9     *Sea. They indicated that the maximum of spring time free tropospheric O<sub>3</sub> over AS is mainly*  
10    *driven by long-range transport, particularly, from India. I recommend the paper for publica-*  
11    *tion after consideration of the points below.*

13    *Page 2, Line 10-12 It would be better to define the region of Arabian Sea in Figure 1. The*  
14    *enhancement is not very obvious. What is the reason for the 30x10 grid box line in Figure 1?*

16    **Response:** The region of Arabian Sea was defined too far back (in Figure 2 as rectangle and  
17    in Page 7, Line 11). The definition is moved ahead to Page 2 Line 10-12. The sentence is now  
18    'A tropospheric ozone maximum is observed over the Arabian Sea (AS, west side of the sub-  
19    continental India).' The caption of Figure 1 is changed to '... and (right) OMI/MLS in 2008,  
20    with bold arrows pointing to AS. The AS region is defined as 10-20 N, 60-70 E in this study  
21    and is marked with red rectangle in Fig. 2).'

22    The 30x10 grid box line is a default setting of the software 'pglobal '.

24    *Page 2, Line 13-16 What is the relation between Southern Hemispheric biomass burning with*  
25    *enhanced TOC over Arabian Sea? I assume detailed description and citations for Southern*  
26    *Hemispheric biomass burning are not necessary here.*

28    **Response:** The study of AS tropospheric ozone columns is inspired by averaging TOCs over  
29    long time period, when the author found four main patterns in a global scale: plumes caused  
30    by biomass burning, by the anthropogenic pollution in midlatitudes northern hemisphere, by

1 STE over Mediterranean, and the ozone enhancement over Arabian Sea. Plenty of studies and  
2 researches have helped us understanding the first three patterns of tropospheric ozone, while  
3 few were about the enhancement over Arabian Sea. Page 2, Line 12-18 states this motivation  
4 and aims to point out the outstanding magnitude of Arabian Sea ozone enhancement by com-  
5 paring it with the other three well-known patterns. The biomass burning pattern is one of  
6 them.

7 The detailed citations may are not necessary, and several citations have been removed. The  
8 sentence is now '... and towards Australia (e.g., Fishman et al., 1986, 1991), 2) TOC attribut-  
9 ed to anthropogenic sources ...'

10

11 *Page 2, Line 20-21 If this phenomenon is not unique, but just a “well-known largen scale*  
12 *phenomenon”, why should we focus on it?*

13

14 **Response:** The authors agree that this sentence weakened the importance of the AS ozone  
15 enhancement. The sentence is now 'Although the TOC enhancement over AS is an important  
16 global pattern of tropospheric ozone, the spring maxima in TOC are not unique over the AS  
17 representing rather a well-known large scale phenomenon in the Northern Hemisphere. '

18

19 *Section 2: Is there any evaluation study for the tropospheric O3 column provided by SCIA-*  
20 *MACHY and OMI/MLS? The TOC is highly depended on the stratosphere-troposphere sepa-*  
21 *ration, which could be an issue for the unpolluted area*

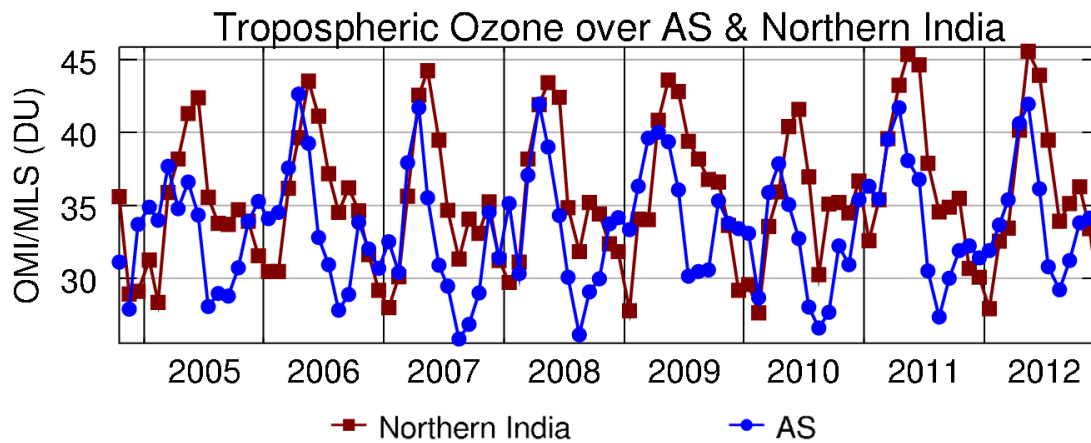
22

23 **Response:** The evaluation studies for the tropospheric ozone column provided by SCIAMACHY  
24 CHY and OMI/MLS were reported by Ebojie et al. (2014) and Ziemke et al. (2006) respec-  
25 tively. The monthly results for both data sets are within 5 DU comparing to ozonesonde  
26 measurements. The stratosphere-troposphere separation is operated by using tropopause  
27 height data. The tropopause height information for SCIAMACHY LNM and OMI/MLS TOC  
28 retrieval is derived from ECMWF and NCEP, respectively. The fact that different databases  
29 are used to retrieve tropopause height for SCIAMACHY and OMI/MLS is not expected to  
30 have a significant effect as tropical region has the most stable tropopause height compared to  
31 the other latitudes.

32

1 Section 4 In Figure 3, can you add a panel to show the O<sub>3</sub> variation over northern India? It  
2 seems that the O<sub>3</sub> seasonality over AS is strongly correlated with the O<sub>3</sub> seasonality over In-  
3 dia (based on Figure 2). Instead of complex source analysis, I am wondering whether the  
4 variation of O<sub>3</sub> over AS can be simply explained by the variation of O<sub>3</sub> formation of India.

5  
6 **Response:** The TOC variations over northern India and AS from OMI/MLS are shown below.  
7 Despite the similar seasonal pattern in general, the variation of ozone over AS cannot be  
8 simply explained by the variation of ozone formation of India. As discussed in the manuscript,  
9 the Northern India is a major source region for air masses over Bay of Bengal, but not for the  
10 Arabian Sea.



11  
12  
13 Section 4.3 The local chemistry production in lower troposphere is small (Figure 10), how-  
14 ever, I am wondering whether the significant O<sub>3</sub> production in upper troposphere has influ-  
15 ences on lower tropospheric O<sub>3</sub>. Does lightning play a role in the O<sub>3</sub> accumulation?

16  
17 **Response:** The HYSPLIT trajectory forward model results (Fig. 7) indicate that the air mass-  
18 es in upper troposphere are transported towards the Pacific Ocean rather than sinking down-  
19 wards. In Page 14, Line 7-9, we also pointed out that ozone amount over ~11 km in pre-  
20 monsoon season has a zonal pattern.  
21 We conducted limited studies on lightning influence by checking the lightning flash rate data  
22 provided from LIS/OTD (Lightning Imaging Sensor/space borne Optical Transient Detector).  
23 The lightning over AS is negligible. Lightning can play a role by influencing the source re-  
24 gion before long range transport. Barret et al. studied lightning NO<sub>x</sub> influence over Arabian  
25 Sea by using GEOS-Chem model. Ozone concentration at 565 hPa can decrease by 20 ppbv

1 when turning off global lightning, while it remains almost unchanged without the local light-  
2 ning. These results were presented in a poster and was not published in journals in accord-  
3 ance with our knowledge.

4

5 *Technical comments:*

6 *Page 13, Line 11 Change Figure 6.11 to Figure 10*

7

8 **Response:** Typo corrected.

9

10 Besides of the comments that were given, the authors would like to clarify some contributors  
11 in the acknowledgements: ‘...We acknowledge the working staffs on MACC reanalysis,  
12 NCEP, and MOZART-4. ... We would like to thank Dr. Anne-Marlene Blechschmidt for her  
13 help. Our gratitude goes to Prof. Christian von Savigny for giving comments during the  
14 preparation of the manuscript. The authors acknowledge the North-German Supercomputing  
15 Alliance (HLRN) for providing HPC resources that have contributed to the research results  
16 reported in this paper’

17

# Tropospheric ozone maxima observed over the Arabian Sea during the pre-monsoon

Jia Jia<sup>1</sup>, Annette Ladstätter-Weißenmayer<sup>1</sup>, Xuewei Hou<sup>2</sup>, Alexei Rozanov<sup>1</sup> and John P. Burrows<sup>1</sup>

<sup>1</sup>Institute of Environmental Physics, Bremen, Germany

<sup>2</sup>Nanjing University of Information Science and Technology, Nanjing, China

*Correspondence to:* Jia Jia (jia@iup.physik.uni-bremen.de)

**Abstract.** An enhancement of the tropospheric ozone column (TOC) over Arabian Sea (AS) during the pre-monsoon season is reported in this study. The potential sources of the AS spring ozone pool are investigated by use of multiple data sets (e.g., SCIAMACHY Limb-Nadir-Matching TOC, OMI/MLS TOC, TES TOC, MACC reanalysis data, MOZART-4 model and HYSPLIT model). 3/4 of the enhanced ozone concentrations are attributed to the 0-8 km height range. The main source of the ozone enhancement is considered to be caused by long range transport of ozone pollutants from India (~ 50% contributions to the lowest 4 km, ~ 20% contributions to the 4-8 km height range), the Middle East, Africa and Europe (~30% in total). In addition, the vertical pollution accumulation in the lower troposphere, especially at 4-8 km, was found to be important for the AS spring ozone pool formation. Local photochemistry, on the other hand, plays a negligible role in producing ozone at the 4-8 km height range. In the 0-4 km height range, ozone is quickly removed by wet-deposition. The AS spring TOC maxima are influenced by the dynamical variations caused by the sea surface temperature (SST) anomaly during the El Niño period in 2005 and 2010 with a ~5 DU decrease.

## 1 1 Introduction

2 Tropospheric ozone is one of the most important green-house gases and one of the most important components  
3 of photochemical smog. Most tropospheric ozone is produced in situ by photochemical reactions of its precursors  
4 ( $\text{NO}_x$  ( $\text{NO} + \text{NO}_2$ ),  $\text{CO}$ ,  $\text{CH}_4$  and VOCs) in the presence of sunlight, while some tropospheric ozone naturally  
5 originates in the stratosphere. High surface ozone values are detrimental to human health by causing respiratory  
6 illnesses, and can also lead to losses in agricultural crops (see Van Dingenen et al., 2009; Mills et al.,  
7 2016 and references therein).

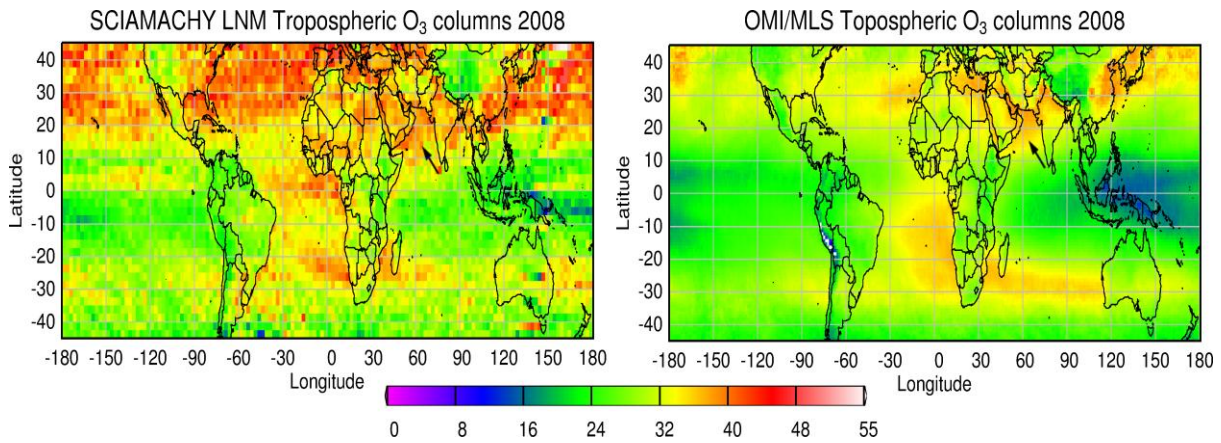
8 In this study, we investigated the global pattern of tropospheric ozone by averaging 7 years (2005-2011) of Tropospheric  
9 Ozone Column (TOC) data products from different satellite instrumentation: SCIAMACHY Limb-Nadir-Matching TOC  
10 (Ebojje et al., 2014; Jia, 2016) and the OMI/MLS TOC (Ziemke et al., 2006). A tropospheric ozone maximum is  
11 observed over the Arabian Sea (AS, [west side of the subcontinental India](#)). This enhancement of TOC can be  
12 observed in yearly mean image as well (Fig. 1). The enhancement of TOC is similar in magnitude as TOC  
13 enhancements observed during the follow events: 1) the well-known biomass burning plume in the Southern  
14 Hemisphere that was transported over the South Atlantic, the coast of South Africa, along the Indian Ocean  
15 and towards Australia (e.g., Fishman et al., 1986, 1991; [Pickering et al., 1996](#); [Thompson et al., 1996, 2001](#);  
16 [Lelieveld and Dentener, 2000](#); [Staudt et al., 2002](#); [Sinha et al., 2004](#)), 2) TOC attributed to anthropogenic  
17 sources in the Northern Hemisphere, and 3) the Mediterranean summer ozone pool attributed to the  
18 stratospheric-tropospheric exchange (STE) (Zanis et al., 2014). A spring (or so called pre-monsoon, see Sect.  
19 2.1) TOC maximum of ~42 DU on monthly average was identified from our study of the seasonality of the TOC.

20 [Although the TOC enhancement over AS is an important global pattern of tropospheric ozone, the sSpring](#)  
21 [maxima in TOC are not unique over the AS representing but](#) rather a well-known large scale phenomenon in the  
22 Northern Hemisphere. Nevertheless, the origin and mechanisms explaining this phenomenon is still a matter for  
23 debate (e.g. Monks, 2000, 2015 and references therein). The increase of tropospheric pollutants, presumably  
24 increase of longer lived VOCs which are ozone precursors, during winter, may play an important role by influencing  
25 the two major contributors to tropospheric ozone concentrations: the STE intrusions and the photochemical  
26 production process (Holton et al., 1995; Penkett et al., 1998; Monks, 2000). In a remote region like AS, an  
27 intuitive hypothesis is that long range transport (LRT) of ozone from more polluted regions or from STE may be  
28 the drivers. This is because of the longer ozone lifetime in spring and the weak local production over remote  
29 areas (Wang et al., 1998).

30 In previous studies using the ozonesonde measurements above the west coast of India and the data from two  
31 campaigns (the 1998 and 1999 INDOEX – INdian Ocean EXperiment campaigns and the ICARB – Integrated  
32 Campaign for Aerosols, Gases and Radiation Budget campaign which was conducted during March-May 2006),  
33 the higher AS TOC during pre-monsoon season was confirmed to be significantly influenced by LRT of the  
34 continental anthropogenically influenced outflows from the Middle East, Western India, Africa, North America  
35 and Europe (Lal and Lawrence, 2001; Chand et al, 2003; Srivastava et al., 2011, 2012; Lal et al., 2013, 2014). In  
36 addition, by comparing the INDOEX ozone measurements from both sides (northern and southern) of the ITCZ  
37 (InterTropical Convergence Zone), the influence of the ITCZ functioning as a sink for ozone was determined by  
38 the observed 4 times higher TOC values on the northern side of AS compared to the southern side (Chand et al.,

1 2003). The seasonal variation of tropospheric ozone at Ahmadabad (23.03 N, 72.54 E) was reported to have an  
2 averaged maximum of ~44 DU in April during the years 2003–2007 (Lal et al., 2014). The possibility of the  
3 STE influencing the ozone mixing ratio up to ~10 km altitude was also discussed. However, the mechanisms  
4 explaining this phenomenon need to be better understood.

5



6  
7

8 Figure 1. Yearly average for TOC retrieved from (left) SCIAMACHY LNM and (right) OMI/MLS in 2008,  
9 with bold arrows pointing to AS. The AS region is defined as 10--20 N, 60-70 E in this study and is marked  
10 with red rectangle in Fig. 2

11

12 Here, the TOC enhancement over the AS is investigated and interpreted by using TOC data products from sev-  
13 eral satellite remote sensors (i.e. SCIAMACHY Limb-Nadir Matching, OMI/MLS and TES), MACC (Monitor-  
14 ing Atmospheric Composition and Climate) reanalysis data (Inness et al., 2013) and simulations from the global  
15 tropospheric chemical transport model (CTM) MOZART-4 model (Model for Ozone and Related Tracers)  
16 (Emmons et al., 2010). This study focuses on the analysis of the regional contribution to LRT, the influence of  
17 the meteorological conditions, the local chemistry and STE, and the inter-annual variability of the spring ozone  
18 maxima, thus to better understand the climate interact with the distribution of tropospheric ozone through tem-  
19 perature, humidity and dynamics. In Sect. 2, the data sets used in this study are briefly discussed. In Sect. 3, the  
20 regional distribution and the time series of tropospheric ozone and its precursors are investigated. Meteorologi-  
21 cal and photochemical sources of ozone plumes due to LRT, local chemistry and STE are discussed in Sect. 4.  
22 The role of accumulation of pollutants is also highlighted in this section. In Sect. 5 the impact of El Ni ño on the  
23 inter-annual variability is identified. Finally, conclusions are given in Sect. 6.

24

## 25 2 Data sets used in this study

26 The SCanning Imaging Absorption spectromETER for Atmospheric CHartographyY (SCIAMACHY) was a pas-  
27 sive spectrometer designed to measure radiances in eight spectral channels, covering a wide range from 214 nm  
28 to 2384 nm with a moderate spectral resolution of 0.21 nm to 1.56 nm (Burrows et al., 1995; Bovensmann et al.,  
29 1999). SCIAMACHY performed observations in three viewing modes: nadir, limb and solar/lunar occultation.

1 The SCIAMACHY Limb-Nadir-Matching TOC is retrieved based on the tropospheric ozone residual (TOR)  
2 method, which subtracting the stratospheric ozone columns retrieved from the limb measurements, from the  
3 collocated total ozone columns acquired from nadir measurements, by using the tropopause height data (Ebojic  
4 et al., 2014). The results showed in this study are from the V1.2 SCIAMACHY Limb-Nadir-Matching TOC data  
5 set. This data set is recently developed in the Institute of Environmental Physics (IUP) in the University of Bre-  
6 men (Details can be found in Jia, 2016). The data set is not complete in a full SCIAMACHY performing time  
7 period (2002-2012), thus is not showed in the time series image.

8 The UV-Vis nadir viewing spectrometer Ozone Monitoring Instrument (OMI), the thermal-emission Microwave  
9 Limb Sounder (MLS) and the infrared Fourier transform spectrometer Tropospheric Emission Spectrometer  
10 (TES) are three of the main instruments onboard the EOS Aura satellite (Levelt et al., 2006; Waters et al., 2006;  
11 Beer, 2006). The OMI/MLS TOC data set is retrieved based on TOR method using data sets from OMI and  
12 MLS. The adjustment for inter-calibration differences of OMI and MLS instruments is performed by using the  
13 CCD method (Ziemke et al., 2006; 2011). Both OMI-CCD and MLS measurements of the stratospheric ozone  
14 are averaged for the comparison over the Pacific (120 °W-120 °E) (Ziemke et al., 2006). The MLS data is ad-  
15 justed according to the observed differences, and then interpolated in two steps along-track and along longitude.  
16 In the end, OMI/MLS is able to provide daily-based global TOCs.

17 TES ozone is retrieved from the 9.6  $\mu\text{m}$  ozone absorption band using the 995 – 1070  $\text{cm}^{-1}$  spectral range. In  
18 cloud-free conditions, the nadir vertical profiles have around four degrees of freedom (DOF) for signal, ap-  
19 proximately two of which are in the troposphere, giving an estimated vertical resolution of about 6 km with a  
20 footprint of 5.3 km  $\times$  8.5 km, covering an altitude range of 0-33 km (see Beer et al., 2001; Nassar et al., 2008  
21 and the references therein).

22 MACC is a research project for the European GMES (Global Monitoring for Environment and Security) initia-  
23 tive (Inness et al., 2013). MACC combines a wealth of atmospheric composition data with a state-of-the-art nu-  
24 merical model and data assimilation system to produce a reanalysis of the atmospheric composition. MACC  
25 reanalysis data of ozone, CO and specific humidity used in this study are available in 6-h time intervals (00, 06,  
26 12 and 18 UTC) and were provided in monthly files with the unit of kg/kg under the website  
27 <http://apps.ecmwf.int/datasets/data/macc-reanalysis/levtype=ml/>. The horizontal resolution of the model is 1.125 °  
28  $\times$  1.125 °. Variables were provided as 3D fields in pressure hybrid vertical coordinates. The vertical coordinate  
29 system is given by 60 hybrid sigma-pressure levels, with a model top at 0.1 hPa.

30 MOZART-4 is a global tropospheric CTM. It was run with the standard chemical mechanism (see Emmons et  
31 al., 2010 for details) in this study. MOZART-4 was driven by the NCEP/ National Center for Atmospheric Re-  
32 search (NCAR) reanalysis meteorological parameters, having a horizontal resolution of approximately 2.8 °  $\times$   
33 2.8 °, with 28 vertical levels from the surface to approximately 2 hPa. The chemical initial condition in 2000 and  
34 emissions from 1997 to 2007 used in MOZART-4 were from the NCAR Community Data Portal  
35 (<http://cdp.ucar.edu/>), which was introduced by Emmons et al. (2010). The model was run with a time step of 20  
36 min from 1 January 1996 to 31 December 2007, and the first year was discarded as spin-up (Hou et al., 2014;  
37 Zhu et al., 2015). The tagged tracer method was used to isolate the contributions from individual source regions.  
38 This method was introduced by Sudo and Akimoto (2007). It treats a chemical species emitted or chemically



1 produced in a certain region as a separate tracer and calculates its transport, chemical transformation and surface  
2 deposition. The results used in this study are simulated by Hou et al. (2014).

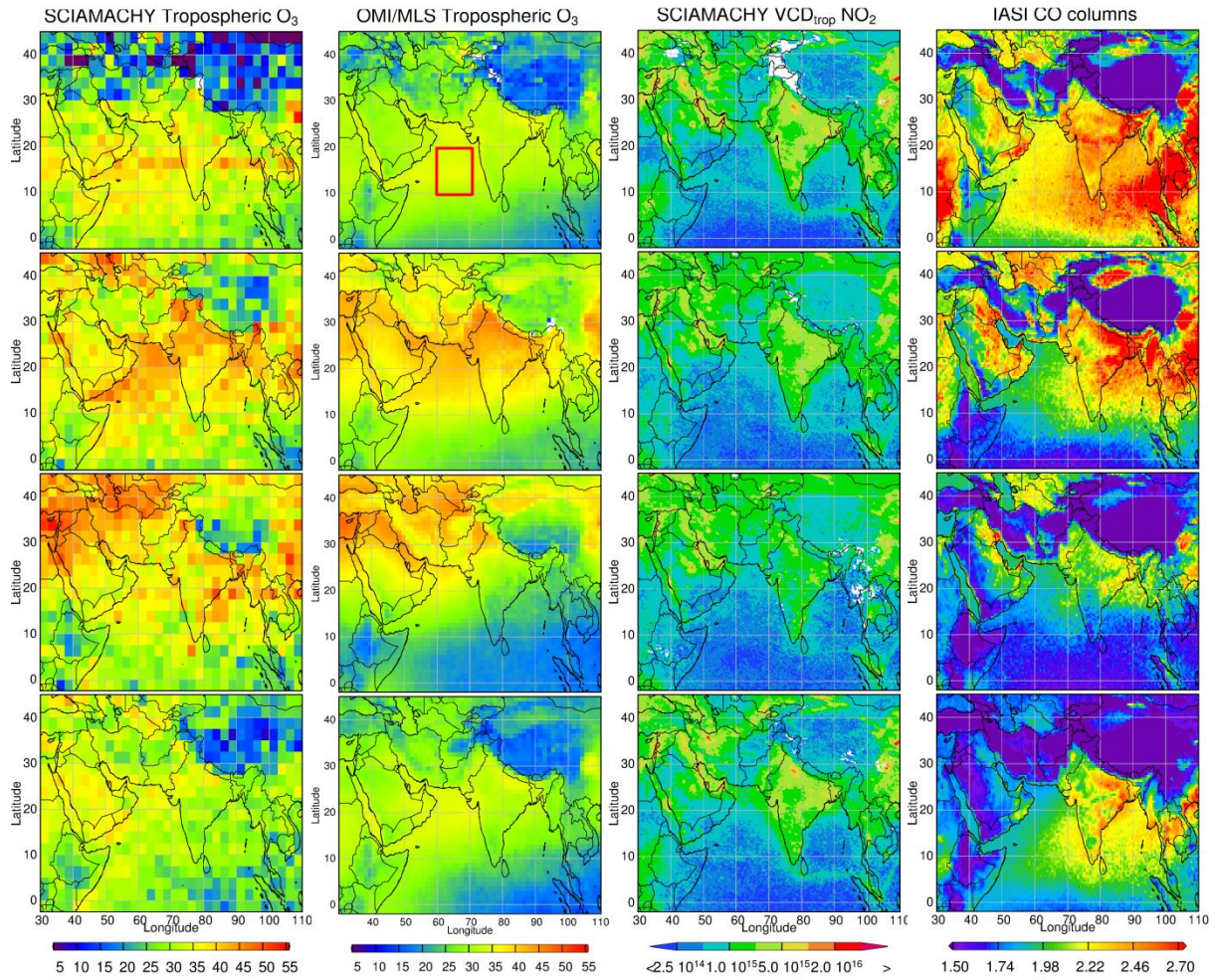
3 HYbrid Single-Particle Lagrangian Integrated Trajectory (HYSPLIT) is a system for the computation of simple  
4 air parcel trajectories from the National Oceanic and Atmospheric Administration (NOAA). In order to investi-  
5 gate the forward and backward trajectory of the air mass, the web-based version of the HYSPLIT model (Stein  
6 et al., 2015) is used for this study: <http://ready.arl.noaa.gov/hypub-bin/trajtype.pl?runtype=archive>.

### 8 **3 Observation of a pre-monsoon enhancement in TOC data products**

9 Satellite retrieved TOCs have a better spatial and temporal coverage compared to ozonesonde measurements.  
10 However in situ measurements of ozone from ozonesondes are considered more accurate. Combining the two  
11 types of measurements provides an opportunity to investigate data-sparse regions such as the AS. In comparison  
12 with the studies using ozonesonde and ship measurements, the analysis of the satellite observations of TOCs  
13 regarding AS region is still a gap in the current state. In this section, the satellite observations and the model  
14 results are presented.

15 Figure 2 shows the regional distribution of the TOC and two of its photochemical precursors: NO<sub>2</sub> and CO. Sea-  
16 sonal cycles of TOC, CO and NO<sub>2</sub> over the AS are shown in Fig. 3. A seasonal pattern of TOC is observed in  
17 both OMI/MLS and TES. An offset of ~5 DU exists between the two investigated TOC data products. A maxi-  
18 mum of TOC over AS is observed (~42/47 DU) in every April during the years 2005–2012, followed by mon-  
19 soon/summer minima of ~20 DU. TOC recovers to ~35 DU in the post monsoon autumn but drops down  
20 slightly during the winter monsoon. This seasonal pattern is consistent with the results from the sonde station  
21 Ahmedabad (Fig. 6 in Lal et al., 2014) and depends on the meteorological conditions (Sect. 3.1). The ozone pre-  
22 cursors, CO and NO<sub>2</sub>, show a different behaviour than ozone. As NO<sub>2</sub> has a short lifetime (2-8 hours, Beirle et  
23 al., 2011), the tropospheric NO<sub>2</sub> data products, retrieved from observations of SCIAMACHY or other related  
24 instrumentation in space, show high values over anthropogenic sources and relatively low values, often below  
25 the detection limit, over the remote regions. Over the AS, tropospheric NO<sub>2</sub> columns are small being around  
26 10<sup>14</sup> molec/cm<sup>2</sup>. This small concentration originates from ship emissions and continental outflow (Richter et al.,  
27 2004). Higher values can be observed during the winter monsoon from transport off the Asian coast. CO has a  
28 longer life time than ozone (~2 months in average for CO and ~23 days for tropospheric ozone, Novelli et al.,  
29 1998; Young et al., 2013). Due to the relatively long lifetime of CO and ozone, both trace gases show a similar  
30 transport pattern. For instance, the biomass burning plume originating from Southern Africa in boreal autumn in  
31 the Southern Hemisphere can be observed as well for CO as for ozone. However, in comparison to ozone, which  
32 is produced due to the photochemical production, the spatial pattern of CO is known to be more driven by emis-  
33 sions than dynamical processes (Logan et al., 2008). Thus, the time series of the data products for tropospheric  
34 CO reveal a similar winter maximum as NO<sub>2</sub>, and it also shows a smaller peak in spring time as TOC. The  
35 spring peaks of CO are observed one month earlier than that those of TOC. This shift can be caused by the com-  
36 bustion emission of CO in Southern Asia (Fig. 6 in Duncan et al., 2003).

1  
2



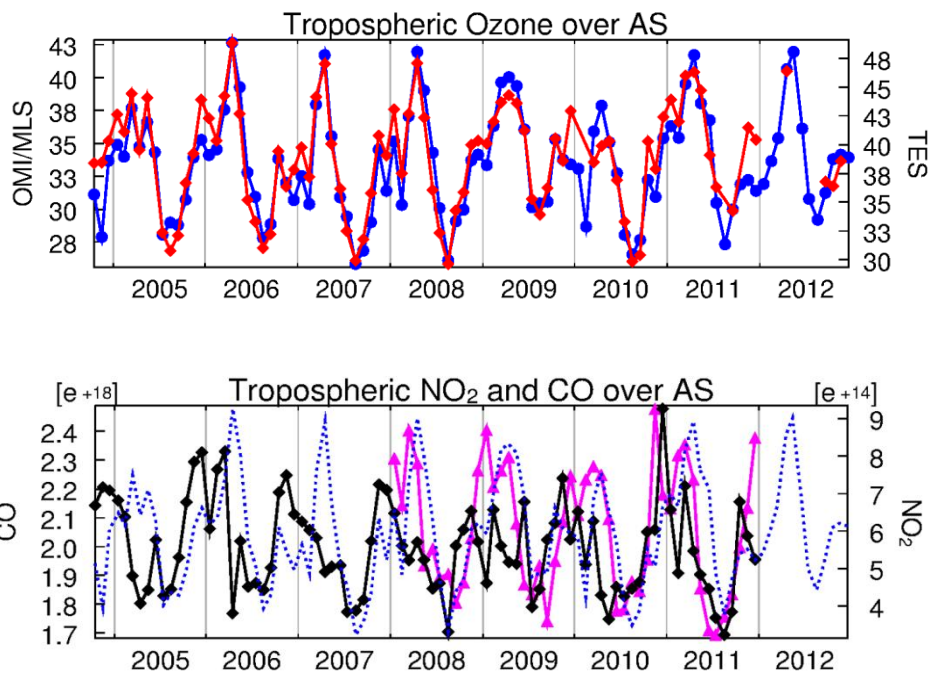
3

4 Figure 2. Plots of the TOC, NO<sub>2</sub> (Hilboll et al., 2013) and CO (x10<sup>18</sup>, George et al., 2009) as a function of sea-  
5 son in 2008. The unit for TOC are DU and that for NO<sub>2</sub> and CO in molec/cm<sup>2</sup>. From top to bottom are DJF (De-  
6 cember to February), MAM (March to May), JJA (June to August) and SON (September to November).

7

8 In this manuscript, MACC reanalysis data is used to provide vertical information of ozone. This choice is moti-  
9 vated by the fact that OMI and MLS satellite ozone data were actively assimilated in the MACC reanalysis and  
10 constrain tropospheric ozone (Inness et al., 2013). Figure 4 shows MACC results of ozone partial columns be-  
11 tween 0 km and the TPH, determined from ECMWF retrieval (Ebojie et al., 2014), and between 0-8 km, respec-  
12 tively. In a year with no ENSO (El Nino-Southern Oscillation) event in spring, for instance in 2006 (upper pan-  
13 els of Fig. 4), the enhanced ozone during pre-monsoon is ~30 DU out of ~40 DU (~3/4) originating from the  
14 lower troposphere (0-8 km). Because of this result, possible origins will be discussed in the following section  
15 (Sect. 3) by analysing 4 various altitude ranges: 0-4 km, 4-8 km, 8-12 km and 12-18 km.

16



1

2

3 Figure 3. Trace gas time series over AS (10-20°N, 60-70°E) from 2004 to 2012. The blue (solid and dotted)  
 4 curves represents OMI/MLS ozone, red is TES ozone, magenta is IASI CO and black stands for SCIAMACHY  
 5 NO<sub>2</sub>. The vertical columns are given in DU for ozone and molec/cm<sup>2</sup> for NO<sub>2</sub> and CO. The region used for this  
 6 time series calculation is marked with red rectangle in Fig. 2. The time series of TOC from SCIAMACHY,  
 7 MACC, OMI.MLS and TES in the year 2008 is presented in appendix Fig. A3.

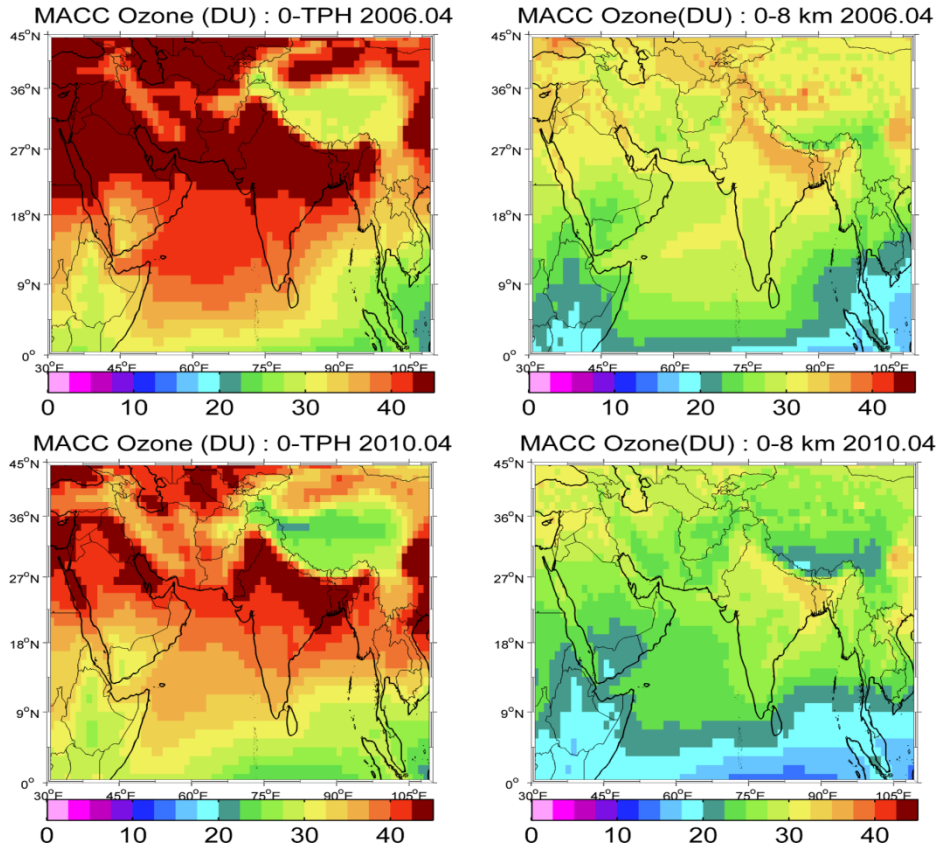
8

9 **4 Potential origins of the AS pre-monsoon ozone pool**

10 **4.1 Influences of meteorology**

11 The AS region is defined in this study as 10-20°N, 60-70°E on the west side of the sub-continental India. This  
 12 location is influenced by the tropical/subtropical air mass exchanges and the sea breeze circulation (e.g., Law-  
 13 rence and Lelieveld, 2010). The climate of AS can be divided into 4 different seasons, due to the seasonal varia-  
 14 tion of the ITCZ: winter-spring monsoon (Dec-Feb), pre-monsoon transition (Mar-May), summer monsoon  
 15 (Jun-Aug), and post-monsoon transition (Sep-Nov). In summer, the ITCZ is at its northernmost position. The  
 16 wind appears to be westerly and strong due to the Somali jet (Fig. 5). This condition causes strong precipitation,  
 17 higher cloud cover frequency and increased air humidity over AS (David and Nair, 2013). The wind and strong  
 18 precipitation 'wash' the air masses and remove soluble pollutants. A summer monsoon minimum for the trace  
 19 gases such as shown in Fig. 3 may be expected. The destruction of ozone by reactive halogens is another poten-  
 20 tial sink for the ozone in the marine boundary layer (Dickerson et al., 1999; Ali et al., 2009). During the pre-  
 21 monsoon transition, surface winds are westerly at the northern AS with an anticyclonic pattern centred over the  
 22 middle AS. At this time, the AS is most of the time cloud-free and dynamically steady. This cloud-free anti-  
 23 cyclonic condition possibly causes subsidence of air masses and results in accumulation of pollutants (Sect. 3.2).

1  
2



3

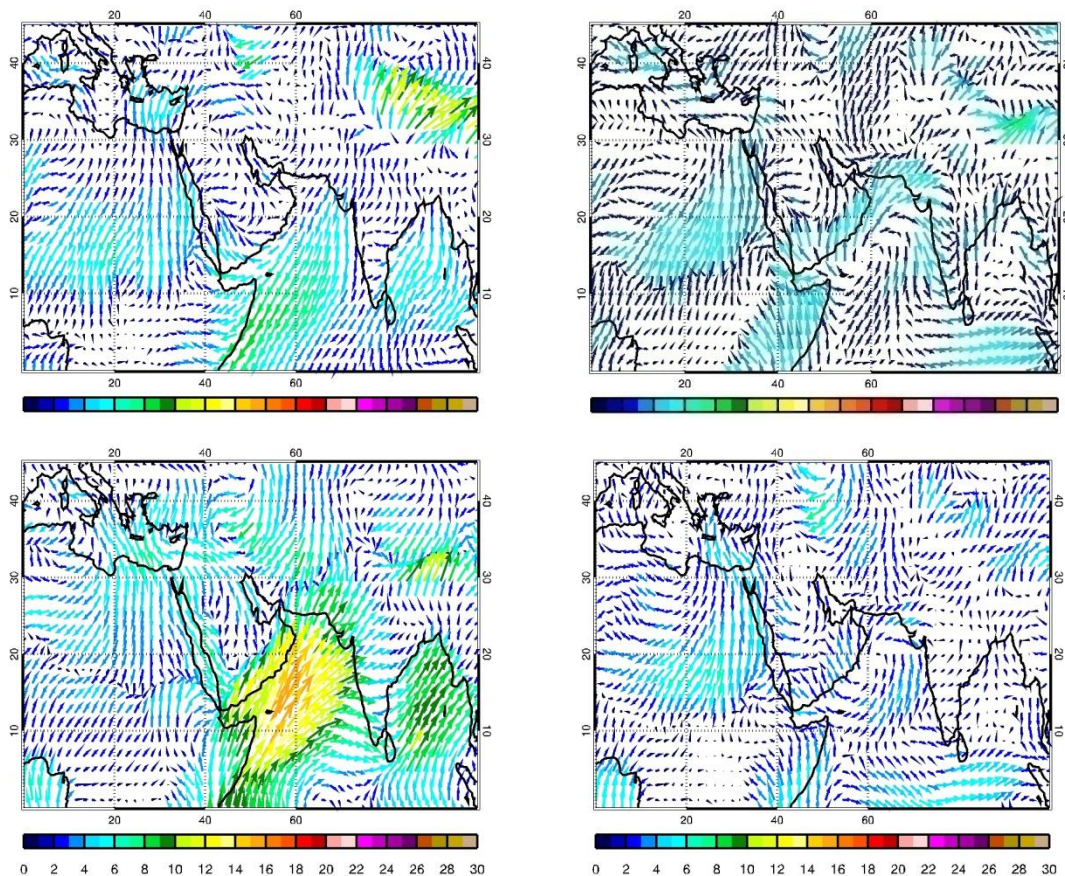
4 Figure 4. Ozone partial columns (TOC in the left panels and 0-8 km column of tropospheric ozone in the right  
5 panels) from MACC reanalysis model in April 2006 (upper panels) and 2010 (lower panels).

6

7 The ITCZ located at the southern part of the AS can become the 'border' that stops the pollutants (in this case,  
8 tropospheric ozone) diffusing to the Indian ocean with ozone depletion on the surface of cloud droplets in the  
9 convective region (Lelieveld and Crutzen, 1990).

10 It is worth mentioning that the solar radiation over the AS, unlike in the middle/high latitudes where it is strong-  
11 est in summer, reaches its maximum during pre-monsoon (Weller et al., 1998; David and Nair, 2013). One  
12 could argue that a maximum solar radiation can cause stronger photochemical reactions and thus an increased  
13 ozone concentration. To answer this question, the contribution of the photochemical production will be investi-  
14 gated in Sect. 3.3.

15



1

2

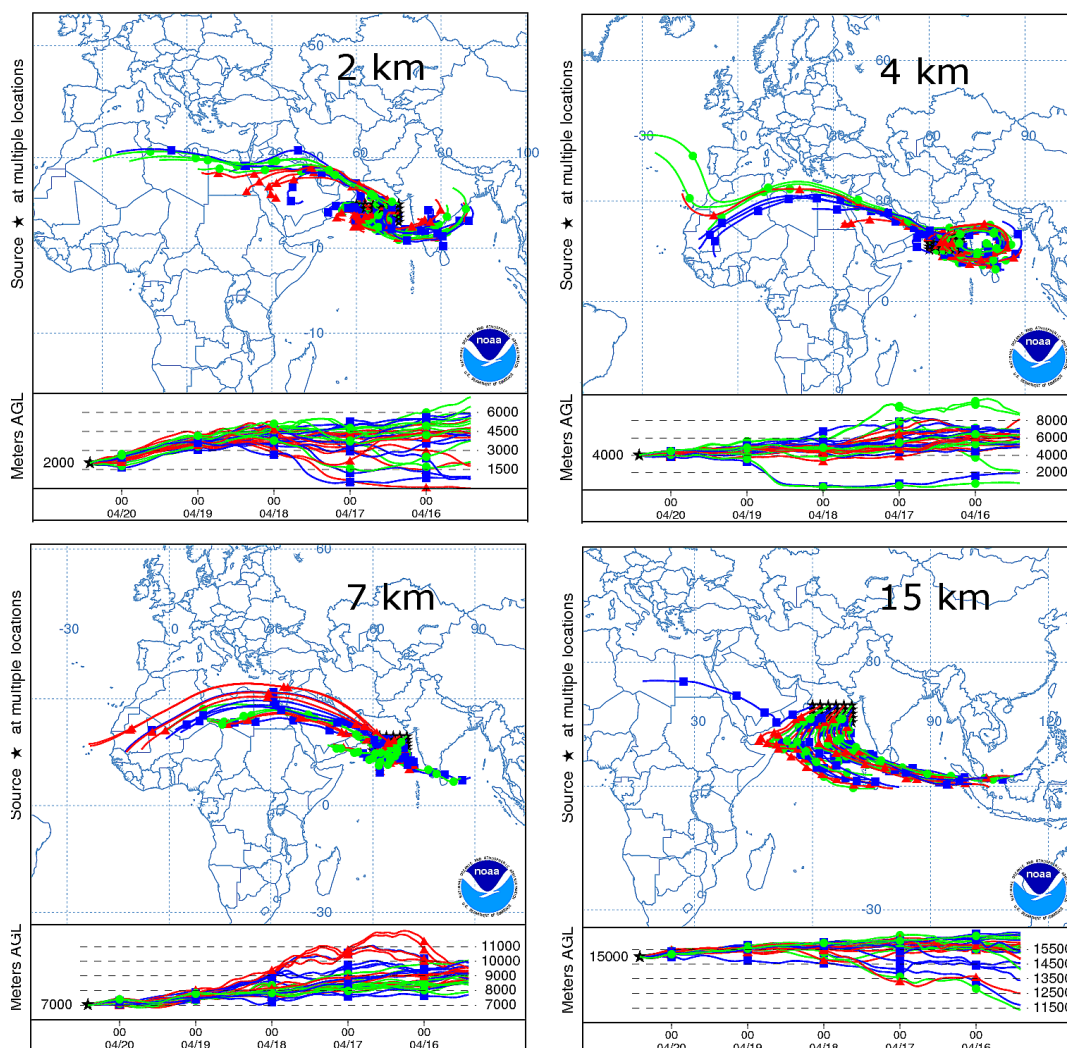
3 Figure 5. 10 meter sea surface wind on January (upper left), April (upper right), July (lower left) and October  
 4 (lower right) over AS at 2008 from NCEP (National Center Environmental Prediction). Figure provided by  
 5 Anne Blechschmidt from the University of Bremen.

6

#### 7 **4.2 Long range transport mechanism and pollutant accumulation**

8 It is established in the previous studies that LRT plays an important role in the AS pre-monsoon ozone pool (Lal  
 9 and Lawrence, 2001; Chand et al, 2003; Srivastava et al., 2011, 2012; Lal et al., 2013, 2014). For example, the  
 10 satellite data products for CO and TOC are highly correlated (Fig. 3). Trajectory models are used to investigate  
 11 the LRT pathways of the air parcels. Figures 6 and 7 show an example of the HYSPLIT backward and forward  
 12 trajectory results for air masses over AS at 2, 4, 7 and 15 km in April 2008. In the lower troposphere (0-8 km),  
 13 the sources are identified as the Middle East, India and North Africa, which are consistent with the previous  
 14 studies. The higher tropospheric ozone (12-18 km) is found in air which was uplifted and transported from the  
 15 North Indian Ocean and Southeast Asia. The air masses in the lower troposphere subside 4-5 km locally within a  
 16 high pressure system within 10 days. This confirms the conclusion on accumulation of pollutant which was de-  
 17 rived from the wind field information in Sect. 3.1 (see Fig. 5). This theory was also proved by Srivastava et al.  
 18 (2011) from the TPSCF (Total Potential Source Contribution Function) results. One explanation for the larger  
 19 TOC over the AS in comparison to surrounded regions is the lower humidity which provides less favorable con-

NOAA HYSPLIT MODEL  
 Backward trajectories ending at 1000 UTC 20 Apr 08  
 GDAS Meteorological Data

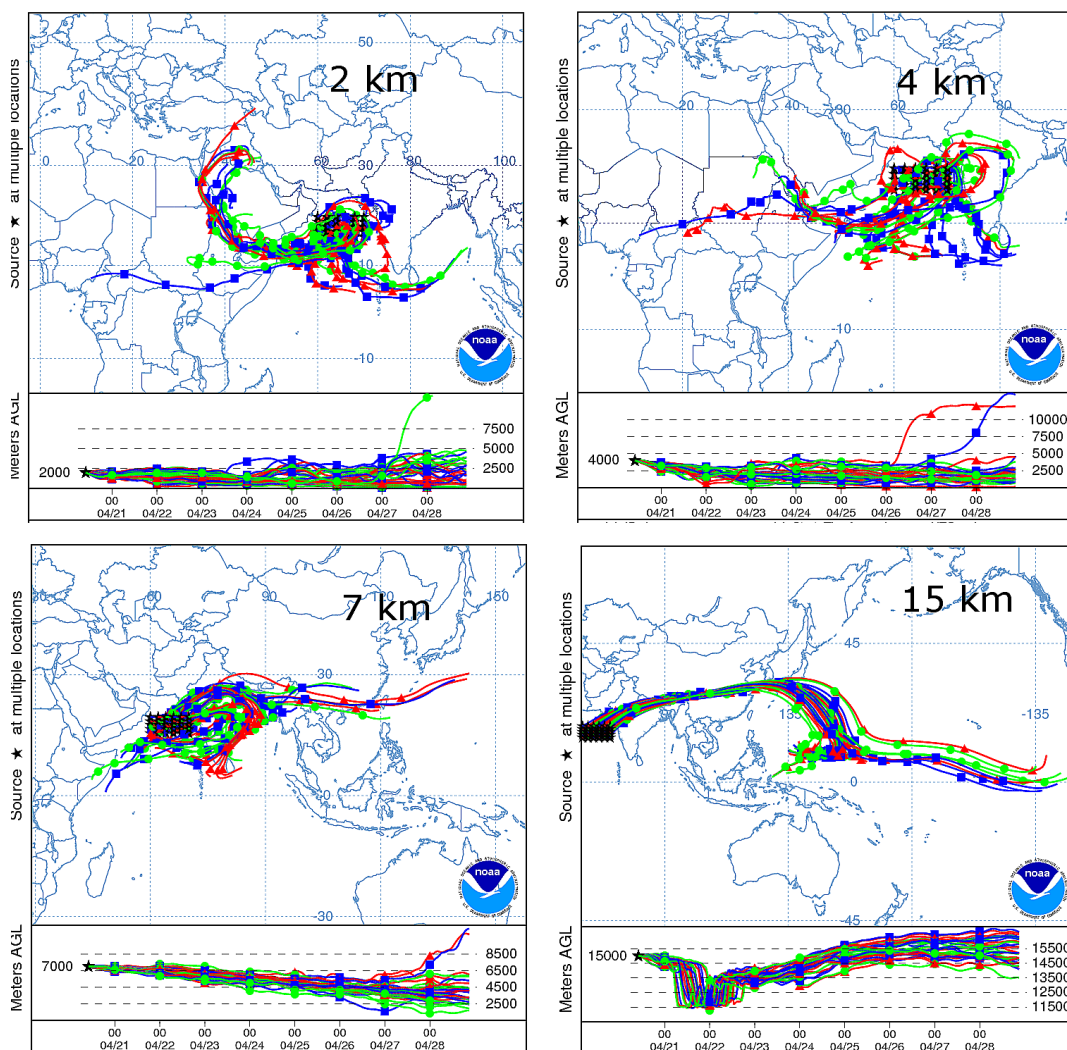


1  
 2 Figure 6. HYSPLIT trajectory 120 hr backward model results for air masses at AS with source location at 2, 4, 7  
 3 and 15 km.

4  
 5 dition for ozone depletion by Hydroxyl radicals (OH) (Fig. 12). This is further discussed in Sect. 3.3. In addition  
 6 to the sources, here we also investigate the areas that are influenced by the AS ozone pool (Fig. 7). The ozone-  
 7 rich air over the AS is transported back to India (lower left panel). HYSPLIT also simulates transport to the Red  
 8 Sea through the Gulf of Aden in the lower troposphere (upper panels), which is expected because of the moun-  
 9 tains aside acting as a barrier for pollution transport. The elevated tropospheric air masses are also transported  
 10 towards the Pacific Ocean via China (lower right panel).

11 To quantify contributions to LRT from different source locations, the tagged tracer simulation with MOZART-4

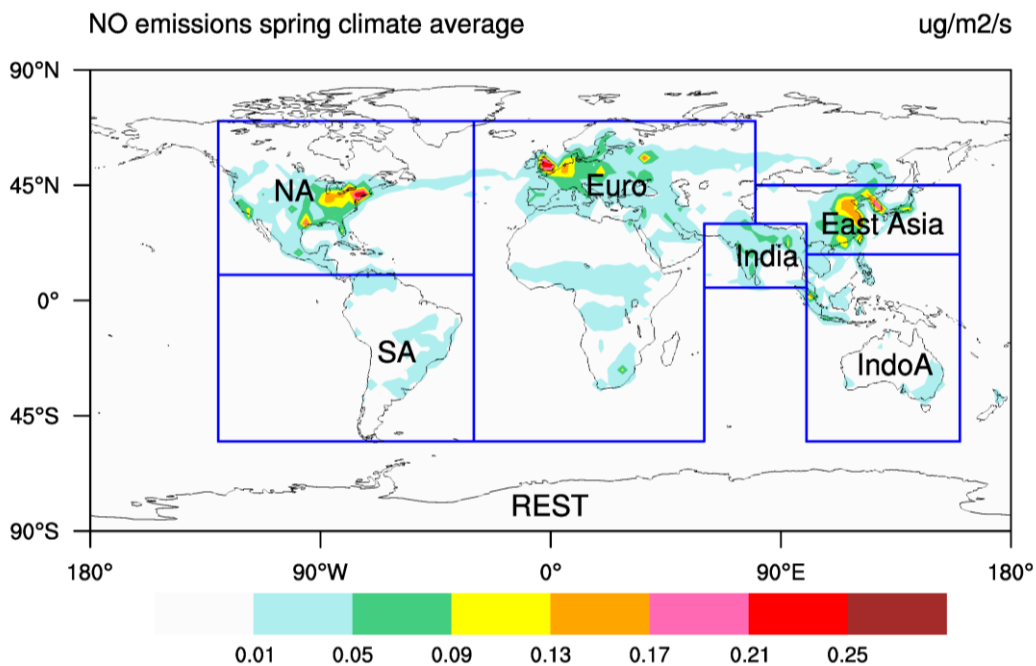
NOAA HYSPLIT MODEL  
 Forward trajectories starting at 1000 UTC 20 Apr 08  
 GDAS Meteorological Data



1  
 2 Figure 7. HYSPLIT trajectory 240 hr forward model results for air masses at AS with source location at 2, 4, 7  
 3 and 15 km.

4  
 5 CTM (Sudo and Akimoto, 2007; Hou et al., 2014) during 1997-2007 was used. Figure 8 shows the seven tagged  
 6 regions. Europe, Africa and the Middle East are combined into one hot spot as the closer western region (named  
 7 'Euro'). India, Bay of Bengal and AS are presented together as the closer eastern region (named 'India'). Note  
 8 that when evaluating the contribution from this region, the influence from pollutant accumulation over the AS  
 9 should always be considered. The Indian Ocean is included in the 'Rest' region. 'NA' and 'SA' represent North  
 10 America and South America respectively. The regions are divided due to the time consumption of the model  
 11 calculation. For further studies, another arrangement can be considered.

12



1

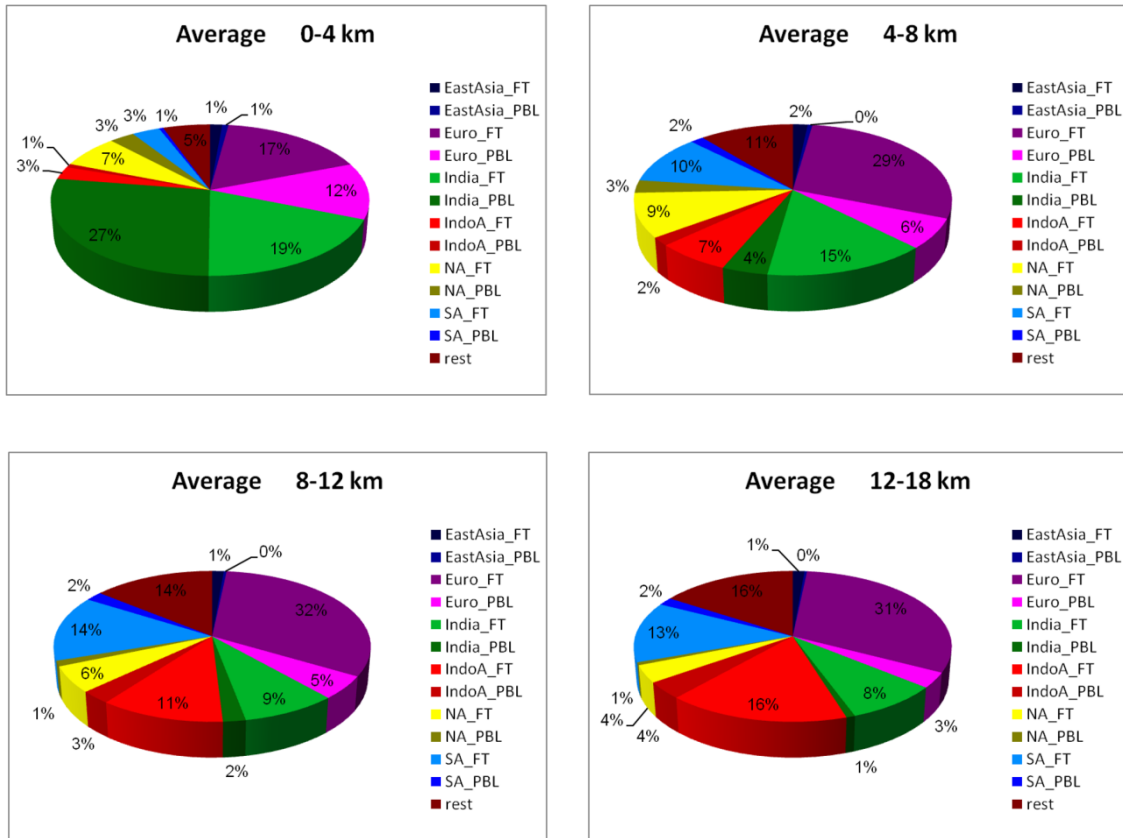
2 Figure 8. Regional separation for tracer tagging with distributions of the spring mean emission rate ( $\mu\text{g}/\text{m}^2/\text{s}$ ) of  
 3 NO (including anthropogenic, biomass burning, and soil emissions) at the surface used in the model simulations  
 4 during 1997–2007.

5

6 The source region distribution varies for different altitude ranges (Fig. 9). In the 0-4 km layer, ~30% of the  
 7 transported ozone comes from the 'Euro' region. The 'India' region is the biggest source region that contributes  
 8 50%, of which 60% comes from the boundary layer. In the 4-8 km layer, the influences of the boundary layers  
 9 are much smaller, while 'Euro\_FT' contributes ~10% more than to the 0-4 km layer. The far-away source re-  
 10 gions ('NA', 'SA' and 'IndoA') become non-negligible (~10% each). The contribution from 'IndoA' increases  
 11 with height. Since the Indian Ocean is included, an increased contribution from 'Rest' with altitude is expected.  
 12 In conclusion, the main contributor to LRT is 'Euro\_FT' with 30% contribution in average, followed by the 'In-  
 13 dia' region with over 20% contribution. The inputs from far-away source regions are similar, with ~10% each.  
 14 The influence from East Asia is negligible. Note that the air masses in the higher altitudes are normally quickly  
 15 removed by the strong advection (Fig. 10). The contributors in the lower altitudes (<12 km) have more influ-  
 16 ences on the ozone accumulation.

17





1

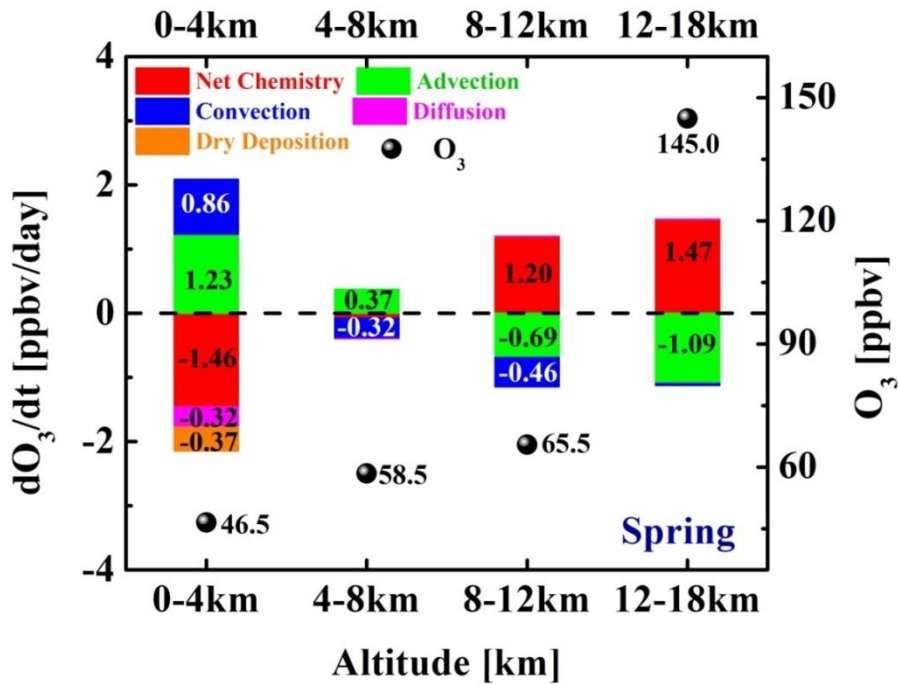
2

3 Figure 9. Averaged LRT contributions to the AS tropospheric ozone concentration from different source regions  
 4 to 4 atmospheric layers over the AS in April 1997-2007. PBL (planetary boundary layer) is defined as the region  
 5 from surface to the top of the boundary layer. FT (free troposphere) is defined as extending to the tropopause  
 6 above the BL.

### 7 4.3 Local chemistry

8 This section addresses two questions: (1), What is the role of the photochemistry for TOC above AS? (2), Is  
 9 more ozone been photochemically produced during the long accumulation time in the middle (4-8 km) or lower  
 10 (0-4 km) troposphere?

11 The ozone budget is calculated in the MOZART-4 model (Fig. 106-4) within the 1997-2007 time periods. Pho-  
 12 tochemistry plays a very different role in the four altitude ranges. In the 0-4 km layer, water vapour acts as a  
 13 source of OH radicals and depletes ozone. Compared to the photochemical production, this depletion process  
 14 dominates (Nair et al., 2011). Thus a net outflow of ozone in chemistry was observed. In the higher layers (8-12  
 15 km, 12-18 km), photochemical production becomes a major source of ozone, while advection being the major



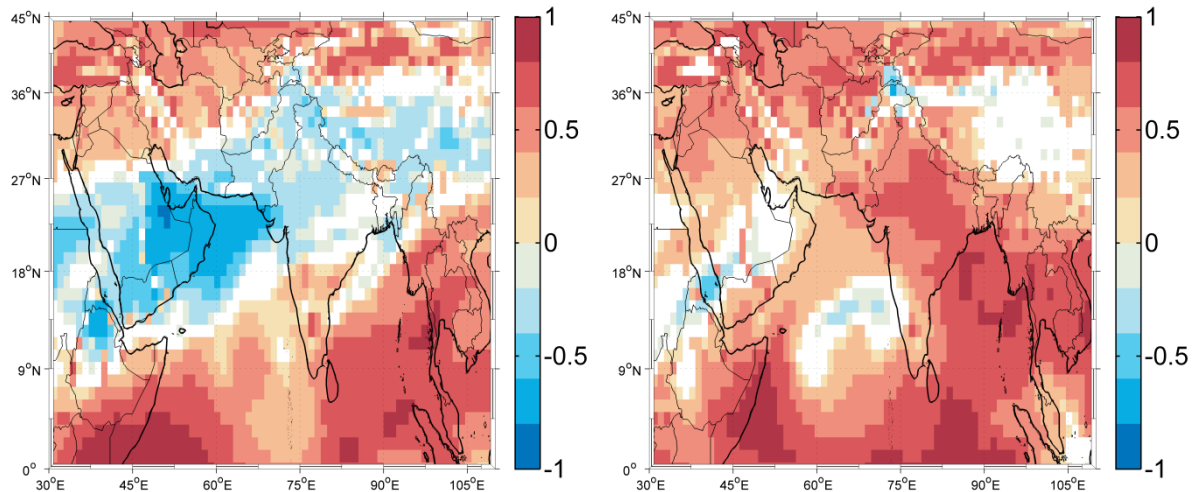
1

2 Figure 10. Averaged ozone budget in pre-monsoon from MOZART-4 at four layers over AS region. The ozone  
 3 partial column volumes (ppbv) calculated from MOZART-4 is presented as black dots.

4

5 sink. Zahn et al. (2002) estimated that the annual net ozone production rates over AS are  $17.6 \times 10^{10}$  molecules  
 6  $\text{cm}^{-2} \text{s}^{-1}$ , by using the CARIBIC (Civil Aircraft for the Regular Investigation of the atmosphere Based on an  
 7 Instrumented Container) aircraft data from 10-11 km altitude. However, Livesey et al. (2013) showed in MLS  
 8 data that such maximum of ozone amount around 215 hPa ( $\sim 11$  km) in pre-monsoon season is most likely a  
 9 zonal pattern. In the 4-8 km layer, the budget is rather small with a net inflow by advection. The net chemistry is  
 10 less than  $-0.1$  ppbv per day, indicating a negligible sink.

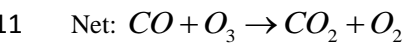
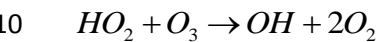
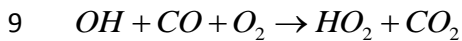
11 The O<sub>3</sub>-CO correlation has been broadly used to indicate tropospheric O<sub>3</sub> sources (Fishman and Seiler, 1983;  
 12 Kim et al., 2013; Inness et al., 2015). A positive O<sub>3</sub>-CO correlation denotes considerable chemical production of  
 13 O<sub>3</sub>. A negative correlation, on the other hand, can originate from chemical O<sub>3</sub> loss or deposition, or can suggest  
 14 that the air mass is either transported from the stratosphere, or moved by advection from the free troposphere.  
 15 Figure 11 shows the O<sub>3</sub>-CO correlation at 4-8 km in April using MACC data. The left panel is a typical correla-  
 16 tion result with strong negative correlations over AS (See also appendix Fig. A1). This correlation suggests that



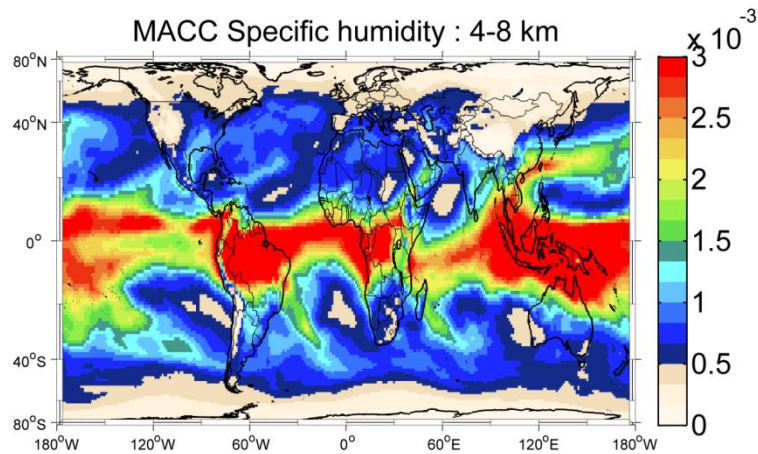
1  
 2 Figure 11.  $O_3$ -CO correlations calculated for 4-8 km column abundances with 3 hr temporal interval in April  
 3 2008 (left panel) and 2006 (right panel) from MACC reanalysis data.

4  
 5 a chemical production of ozone is most likely not the cause for the observed ozone enhancement. Some ozone  
 6 production is expected (e.g., year 2006 in the right panel), but this kind of situation is rare.

7 The averaged specific humidity in-between 4-8 km was used to investigate evidence for the impact of  $HO_x$  re-  
 8 moval on ozone in clean air conditions (Fig. 12):



12 Unlike the humid lowest troposphere, the air masses over the AS at 4-8 km are rather dry compared to the sur-  
 13 roundings. This can be explained by adiabatic lifting and expansion of marine boundary air followed by conden-  
 14 sation and removal for  $H_2O$ . The lifting is stronger over land than over ocean due to the temperature differences.  
 15 This is also one of the reasons that Southeast Asia has strongest convection. The dry air at 4-8 km can lead to a  
 16 smaller depletion contribution from OH radicals, thus it is more suitable for ozone accumulation. Hence, the AS  
 17 ozone columns in the 4-8 km altitude region are expected to be higher than its surroundings.

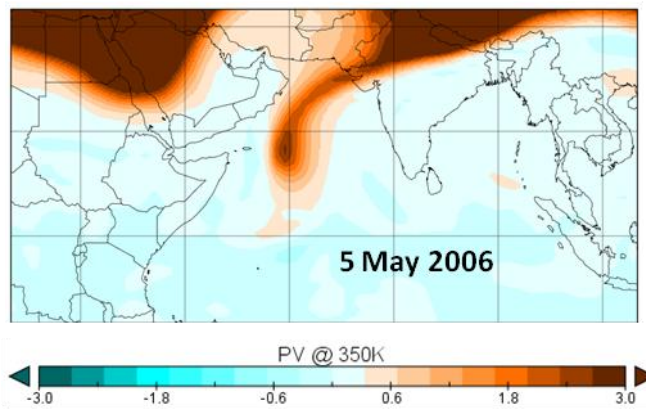


1  
2 Figure 12. Specific humidity (kg/kg) at 4-8 km in April 2006 from MACC reanalysis dataset.

3 **4.4 Stratosphere-troposphere exchange**

4 The STE is not the focus of this study, thus is only briefly mentioned here. The ozone concentrations in the ex-  
 5 tra-tropical lower stratosphere show a maximum in late winter/early spring as driven by the Brewer-Dobson  
 6 circulation (e.g., Fortuin and Kelder, 1998; IPCC/TEAP, 2005). Fadnavis et al (2010) indicated ozone strato-  
 7 spheric intrusion during winter and pre-monsoon season over the Indian region (5-40°N, 65-100°E) by using  
 8 both satellite and model data. One stratospheric intrusion was observed over AS during the ICARB campaign  
 9 (Lal et al., 2013) in 5 May 2006 (Fig. 13). However, it is not clear yet how much and how deep the influence  
 10 can be. In our study, the STE contribution simulated by MOZART-4 tagged tracer method is comparable with  
 11 the ones transported from 'Euro\_FT' in each altitude range. The STE origin might be a reason for the strong  
 12 negative O<sub>3</sub>-CO correlation since the chemical loss and deposition are excluded (Sect. 3.3).

13



14  
15 Figure 13. Potential Vorticity from ECMWF.

16

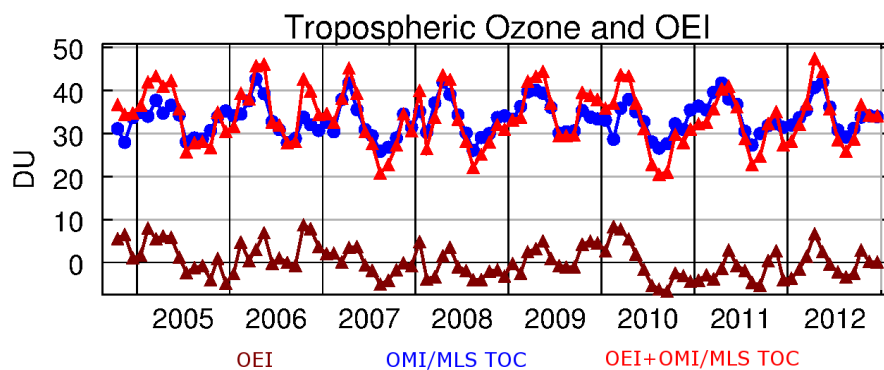
## 5 ENSO and Interannual variation

Two spring anomalies are depicted in 2005 and 2010 where ozone is ~5 DU lower compared to other years (upper panel of Fig. 3). The decrease in 2010 is most likely to be the anomaly of the lower troposphere ozone as observed in Fig. 4. The two following facts suggest the anomaly to be dynamical: (1), the ozone reduced in a similar amount at continental surroundings; (2), similar to ozone, a lower CO maximum appeared in 2010 (lower panel of Fig. 3).

The El Niño events, as driven by a reversal of the Walker Circulation, affect the temperature, humidity and biomass burning emissions, thus influence the trace gases including ozone. Particularly, the tropospheric ozone anomaly related to the El Niño event during the year 1997-1998 was intensively studied (e.g. Chandra et al., 1998; Sudo and Takahashi, 2001). The tropospheric ozone increased (up to 25 DU in the burning season) over the equatorial western Pacific due to a reduced convection and growing burning emissions, whereas decreased (4-8 DU) over the eastern Pacific because of the change in meteorological conditions. By using a model simulation, Zeng and Pyle (2005) reported that the tropospheric ozone concentration at specifically the equatorial region 40-70 °E decreases with similar amount as over the eastern Pacific during El Niño events. Ziemke et al. (2010) showed that the ENSO related response of tropospheric ozone over the western and eastern Pacific dominated interannual variability. An Ozone ENSO Index (OEI) was formed to represent the ENSO impact. The OEI was calculated by subtracting the eastern and central tropical Pacific region tropospheric ozone (15 °S-15 °N, 110-180 °W) from the western tropical Pacific-Indian Ocean region (15 °S-15 °N, 70-140 °E) with the fact that the zonal variability of tropic stratospheric ozone is only ~1 DU.

Figure 14 shows the OEI index that is produced from OMI/MLS data for the related time period (dark red curve). A 'correction' of OMI/MLS TOCs over the AS by adding the OEI index is performed. The ozone spring maxima anomalies at pre-monsoon season in 2005 and 2010 (blue curve) can no more be seen after the 'correction'. This indicates that the El Niño induced dynamics might contribute to the interannual variability over pre-monsoon AS ozone. Since OEI contains both chemical (fire) and dynamical influences in the burning season, ozone peaks (in the red curve) can be observed in the winter of 2006 and 2009 when strong fires happened in Indonesia.

26



27

Figure 14. Time series of tropospheric ozone columns 'corrected' with OEI over AS (10-20 °N, 60-70 °E) from 2004 to 2012. The blue curve represents OMI/MLS TOCs, dark red is OEI calculated from OMI/MLS and red stands for OMI/MLS TOCs with OEI 'correction'.

30

1

2 The dynamical influence of El Niño can be found in two aspects. El Niño can induce an increase of Sea Surface  
3 Temperature (SST) thus strengthens the water vapor upwelling to the middle troposphere, and then reduces the  
4 life time of ozone. It also possibly triggers changes in STE flux as mentioned by e.g. Neu et al. (2014). Moist  
5 air masses are observed from MACC reanalysis data in April 2010 (appendix Fig. A2). This confirms the as-  
6 sumption of the SST influence over AS. A STE flux variation can be caused by both El Niño and La Niña  
7 events. In this case La Niña events (in 2011) didn't contribute as much as El Niño events (in 2005 and 2010).  
8 The impact of El Niño is mainly expressed by the SST anomaly instead of the STE anomaly.

9

## 10 **6 Conclusions**

11 The 7 years composite averaged values for TOC presented over AS exhibit a seasonal pattern and have values  
12 similar to those in the Southern hemispheric biomass burning plume. A disciplined tropospheric ozone seasonal-  
13 ity with a ~42 DU maximum at the pre-monsoon season was shown in the satellite based OMI/MLS and TES  
14 observations as well as in the MACC reanalysis model. The seasonal feature is found to be strongly related to  
15 the meteorological conditions.

16 Previous studies illustrated the importance of LRT to the pre-monsoon ozone enhancement and confirmed the  
17 source locations to be the Middle East, West India, Africa, North America and Europe. Here various regional  
18 contributions to the AS pre-monsoon ozone through LRT were analysed by dividing the global range into 7 re-  
19 gions using the MOZART-4 tagging tracer simulation method. In the lowest 4 km, the sources from India con-  
20 tributed ~50% of the transported AS ozone amount. The free troposphere of the Middle East, Africa and Europe  
21 (so called 'Euro\_FT') started to play a major role from 4 km altitude and higher. The contribution is on average  
22 30%. The Indian region is still the second important source region at 4-8 km with ~20%. Its contribution is  
23 slowly replaced by the further-away source regions at higher altitude range. It is worth mentioning that South  
24 America plays a more important role compared to North America, yet there is no explanation for this result so  
25 far.

26 In addition, the vertical pollutant accumulation in the lower troposphere, especially at 4-8 km, is important to  
27 the AS spring ozone pool. The suitable meteorological conditions were discovered from wind field data from  
28 NECP and specific humidity data from MACC. First, the cloud-free anticyclonic condition that is observed from  
29 the wind field data can cause air to be transported upside down. This point is supported by the forward model  
30 results of HYSPLIT showing that at ~7/8 km or lower, the air circles down over the AS region for around 10  
31 days without diffusion. Second, at 4-8 km the air over AS is much dryer than the surroundings. This is most  
32 probably due to relatively lower temperature over the sea which caused that the moisture cannot be lifted up as  
33 high as over land. The dry conditions induce the accumulation of ozone with a longer life time thus cause the  
34 AS ozone to be outstanding from the sub continental regions.

35 The averaged spring ozone budget was calculated using MOZART-4 to improve our understanding of the addi-  
36 tional local chemical activity. Ozone is photochemically produced at high altitudes (8-18 km) and is removed by  
37 advection. In the lowest 4 km ozone is depleted by OH radicals. Positive ozone budgets from advection and  
38 convection can be observed, which supported the LRT and accumulation mechanisms. At 4-8 km, despite the

1 weak ozone destruction from OH radicals, the net chemical budget is negligible. This suggests a low photo-  
2 chemical production, which is also supported by the negative O<sub>3</sub>-CO correlation. According to the simulation  
3 results and the O<sub>3</sub>-CO correlation, a net contribution from STE can also influence the local ozone amount.

4 The two spring ozone interannual anomalies are believed to be influenced by the dynamical variations (SST  
5 anomaly) during the El Niño events. The climate interacts with the distribution of tropospheric ozone through  
6 temperature, humidity and dynamics.

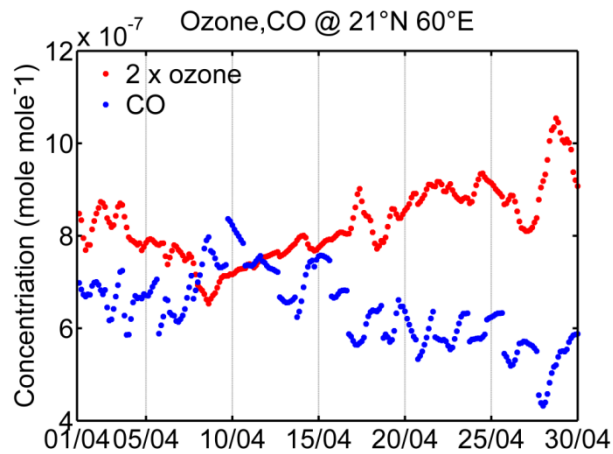
7

## 8 **Acknowledgements**

9 We would like to thank the SCIAMACHY LNM NO<sub>2</sub>, OMI/MLS, TES tropospheric ozone, IASI CO and teams  
10 for providing the data. We acknowledge the two working staffs on ~~models~~ MACC reanalysis, [NCEP](#), and MO-  
11 ZART-4. Jia Jia acknowledges funding by CSC (China Scholarship Council) and scientific support from ESS-  
12 ReS (Earth System Science Research School). We also acknowledge financial support provided by the Univer-  
13 sity and State of Bremen. We would like to thank Anne-Marlene Blechschmidt for [her help](#) ~~helping preparing~~  
14 ~~the wind field and MACC data~~. Our gratitude goes to Prof. Christian von Savigny for giving comments during  
15 the preparation of the manuscript. [The authors acknowledge the North-German Supercomputing Alliance](#)  
16 [\(HLRN\) for providing HPC resources that have contributed to the research results reported in this paper.](#)

17

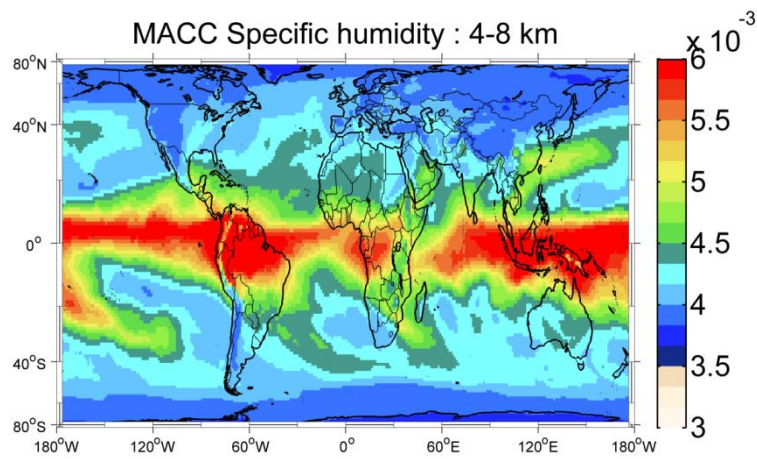
1 **Appendix**



2

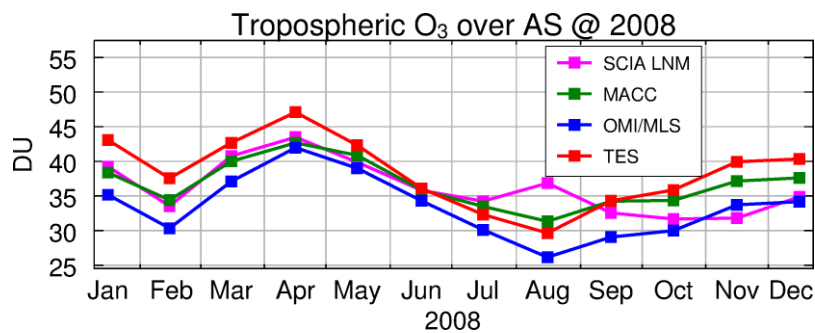
3 Figure A1. O<sub>3</sub> and CO partial column (4-8 km) time series at 21°N, 60°E over AS at April 2008 from MACC  
 4 reanalysis data. The plot is a 'point' example of Fig. 10.

5



6

7 Figure A2. Same as Fig. 12 but for the year 2010.



8

9 Figure A3. TOCs results over AS from SCIAMACHY Limb-Nadir-Matching, OMI/MLS, TES, and MACC  
 10 reanalysis data sets in 2008.



## 1 **References**

- 2 Ali, K., Beig, G., Chate, D. M., Momin, G. A., Sahu, S. K., and Safai, P. D.: Sink mechanism for significantly  
3 low level of ozone over the Arabian Sea during monsoon, *J. Geophys. Res.*, 114, D17306,  
4 doi:10.1029/2008JD011256, 2009.
- 5 Beer, R.: TES on the Aura mission: Scientific objectives, measurements, and analysis overview. *IEEE T. Geosci.*  
6 *Remote*, 44, 1102 – 1105. 20, 60, 2006.
- 7 Beirle, S., Boersma, K. F., Platt, U., Lawrence, M. G., and Wagner, T.: Megacity emissions and lifetimes of  
8 nitrogen oxides probed from space, *Science*, 333, 1737–1739, doi:10.1126/science.1207824, 2011.
- 9 Bovensmann, H., Burrows, J. P., Buchwitz, M., Frerick, J., No ě, S., Rozanov, V. V., Chance, K. V., and Goede,  
10 A. P. H.: SCIAMACHY: mission objectives and measurement modes. *J. Atmos. Sci.*, 56, 127–150, 1999.
- 11 Burrows, J. P., Hőzle, E., Goede, A., Visser, H., and Fricke, W.: SCIAMACHY – scanning imaging absorption  
12 spectrometer for atmospheric cartography, *Acta Astronaut.*, 35, 445–451, 1995.
- 13 Chand, D., Lal, S., and Naja, M.: Variations of ozone in the marine boundary layer over the Arabian Sea and the  
14 Indian Ocean during the 1998 and 1999 INDOEX campaigns, *J. Geophys. Res.*, 108, 4190,  
15 doi:10.1029/2001JD001589, 2003.
- 16 Chandra, S., Ziemke, J. R., Min, W., and Read, W. G.: Effects of 1997–1998 El Ni űo on tropospheric ozone.  
17 *Geophys. Res. Lett.*, 25, 3867–3870, 1998.
- 18 David, L. M. and Nair, P. R.: Tropospheric column O<sub>3</sub> and NO<sub>2</sub> over the Indian region observed by Ozone  
19 Monitoring Instrument (OMI): seasonal changes and long-term trends, *Atmos. Environ.*, 65, 25–39,  
20 doi:10.1016/j.atmosenv.2012.09.033, 2013.
- 21 Dickerson, R. R., Rhoads, K. P., Carsey, T. P., Oltmans, S. J., Burrows, J. P., and Crutzen, P. J.: Ozone in the  
22 remote marine boundary layer: a possible role for halogens, *J. Geophys. Res.*, 104, 21385–21395, 1999.
- 23 Duncan, B. N., Martin, R. V., Staudt, A. C., Yevich, R., and Logan, J. A.: Interannual and seasonal variability of  
24 biomass burning emissions constrained by satellite observations, *J. Geophys. Res.*, 108(D2), 4100,  
25 doi:10.1029/2002JD002378, 2003.
- 26 Ebojie, F., von Savigny, C., Ladst äter-Wei ßenmayer, A., Rozanov, A., Weber, M., Eichmann, K.-U., B ätel, S.,  
27 Rahpoe, N., Bovensmann, H., and Burrows, J. P.: Tropospheric column amount of ozone retrieved from SCIA-  
28 MACHY limb–nadir-matching observations, *Atmos. Meas. Tech.*, 7, 2073-2096, doi:10.5194/amt-7-2073-2014,  
29 2014.
- 30 Emmons, L. K., Walters, S., Hess, P. G., Lamarque, J.-F., Pfister, G. G., Fillmore, D., Granier, C., Guenther, A.,  
31 Kinnison, D., Laepple, T., Orlando, J., Tie, X., Tyndall, G., Wiedinmyer, C., Baughcum, S. L., and Kloster, S.:  
32 Description and evaluation of the Model for Ozone and Related chemical Tracers, version 4 (MOZART-4),  
33 *Geosci. Model Dev.*, 3, 43-67, doi:10.5194/gmd-3-43-2010, 2010.
- 34 Fadnavis, S., Chakraborty, T., and Beig, G.: Seasonal stratospheric intrusion of ozone in the upper troposphere  
35 over India, *Ann. Geophys.*, 28, 2149-2159, doi:10.5194/angeo-28-2149-2010, 2010.

1 Fishman, J. and Seiler, W.: Correlative nature of ozone and carbon monoxide in the troposphere: Implications  
2 for the tropospheric ozone budget, *J. Geophys. Res.*, 88, 3662–3670, doi:10.1029/JC088iC06p03662, 1983.

3 Fishman, J., P. Minnis, and H. G. Reichle, Jr., The use of satellite data to study tropospheric ozone in the trop-  
4 ics, *J. Geophys. Res.*, 91, 14,451-14,465, 1986.

5 Fishman, J., Fakhruzzaman, K., Cros, B., and Nganga, D.: Identification of widespread pollution in the  
6 Southern Hemisphere deduced from satellite analyses, *Science*, 252, 1693–1696, 1991.

7 Fortuin, J. P. F., and Kelder, H.: An ozone climatology based on ozonesonde and satellite measurements, *J.*  
8 *Geophys. Res.*, 103(D24), 31,709 – 31,734, 1998.

9 George, M., Clerbaux, C., Hurtmans, D., Turquety, S., Coheur, P.-F., Pommier, M., Hadji-Lazaro, J., Edwards,  
10 D.P., Worden, H., Luo, M., Rinsland, C., and McMillan, W.: Carbon monoxide distributions from the  
11 IASI/METOP mission: evaluation with other space-borne remote sensors, *Atmos. Chem. Phys.*, 9, 8317-8330,  
12 2009

13 Hilboll, A., Richter, A., and Burrows, J. P.: Long-term changes of tropospheric NO<sub>2</sub> over megacities derived  
14 from multiple satellite instruments, *Atmos. Chem. Phys.*, 13, 4145-4169, doi:10.5194/acp-13-4145-2013, 2013.

15 Holton, J.R., Haynes, P.H., McIntyre, M.E., Douglass, A.R., Rood, R.B., Pfister, L.: Stratosphere-troposphere  
16 exchange, *Reviews of Geophysics* 33, 403-439, 1995.

17 Hou, X., Zhu, B., Kang, H., and Gao, J.: Analysis of seasonal ozone budget and spring ozone latitudinal gradient  
18 variation in the boundary layer of the Asia-Pacific region, *Atmos. Environ.*, 94, 734–741,  
19 doi:10.1016/j.atmosenv.2014.06.006, 2014.

20 Inness, A., Baier, F., Benedetti, A., Bouarar, I., Chabrillat, S., Clark, H., Clerbaux, C., Coheur, P., Engelen, R. J.,  
21 Errera, Q., Flemming, J., George, M., Granier, C., Hadji-Lazaro, J., Huijnen, V., Hurtmans, D., Jones, L., Kaiser,  
22 J. W., Kapsomenakis, J., Lefever, K., Leitão, J., Razinger, M., Richter, A., Schultz, M. G., Simmons, A. J., Sut-  
23 tie, M., Stein, O., Thépaut, J.-N., Thouret, V., Vrekoussis, M., Zerefos, C., and the MACC team: The MACC  
24 reanalysis: an 8 yr data set of atmospheric composition, *Atmos. Chem. Phys.*, 13, 4073-4109, doi:10.5194/acp-  
25 13-4073-2013, 2013.

26 Inness, A., Benedetti, A., Flemming, J., Huijnen, V., Kaiser, J. W., Parrington, M., and Remy, S.: The ENSO  
27 signal in atmospheric composition fields: emission-driven versus dynamically induced changes, *Atmos. Chem.*  
28 *Phys.*, 15, 9083-9097, doi:10.5194/acp-15-9083-2015, 2015.

29 IPCC/TEAP, Bert Metz, Lambert Kuijpers, Susan Solomon, Stephen O. Andersen, Ogunlade Davidson, José  
30 Pons, David de Jager, Tahl Kestin, Martin Manning, and Leo Meyer (Eds), Cambridge University Press, UK. pp  
31 478, 2005.

32 Jia, J.: Improvement and interpretation of the tropospheric ozone columns retrieved based on SCIAMACHY  
33 Limb-Nadir Matching approach, PhD thesis, <http://nbn-resolving.de/urn:nbn:de:gbv:46-00105374-15>, Univer-  
34 sity of Bremen, Bremen, Germany, 2016.

1 Kim, P. S., Jacob, D. J., Liu, X., Warner, J. X., Yang, K., Chance, K., Thouret, V., and Nedelec, P.: Global  
2 ozone–CO correlations from OMI and AIRS: constraints on tropospheric ozone sources, *Atmos. Chem. Phys.*,  
3 13, 9321–9335, doi:10.5194/acp-13-9321-2013, 2013.

4 Lal, S., and Lawrence, M. G.: Elevated mixing ratios of surface ozone over the Arabian Sea, *Geophys. Res.*  
5 *Lett.*, 28(8), 1487–1490, doi:10.1029/2000GL011828, 2001.

6 Lal, S., Venkataramani, S., Srivastava, S., Gupta, S., Mallik, C., Naja, M., Sarangi, T., Acharya, Y. B., and Liu,  
7 X.: Transport effects on the vertical distribution of tropospheric ozone over the tropical marine regions sur-  
8 rounding India, *J. Geophys. Res. Atmos.*, 118, 1513–1524, doi:10.1002/jgrd.50180, 2013.

9 Lal, S., Venkataramani, S., Chandra, N., Cooper, O. R., Brioude, J., and Naja, M.: Transport effects on the ver-  
10 tical distribution of tropospheric ozone over western India, *J. Geophys. Res. Atmos.*, 119, 10012–10026,  
11 doi:10.1002/2014JD021854, 2014.

12 Lawrence, M. G. and Lelieveld, J.: Atmospheric pollutant outflow from southern Asia: a review, *Atmos. Chem.*  
13 *Phys.*, 10, 11017–11096, doi:10.5194/acp-10-11017-2010, 2010.

14 Lelieveld, J. and Crutzen, P. J.: Influences of cloud photochemical processes on tropospheric ozone, *Nature*, 343,  
15 227–233, 1990.

16 ~~Lelieveld, J. and Dentener, F. J.: What controls tropospheric ozone?, *J. Geophys. Res. Atmos.*, 105, 3531–3551,~~  
17 ~~doi:10.1029/1999jd901011, 2000.~~

18 Levelt, P. F., van den Oord, G. H. J., Dobber, M. R., Mäkki, A., Visser, H., de Vries, J., Stammes, P., Lundell,  
19 J., and Saari, H.: The Ozone Monitoring Instrument (OMI). *IEEE T. Geosci. Remote*, 44(5), 1093–1101. 16, 20,  
20 2006.

21 Livesey, N. J., Logan, J. A., Santee, M. L., Waters, J. W., Doherty, R. M., Read, W. G., Froidevaux, L., and  
22 Jiang, J. H.: Interrelated variations of O<sub>3</sub>, CO and deep convection in the tropical/subtropical upper troposphere  
23 observed by the Aura Microwave Limb Sounder (MLS) during 2004–2011, *Atmos. Chem. Phys.*, 13, 579–598,  
24 doi:10.5194/acp-13-579-2013, 2013.

25 Logan, J. Megretskaia, A., Nassar, I. R., Murray, L. T., Zhang, L., Bowman, K. W., Worden, H. M., and Luo,  
26 M.: Effects of the 2006 El Niño on tropospheric composition as revealed by data from the Tropospheric Emis-  
27 sion Spectrometer (TES), *Geophys. Res. Lett.*, 35, L03816, doi:10.1029/2007GL031698, 2008.

28 Mills, G., Harmens, H., Wagg, S., Sharps, K., Hayes, F., Fowler, D., Sutton, M., and Davies, B.: Ozone impacts  
29 on vegetation in a nitrogen enriched and changing climate, *Environmental Pollution*, 208, 898–908, doi:  
30 10.1016/j.envpol.2015.09.038, 2016.

31 Monks, P. S.: A review of the observations and origins of the spring ozone maximum, *Atmos. Environ.*, 34,  
32 3545–3561, 2000.

33 Monks, P. S., Archibald, A. T., Colette, A., Cooper, O., Coyle, M., Derwent, R., Fowler, D., Granier, C., Law,  
34 K. S., Mills, G. E., Stevenson, D. S., Tarasova, O., Thouret, V., von Schneidmesser, E., Sommariva, R., Wild,  
35 O., and Williams, M. L.: Tropospheric ozone and its precursors from the urban to the global scale from air qual-  
36 ity to short-lived climate forcer, *Atmos. Chem. Phys.*, 15, 8889–8973, doi:10.5194/acp-15-8889-2015, 2015.

1 Nair, P.R., David, L.M., Girach, I.A., and George, S.K.: Ozone in the marine boundary layer of Bay of Bengal  
2 during post-winter period: spatial pattern and role of meteorology, *Atmos. Environ.*, 45, 4671e4681, 2011.

3 Nassar, R., Logan, J. A., Worden, H. M., Megretskaia, I. A., Bowman, K. W., Osterman, G. B., Thompson, A.  
4 M., Tarasick, D. W., Austin, S., Claude, H., Dubey, M. K., Hocking, W. K., Johnson, B. J., Joseph, E., Merrill,  
5 J., Morris, G. A., Newchurch, M., Oltmans, S. J., Posny, F., Schmidlin, F. J., Vömel, H., Whiteman, D. N., and  
6 Witte, J. C.: Validation of Tropospheric Emission Spectrometer (TES) nadir ozone profiles using ozonesonde  
7 measurements, *J. Geophys. Res.*, 113, D15S17, doi:10.1029/2007JD008819, 2008.

8 Neu, J. L., Flury, T., Manney, G. L., Santee, M. L., Livesey, N. J., and Worden, J.: Tropospheric ozone varia-  
9 tions governed by changes in stratospheric circulation, *Nat. Geosci.*, 7, 340–344, doi:10.1038/ngeo2138, 2014.

10 Novelli, P. C., Masarie, K. A., and Lang, P. M.: Distributions and recent changes of carbon monoxide in the  
11 lower troposphere, *J. Geophys. Res.-Atmos.*, 103, 19015–19033, 1998.

12 Penkett, S.A., Reeves, C.E., Bandy, B.J., Kent, J.M., Richer, H.R.: Comparison of calculated and measured per-  
13 oxide data collected in marine air to investigate prominent features of the annual cycle of ozone in the tropo-  
14 sphere, *J. Geophys. Res.*, 103, 13377-13388, 1998.

15 ~~Pickering, K.E., Thompson, A.M., Wang, Y., Tao, W., McNamara, D.P., Kirchhoff, V.W.J.H., Heikes, B.G.,~~  
16 ~~Sachse, G.W., Bradshaw, J.D., Gregory, G.L., Blake, D.R.: Convective transport of biomass burning emissions~~  
17 ~~over Brazil during TRACE A. *Journal of Geophysical Research* 101, 23993–24012, 1996.~~

18 Richter, A., Eyring, V., Burrows, J. P., Bovensmann, H., Lauer, A., Sierk, B., and Crutzen, P. J.: Satellite meas-  
19 urements of NO<sub>2</sub> from international shipping emissions, *Geophys. Res. Lett.*, 31, L23110,  
20 doi:10.1029/2004GL020822, 2004.

21 ~~Sinha, P., Jaegle, L., Hobbs, P., Liang, Q.: Transport of biomass burning emissions from southern Africa. *Jour-*  
22 ~~*nal of Geophysical Research Atmospheres* 109, D20204, 2004.~~~~

23 Srivastava, S., Lal, S., Venkataramani, S., Gupta, S., and Acharya, Y. B.: Vertical distribution of ozone in the  
24 lower troposphere over the Bay of Bengal and the Arabian Sea during ICARB-2006: Effects of continental out-  
25 flow, *J. Geophys. Res.*, 116, D13301, doi:10.1029/2010JD015298, 2011.

26 Srivastava, S., Lal, S., Naja, M., Venkataramani, S., and Gupta, S.: Influence of regional pollution and long  
27 range transport over Western India: analysis of ozonesonde data, *Atmos. Environ.*, 47 (2012), pp. 174–182,  
28 2012.

29 ~~Staudt, A.C., Jacob, D.J., Logan, J.A., Bachiochi, D., Krishnamurti, T.N., Poisson, N.: Global chemical model~~  
30 ~~analysis of biomass burning and lightning influences over the South Pacific in austral spring, *J. Geophys. Res.*,~~  
31 ~~107, 4200, 2002.~~

32 Sudo, K. and Akimoto, H.: Global source attribution of tropospheric ozone: Long-range transport from various  
33 source regions, *J. Geophys. Res.*, 112, D12302, doi:10.1029/2006JD007992, 2007.

34 Sudo, K., and Takahashi, M.: Simulation of tropospheric ozone changes during 1997–1998 El Niño: Meteorolo-  
35 gical impact on tropospheric photochemistry, *Geophys. Res. Lett.*, 28, 4091–4094, 2001.

- 1 [Thompson, A.M., Pickering, K.E., McNamara, D.P., Schoeberl, M.R., Hudson, R.D., Kim, J.H., Browell, E.V.,](#)  
2 [Kirchhoff, V.W.J.H., Nganga, D.: Where did tropospheric ozone over southern Africa and the tropical Atlantic](#)  
3 [come from in October 1992? Insights from TOMS, GTE TRACE A, and SAFARI 1992 J. Geophys. Res.,](#)  
4 [\(D19\), 24,251–24,278, 1996.](#)
- 5 [Thompson, A.M., Witte, J.C., Hudson, R.D., Guo, H., Herman, J.R., Fujiwara, M.: Tropical tropospheric ozone](#)  
6 [and biomass burning, Science 291, 2128–2132, 2001.](#)
- 7 Van Dingenen, R., Dentener, F. J., Raes, F., Krol, M. C., Emberson, L., and Cofala, J.: The global impact  
8 of ozone on agricultural crop yields under current and future air quality legislation, *Atmos. Envi-*  
9 *ron.*, 43, 604–618, doi:10.1016/j.atmosenv.2008.10.033, 2009.
- 10 Wang, Y., Jacob, D.J., Logan, J.A.: Global simulation of tropospheric O<sub>3</sub>-NO<sub>x</sub>-hydrocarbon chemistry: 3. Ori-  
11 gin of tropospheric ozone and effects of nonmethane hydrocarbons, *Journal of Geophysical Research* 103,  
12 10757-10767, 1998.
- 13 Waters, J. W., Froidevaux, L., Harwood, R. S., Jarnot, R. F., Pickett, H. M., Read, W. G., Siegel, P. H., Cofield,  
14 R. E., Filipiak, M. J., Flower, D. A., Holden, J. R., Lau, G. K. K., Livesey, N. J., Manney, G. L., Pumphrey, H.  
15 C., Santee, M. L., Wu, D. L., Cuddy, D. T., Lay, R. R., Loo, M. S., Perun, V. S., Schwartz, M. J., Stek, P. C.,  
16 Thurstans, R. P., Boyles, M. A., Chandra, K. M., Chavez, M. C., Chen, G. S., Chudasama, B. V., Dodge, R.,  
17 Fuller, R. A., Girard, M. A., Jiang, J. H., Jiang, Y. B., Knosp, B. W., LaBelle, R. C., Lam, J. C., Lee, K. A.,  
18 Miller, D., Oswald, J. E., Patel, N. C., Pukala, D. M., Quintero, O., Scaff, D. M., Van Snyder, W., Tope, M. C.,  
19 Wagner, P. A., and Walch, M. J.: The Earth Observing System Microwave Limb Sounder (EOS MLS) on the  
20 Aura satellite, *IEEE Trans. Geosci. Remote Sens.*, 44 (5), 1075–1092, doi:10.1109/TGRS.2006.873771, 2006.
- 21 Weller, R. A., Baumgartner, M. F., Josey, S. A., Fischer, A. S., and Kindle, J. C.: Atmospheric Forcing in the  
22 Arabian Sea during 1994–1995: Observations and Comparisons with Climatology and Models, *Deep Sea*  
23 *Research Part II: Topical Studies in Oceanography* 45: 1961–1999. doi:10.1016/S0967-0645(98)00060-5, 1998.
- 24 Young, P. J., Archibald, A. T., Bowman, K. W., Lamarque, J.-F., Naik, V., Stevenson, D. S., Tilmes,  
25 S., Voulgarakis, A., Wild, O., Bergmann, D., Cameron-Smith, P., Cionni, I., Collins, W. J., Dalsøren, S.  
26 B., Doherty, R. M., Eyring, V., Faluvegi, G., Horowitz, L. W., Josse, B., Lee, Y. H., MacKenzie, I. A., Na-  
27 gashima, T., Plummer, D. A., Righi, M., Rumbold, S. T., Skeie, R. B., Shindell, D. T., Strode, S. A., Sudo,  
28 K., Szopa, S., and Zeng, G.: Pre-industrial to end 21st century projections of tropospheric ozone from the  
29 Atmospheric Chemistry and Climate Model Intercomparison Project (ACCMIP), *Atmos. Chem. Phys.*, 13,  
30 2063–2090, doi:10.5194/acp-13-2063-2013, 2013.
- 31 Zahn, A., Brenninkmeijer, C. A. M., Asman, W. A. H., Crutzen, P. J., Heinrich, G., Fischer, H., Cuijpers, J. W.  
32 M., and van Velthoven, P. F. J.: Budgets of O<sub>3</sub> and CO in the upper troposphere: CARIBIC passenger aircraft  
33 results 1997–2001, *J. Geophys. Res.*, 107(D17), 4337, doi:10.1029/2001JD001529, 2002.
- 34 Zanis, P., Hadjinicolaou, P., Pozzer, A., Tyrlis, E., Dafka, S., Mihalopoulos, N., and Lelieveld, J.: Summertime  
35 free-tropospheric ozone pool over the eastern Mediterranean/Middle East, *Atmos. Chem. Phys.*, 14, 115-132,  
36 doi:10.5194/acp-14-115-2014, 2014.

- 1 Zeng, G. and Pyle, J. A.: Influence of El Niño Southern Oscillation on stratosphere/troposphere exchange and  
2 the global tropospheric ozone budget, *Geophys. Res. Lett.*, 32, L01814, doi:10.1029/2004GL021353, 2005.
- 3 Zhu, B., Hou, X., and Kang, H.: Analysis of the seasonal ozone budget and the impact of the summer monsoon  
4 on the northeastern Qinghai-Tibetan Plateau, *J. Geophys. Res. Atmos.*, 121, 2029–2042,  
5 doi:10.1002/2015JD023857, 2016.
- 6 Ziemke, J. R., Chandra, S., Duncan, B. N., Froidevaux, L., Bhartia, P. K., Levelt, P. F., and Waters, J. W.: Tro-  
7 pospheric ozone determined from Aura OMI and MLS: Evaluation of measurements and comparison with the  
8 Global Modeling Initiative’s Chemical Transport Model, *J. Geophys. Res.*, 111, D19303,  
9 doi:10.1029/2006JD007089, 2006.
- 10 Ziemke, J. R., Chandra, S., Labow, G. J., Bhartia, P. K., Froidevaux, L., and Witte, J. C.: A global climatology  
11 of tropospheric and stratospheric ozone derived from Aura OMI and MLS measurements, *Atmos. Chem. Phys.*,  
12 11, 9237–9251, doi:10.5194/acp-11-9237-2011, 2011.
- 13 Ziemke, J. R., Chandra, S., Oman, L. D., and Bhartia, P. K.: A new ENSO index derived from satellite meas-  
14 urements of column ozone, *Atmos. Chem. Phys.*, 10, 3711–3721, doi:10.5194/acp-10-3711-2010, 2010.

1           **Tropospheric ozone maxima observed over the Arabian Sea during the**  
2                                           **pre-monsoon**  
3                                           **by J. Jia et al.**

4                                           **Answers to referee comments, Referee #3**

5   The authors would like to thank Referee #3 for reviewing the manuscript.

6  
7   **Comments:**

8   *This work describes variations in the tropospheric ozone column over the Arabian Sea using*  
9   *satellite data (SCIAMACHY, OMI/MLS, TES), MACC reanalysis data, MOZART-4 results &*  
10   *HYSPLIT trajectories and indicates that spring time ozone maximum over a region in the*  
11   *Arabian sea is largely (50% in 0-4 km and 20% in 4-8 km) due to LRT from India apart from*  
12   *some contribution from Middle East, Africa and Europe. Major findings are based on MACC*  
13   *reanalysis data and MOZART-4 output (Hou et al. 2014). Quantitative contributions from*  
14   *different regions are mentioned, where detailed explanation and in-depth analysis for these*  
15   *regions was expected. It has been mentioned (page 2, line 20) that spring time maximum*  
16   *ozone is not unique but rather well-known. It has also been confirmed by other studies (line*  
17   *32) that this is due to LRT from Middle East, Western India, Africa, etc. Therefore, it was ex-*  
18   *pected that this work should have provided some additional knowledge with more quantita-*  
19   *tive analysis.*

20   *There are significant differences in spatial distribution among SCIAMACHY, OMI/MLS and*  
21   *MACC reanalysis data over the Arabian Sea during spring. In my opinion, few of my below*  
22   *comments might be helpful in making it a better manuscript.*

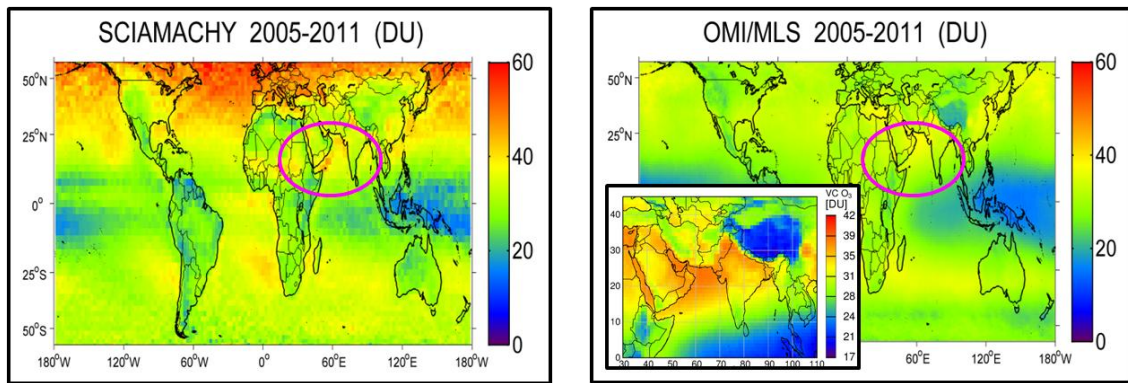
23  
24   *Specific comments:*

25   *Introduction, Page 2, 2nd para – Enhancement in ozone over the Arabian Sea is not promi-*  
26   *nent. It would be better to include some discussion on enhancement in ozone over northern*  
27   *India. Additionally, higher ozone could also be seen over the Bay of Bengal in SCIAMACHY*  
28   *but not in OMI/MLS, any reason for it!*

29

1 **Response:** The enhancement in ozone over the Arabian Sea can be observed better in a 7-  
 2 years averaged image as shown below. This enhancement is exciting as AS is a remote ma-  
 3 rine region. The enhancement in ozone over northern India is expected with anthropogenic  
 4 pollution and biomass burning over Indo-Gangenic Plain. The authors agree that this en-  
 5 hancement should also be mentioned. The sentence in Page 2 Line 12-18 is changed to '..., 2)  
 6 TOC attributed to anthropogenic sources in the Northern Hemisphere, for instance, Northern  
 7 India, and 3) the Mediterranean ...'  
 8 High ozone values can also be seen over the BoB in OMI/MLS during spring time (Figure 2).  
 9 The higher values in SCIAMACHY seem to be contributed from summer-monsoon. General-  
 10 ly, if any feature is seen by one instrument and not seen by another, the difference might be  
 11 explained either by different samplings of the instruments or by quality problems in one of  
 12 the data set. Here the second explanation is more probable. A validation with respect to inde-  
 13 pendent data is needed to decide which data set is more correct. Unfortunately, no sufficient  
 14 balloon/ship measurement was taken over BoB.

15



16

17

18 *Section 3: CO and NO2 are ozone precursors and springtime CO column (Fig 2) values are*  
 19 *observed to be much higher in the Bay of Bengal region than over the Arabian Sea. NO2 is*  
 20 *also seen to be similar over AS and BoB. Any comment !!! Additionally, CO is also higher in*  
 21 *southern region of the Arabian Sea and southwest boundaries of India. But higher ozone*  
 22 *(particularly SCIAMACHY) is seen in the northern part of the Arabian Sea and close to*  
 23 *Oman, Yemen, Pakistan, etc. Why ozone is not higher close to western coast of India? Expla-*  
 24 *nation should be added in this regard. Considering these facts, source of ozone maximum*  
 25 *should be discussed.*

26



1 **Response:** One difference between CO and tropospheric ozone is that CO is emitted directly  
2 from pollutions, while ozone is produced through secondary photochemical reactions. CO is  
3 mostly observed near the boundary layer close to the emission sources; in this case, biomass  
4 burnings in Southeast Asia and Indo-Gangetic Plain. Srivastava et al. (2011) reported that  
5 transport from highly polluted Indo-Gangetic Plain is the major source for polluted air  
6 masses over Bay of Bengal. Thus, CO column values are much higher in the Bay of Bengal  
7 region. NO<sub>2</sub>, on the other hand, is a short lived trace gas, which is often observed at source  
8 region. The similar value of NO<sub>2</sub> over AS and BoB is at its background level. At this situa-  
9 tion, the present of higher CO in southern region of the Arabian Sea and southwest bounda-  
10 ries of India would not contribute to ozone production due to wet-deposition. The different  
11 spatial distribution among ozone precursors and ozone indicate a dynamic origin of high  
12 TOC over AS from long range transport of ozone. This sentence has been added to Page 5  
13 Line 34. The air masses over AS is not mainly transported from northern India, but is trans-  
14 ported from central/south India and Southwest Asia, i.e., Oman, Yemen, Pakistan, etc. Our  
15 study shows later that the source from India contributes to the lower altitude of ozone over  
16 AS, while Southwest Asia and Europe are the major sources for ozone columns from 4 km  
17 above (Fig. 9). Therefore, ozone over AS is higher close to Southwest Asia instead of western  
18 coast of India. The authors agree that this ozone distribution is worth to be pointed out and  
19 explained in the manuscript. We have added 'The spring TOC are higher over western AS  
20 than over eastern AS (Fig. 2). This distribution is further discussed in Sect. 4.2.' in Page 5,  
21 Line 19 and '... with over 20% contribution. Since 'Euro FT' is the major source of TOC  
22 over AS, higher TOCs are observed over the western AS that is close to Southwest Asia, i.e.,  
23 Oman, Yemen, Pakistan, etc., instead of the eastern AS near west coast of India. ...' in Page  
24 12, Line 13.

25

26 *Section 3: Figure 2 is for year 2008 and Figure 4 is for years 2006 and 2010. It will be good*  
27 *to add results for year 2008 in Figure 4 or make figure 2 for years 2006 or 2010. A signifi-*  
28 *cant difference in spatial distribution is seen over AS during spring/April. Figure 2 shows*  
29 *higher ozone (SCIAMACHY) having proximity to western region of AS, while this is not seen*  
30 *in Fig 4. It would be better to add monthly variations from MACC reanalysis (TOC, 0-4 km,*  
31 *4-8 km, 8-12 km, 12-18 km) in a separate panel of figure 3.*

32

33 **Response:** The results for year 2008 are added in Figure 4.

1 Both satellite and model shows maxima in April (Fig. A3). As model data preparing is time  
2 consuming, we have chosen April instead of long time series. Analyzing monthly variations  
3 from MACC reanalysis data cannot help better understanding the spatial distribution differ-  
4 ences seen between Fig.2 and Fig. 4 since the time series represent a regional average. Never-  
5 theless, the authors found this review very interesting, we will consider putting this idea into  
6 the framework of the next study.

7

8 *Section 4.2: Line 10 "...CO and TOC are highly correlated..." please clarify. This is in con-*  
9 *tradiction with statement at page 5 line 20 ("...CO and NO2 show a different...").*

10

11 **Response:** The sentence '...CO and TOC are highly correlated...' is deleted.

12

13 *Figure 6: Backward trajectories (mainly 2 and 4 km) are from southern India or some time*  
14 *from central region. Both these regions are showing much lower levels of ozone than those*  
15 *over northern India (Fig 1, 2, and 4).*

16

17 **Response:** The high ozone over northern India (mainly over Indo-Gangetic Plain) is mainly  
18 due to the anthropogenic pollution with intensive population and rapidly growing industry. It  
19 is the most polluted region not only for ozone but also other trace gases. Despite the TOC  
20 values over northern India are much higher than in other surrounding regions, our study  
21 shows that the source of increased TOC in AS region are located in central/southern India.

22

23 *Page 9, Line 14: Is this statement based on backward air trajectory of 15 km (Fig 6) alone or*  
24 *are there other supporting evidences? Lines 15-16 are also very qualitative.*

25

26 **Response:** Thank you very much for this comment. The conclusions are based on the trajec-  
27 tory of AS in different years and at different altitudes in April. Figure 6 and 7 only give ex-  
28 amples of the trajectories. The statement at Page 9 Line 14 is indeed misleading the reader.  
29 The sentence has been changed into 'The higher tropospheric ozone (12-18 km) is found in  
30 air which was uplifted and transported not only from the North Africa, but also from the  
31 North Indian Ocean and Southeast Asia.'

1  
2  
3  
4  
5  
6  
7  
8  
9  
10  
11  
12  
13  
14  
15  
16  
17  
18  
19  
20  
21  
22  
23  
24  
25  
26  
27  
28  
29  
30  
31

*Page 11, Line 7: Considering the broad region, it is better to name it as “South Asia”. It would be beneficial to the reader to give some details on methodology adopted in estimating percentage contribution from different regions (Page 12). What/how was the background/reference levels considered while making these estimates?*

**Response:** We agree that the name 'South Asia' would be more appropriate. Unfortunately, due to technical reasons it is extremely time expensive to replace the name in the plot. As this is not crucial for the general content of the paper, we decided to keep the name 'India'. We have added a sentence in Page 11, Line 11 to clarify: 'The selected names are rather symbolic and do not pretend to be geographically fully correct.'

The methodology in estimating contributions from different regions is briefly mentioned in page 4, line 34. We added a sentence in page 12 Line 6 to help readers understand more about the percentage estimation. 'The percentage contributions from different regions are calculated by first estimating the ozone concentration (in ppbv) from a separated region using tagged tracer method (Sudo and Akimoto, 2007), then dividing this value by the sum of ozone concentrations.'

*Section 4.4: It would be worthwhile to list down the contribution from STE in the AS region. As mentioned that it is comparable with that of 'Euro\_FT', which is significant (17%, 29%, 32%, and 31%).*

**Response:** The contributions from STE are now listed as you can see here: This information is added on Page 16, line 11. '... is comparable with the ones transported from 'Euro\_FT' in most altitude ranges (STE to Euro\_FT contributions are 0.955 at 0-4 km, 0.861 at 4-8 km, 0.997 at 8-12 km, and 16.858 at 12-18 km). The STE origin ...'

*Minor comments:*  
*TPH information can be given in the caption of figure 4.*

1 **Response:** The TPH information has been added in the caption of figure 4 as: 'Ozone partial  
2 columns (TOC: 0 km - TPH(~17 km over AS) column of tropospheric ozone in the left pan-  
3 els and 0-8 km ...'

4  
5 *Referencing of figure needs to be in sequence. Figure 12 (@ page 10) is referred after figure*  
6 *7 (@ page 9).*

7  
8 **Response:** The text at Page 10, line 5 has been changed to '... by Hydroxyl radicals (OH).  
9 This is further ...', where figure 12 is no longer referred before figure 7.

10  
11 *Hou et al. (2014) used MOZART-4 model run during 2000-2007, however this study used*  
12 *1997-2007 model run. Please mention it explicitly if a separate run is made for this study.*

13  
14 **Response:** The data used in this study was obtained by Zhu et al.(2016) using the same sce-  
15 nario as Hou et al. (2014). This run was not made specifically for this study. The description  
16 is added in Page 4, Line 30-37: '... from the surface to approximately 2 hPa. The data used in  
17 this study are simulation results obtained by Zhu et al. (2016), using MOZART-4 model for  
18 1997-2007. The chemical initial condition in 2000 and emissions from 1997 to 2007 used ...  
19 it's transport, chemical transformation and surface deposition. More details of the simulation  
20 settings can be found in Hou et al. (2014).'

21  
22 *Page 13: Change "Fig 6.11" to "Fig 10"*

23  
24 **Response:** Typo has been corrected

25  
26 *Conclusion: Line 12: Reference of Southern hemisphere biomass burning is appearing not to*  
27 *be relevant here. This has also been referred in the main text without much relevance.*

28  
29 **Response:** The study of AS tropospheric ozone columns is inspired by averaging TOCs over  
30 long time period, when the author found four main patterns in a global scale: plumes caused  
31 by biomass burning, by the anthropogenic pollution in midlatitudes northern hemisphere, by

1 STE over Mediterranean, and the ozone enhancement over Arabian Sea. Plenty of studies and  
2 researches have helped us understanding the first three patterns of tropospheric ozone, while  
3 few were about the enhancement over Arabian Sea. Page 2, Line 12-18 states this motivation  
4 and aims to point out the outstanding magnitude of Arabian Sea ozone enhancement by com-  
5 paring it with the other three well-known patterns. The biomass burning pattern is one of  
6 them.

7

8 Besides of the comments that were given, the authors would like to clarify some contributors  
9 in the acknowledgements: ‘...We acknowledge the working staffs on MACC reanalysis,  
10 NCEP, and MOZART-4. ... We would like to thank Dr. Anne-Marlene Blechschmidt for her  
11 help. Our gratitude goes to Prof. Christian von Savigny for giving comments during the  
12 preparation of the manuscript. The authors acknowledge the North-German Supercomputing  
13 Alliance (HLRN) for providing HPC resources that have contributed to the research results  
14 reported in this paper’

# Tropospheric ozone maxima observed over the Arabian Sea during the pre-monsoon

Jia Jia<sup>1</sup>, Annette Ladstätter-Weißenmayer<sup>1</sup>, Xuwei Hou<sup>2</sup>, Alexei Rozanov<sup>1</sup> and John P. Burrows<sup>1</sup>

<sup>1</sup>Institute of Environmental Physics, Bremen, Germany

<sup>2</sup>Nanjing University of Information Science and Technology, Nanjing, China

*Correspondence to:* Jia Jia (jia@iup.physik.uni-bremen.de)

**Abstract.** An enhancement of the tropospheric ozone column (TOC) over Arabian Sea (AS) during the pre-monsoon season is reported in this study. The potential sources of the AS spring ozone pool are investigated by use of multiple data sets (e.g., SCIAMACHY Limb-Nadir-Matching TOC, OMI/MLS TOC, TES TOC, MACC reanalysis data, MOZART-4 model and HYSPLIT model). 3/4 of the enhanced ozone concentrations are attributed to the 0-8 km height range. The main source of the ozone enhancement is considered to be caused by long range transport of ozone pollutants from India (~ 50% contributions to the lowest 4 km, ~ 20% contributions to the 4-8 km height range), the Middle East, Africa and Europe (~30% in total). In addition, the vertical pollution accumulation in the lower troposphere, especially at 4-8 km, was found to be important for the AS spring ozone pool formation. Local photochemistry, on the other hand, plays a negligible role in producing ozone at the 4-8 km height range. In the 0-4 km height range, ozone is quickly removed by wet-deposition. The AS spring TOC maxima are influenced by the dynamical variations caused by the sea surface temperature (SST) anomaly during the El Niño period in 2005 and 2010 with a ~5 DU decrease.

## 1 1 Introduction

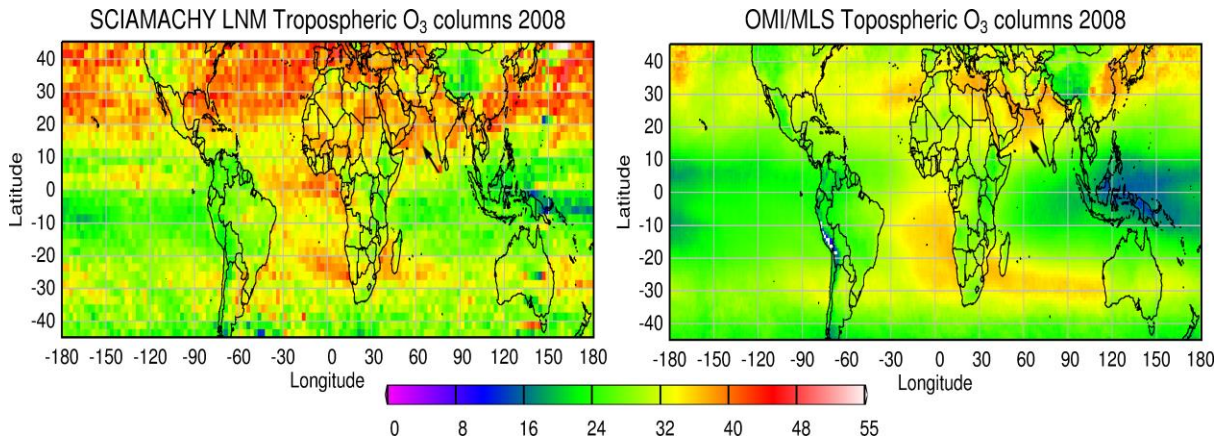
2 Tropospheric ozone is one of the most important green-house gases and one of the most important components  
3 of photochemical smog. Most tropospheric ozone is produced in situ by photochemical reactions of its precursors  
4 ( $\text{NO}_x$  ( $\text{NO} + \text{NO}_2$ ),  $\text{CO}$ ,  $\text{CH}_4$  and VOCs) in the presence of sunlight, while some tropospheric ozone naturally  
5 originates in the stratosphere. High surface ozone values are detrimental to human health by causing respiratory  
6 illnesses, and can also lead to losses in agricultural crops (see Van Dingenen et al., 2009; Mills et al.,  
7 2016 and references therein).

8 In this study, we investigated the global pattern of tropospheric ozone by averaging 7 years (2005-2011) of  
9 Tropospheric Ozone Column (TOC) data products from different satellite instrumentation: SCIAMACHY  
10 Limb-Nadir-Matching TOC (Ebojie et al., 2014; Jia, 2016) and the OMI/MLS TOC (Ziemke et al., 2006). A  
11 tropospheric ozone maximum is observed over the Arabian Sea (AS, west side of the subcontinental India). This  
12 enhancement of TOC can be observed in yearly mean image as well (Fig. 1). The enhancement of TOC is similar  
13 in magnitude as TOC enhancements observed during the follow events: 1) the well-known biomass burning  
14 plume in the Southern Hemisphere that was transported over the South Atlantic, the coast of South Africa, along  
15 the Indian Ocean and towards Australia (e.g., Fishman et al., 1986, 1991), 2) TOC attributed to anthropogenic  
16 sources in the Northern Hemisphere, [for instance, Northern India](#), and 3) the Mediterranean summer ozone pool  
17 attributed to the stratospheric-tropospheric exchange (STE) (Zanis et al., 2014). A spring (or so called pre-  
18 monsoon, see Sect. 2.1) TOC maximum of  $\sim 42$  DU on monthly average was identified from our study of the  
19 seasonality of the TOC. Although the TOC enhancement over AS is an important global pattern of tropospheric  
20 ozone, the spring maxima in TOC are not unique over the AS representing rather a well-known large scale phenomenon  
21 in the Northern Hemisphere. Nevertheless, the origin and mechanisms explaining this phenomenon is  
22 still a matter for debate (e.g. Monks, 2000, 2015 and references therein). The increase of tropospheric pollutants,  
23 presumably increase of longer lived VOCs which are ozone precursors, during winter, may play an important  
24 role by influencing the two major contributors to tropospheric ozone concentrations: the STE intrusions and the  
25 photochemical production process (Holton et al., 1995; Penkett et al., 1998; Monks, 2000). In a remote region  
26 like AS, an intuitive hypothesis is that long range transport (LRT) of ozone from more polluted regions or from  
27 STE may be the drivers. This is because of the longer ozone lifetime in spring and the weak local production  
28 over remote areas (Wang et al., 1998).

29 In previous studies using the ozonesonde measurements above the west coast of India and the data from two  
30 campaigns (the 1998 and 1999 INDOEX – INDIan Ocean EXperiment campaigns and the ICARB – Integrated  
31 Campaign for Aerosols, Gases and Radiation Budget campaign which was conducted during March-May 2006),  
32 the higher AS TOC during pre-monsoon season was confirmed to be significantly influenced by LRT of the  
33 continental anthropogenically influenced outflows from the Middle East, Western India, Africa, North America  
34 and Europe (Lal and Lawrence, 2001; Chand et al, 2003; Srivastava et al., 2011, 2012; Lal et al., 2013, 2014). In  
35 addition, by comparing the INDOEX ozone measurements from both sides (northern and southern) of the ITCZ  
36 (InterTropical Convergence Zone), the influence of the ITCZ functioning as a sink for ozone was determined by  
37 the observed 4 times higher TOC values on the northern side of AS compared to the southern side (Chand et al.,  
38 2003). The seasonal variation of tropospheric ozone at Ahmadabad ( $23.03^\circ\text{N}$ ,  $72.54^\circ\text{E}$ ) was reported to have an  
39 averaged maximum of  $\sim 44$  DU in April during the years 2003–2007 (Lal et al., 2014). The possibility of the

1 STE influencing the ozone mixing ratio up to ~10 km altitude was also discussed. However, the mechanisms  
2 explaining this phenomenon need to be better understood.

3



4  
5

6 Figure 1. Yearly average for TOC retrieved from (left) SCIAMACHY LNM and (right) OMI/MLS in 2008,  
7 with bold arrows pointing to AS. The AS region is defined as 10--20°N, 60-70°E in this study and is marked  
8 with red rectangle in Fig. 2

9

10 Here, the TOC enhancement over the AS is investigated and interpreted by using TOC data products from sev-  
11 eral satellite remote sensors (i.e. SCIAMACHY Limb-Nadir Matching, OMI/MLS and TES), MACC (Monitor-  
12 ing Atmospheric Composition and Climate) reanalysis data (Inness et al., 2013) and simulations from the global  
13 tropospheric chemical transport model (CTM) MOZART-4 model (Model for Ozone and Related Tracers)  
14 (Emmons et al., 2010). This study focuses on the analysis of the regional contribution to LRT, the influence of  
15 the meteorological conditions, the local chemistry and STE, and the inter-annual variability of the spring ozone  
16 maxima, thus to better understand the climate interact with the distribution of tropospheric ozone through tem-  
17 perature, humidity and dynamics. In Sect. 2, the data sets used in this study are briefly discussed. In Sect. 3, the  
18 regional distribution and the time series of tropospheric ozone and its precursors are investigated. Meteorologi-  
19 cal and photochemical sources of ozone plumes due to LRT, local chemistry and STE are discussed in Sect. 4.  
20 The role of accumulation of pollutants is also highlighted in this section. In Sect. 5 the impact of El Niño on the  
21 inter-annual variability is identified. Finally, conclusions are given in Sect. 6.

22

## 23 2 Data sets used in this study

24 The SCanning Imaging Absorption spectroMeter for Atmospheric CHartographyY (SCIAMACHY) was a pas-  
25 sive spectrometer designed to measure radiances in eight spectral channels, covering a wide range from 214 nm  
26 to 2384 nm with a moderate spectral resolution of 0.21 nm to 1.56 nm (Burrows et al., 1995; Bovensmann et al.,  
27 1999). SCIAMACHY performed observations in three viewing modes: nadir, limb and solar/lunar occultation.  
28 The SCIAMACHY Limb-Nadir-Matching TOC is retrieved based on the tropospheric ozone residual (TOR)  
29 method, which subtracting the stratospheric ozone columns retrieved from the limb measurements, from the



1 collocated total ozone columns acquired from nadir measurements, by using the tropopause height data (Ebojie  
2 et al., 2014). The results showed in this study are from the V1.2 SCIAMACHY Limb-Nadir-Matching TOC data  
3 set. This data set is recently developed in the Institute of Environmental Physics (IUP) in the University of Bre-  
4 men (Details can be found in Jia, 2016). The data set is not complete in a full SCIAMACHY performing time  
5 period (2002-2012), thus is not showed in the time series image.

6 The UV-Vis nadir viewing spectrometer Ozone Monitoring Instrument (OMI), the thermal-emission Microwave  
7 Limb Sounder (MLS) and the infrared Fourier transform spectrometer Tropospheric Emission Spectrometer  
8 (TES) are three of the main instruments onboard the EOS Aura satellite (Levelt et al., 2006; Waters et al., 2006;  
9 Beer, 2006). The OMI/MLS TOC data set is retrieved based on TOR method using data sets from OMI and  
10 MLS. The adjustment for inter-calibration differences of OMI and MLS instruments is performed by using the  
11 CCD method (Ziemke et al., 2006; 2011). Both OMI-CCD and MLS measurements of the stratospheric ozone  
12 are averaged for the comparison over the Pacific (120° W-120° E) (Ziemke et al., 2006). The MLS data is ad-  
13 justed according to the observed differences, and then interpolated in two steps along-track and along longitude.  
14 In the end, OMI/MLS is able to provide daily-based global TOCs.

15 TES ozone is retrieved from the 9.6  $\mu\text{m}$  ozone absorption band using the 995 – 1070  $\text{cm}^{-1}$  spectral range. In  
16 cloud-free conditions, the nadir vertical profiles have around four degrees of freedom (DOF) for signal, approx-  
17 imately two of which are in the troposphere, giving an estimated vertical resolution of about 6 km with a foot-  
18 print of 5.3 km  $\times$  8.5 km, covering an altitude range of 0-33 km (see Beer et al., 2001; Nassar et al., 2008 and  
19 the references therein).

20 MACC is a research project for the European GMES (Global Monitoring for Environment and Security) initia-  
21 tive (Inness et al., 2013). MACC combines a wealth of atmospheric composition data with a state-of-the-art nu-  
22 merical model and data assimilation system to produce a reanalysis of the atmospheric composition. MACC  
23 reanalysis data of ozone, CO and specific humidity used in this study are available in 6-h time intervals (00, 06,  
24 12 and 18 UTC) and were provided in monthly files with the unit of kg/kg under the website  
25 <http://apps.ecmwf.int/datasets/data/macc-reanalysis/levtype=ml/>. The horizontal resolution of the model is 1.125°  
26  $\times$  1.125°. Variables were provided as 3D fields in pressure hybrid vertical coordinates. The vertical coordinate  
27 system is given by 60 hybrid sigma-pressure levels, with a model top at 0.1 hPa.

28 MOZART-4 is a global tropospheric CTM. It was run with the standard chemical mechanism (see Emmons et  
29 al., 2010 for details) in this study. MOZART-4 was driven by the NCEP/ National Center for Atmospheric Re-  
30 search (NCAR) reanalysis meteorological parameters, having a horizontal resolution of approximately 2.8°  $\times$   
31 2.8°, with 28 vertical levels from the surface to approximately 2 hPa. The data used in this study are simulation  
32 results obtained by Zhu et al. (2016), using MOZART-4 model for 1997-2007. The chemical initial condition in  
33 2000 and emissions from 1997 to 2007 used in MOZART-4 were from the NCAR Community Data Portal  
34 (<http://cdp.ucar.edu/>), which was introduced by Emmons et al. (2010). The model was run with a time step of 20  
35 min from 1 January 1996 to 31 December 2007, and the first year was discarded as spin-up (Hou et al., 2014;  
36 Zhu et al., 2016). The tagged tracer method was used to isolate the contributions from individual source re-  
37 gions. This method was introduced by Sudo and Akimoto (2007). It treats a chemical species emitted or chemi-  
38 cally produced in a certain region as a separate tracer and calculates its transport, chemical transformation and

1 surface deposition. [More details of the simulation settings can be found in Hou et al. \(2014\). The results used in](#)  
2 [this study are simulated by Hou et al. \(2014\).](#)

3 HYbrid Single-Particle Lagrangian Integrated Trajectory (HYSPLIT) is a system for the computation of simple  
4 air parcel trajectories from the National Oceanic and Atmospheric Administration (NOAA). In order to investi-  
5 gate the forward and backward trajectory of the air mass, the web-based version of the HYSPLIT model (Stein  
6 et al., 2015) is used for this study: <http://ready.arl.noaa.gov/hypub-bin/trajtype.pl?runtype=archive>.

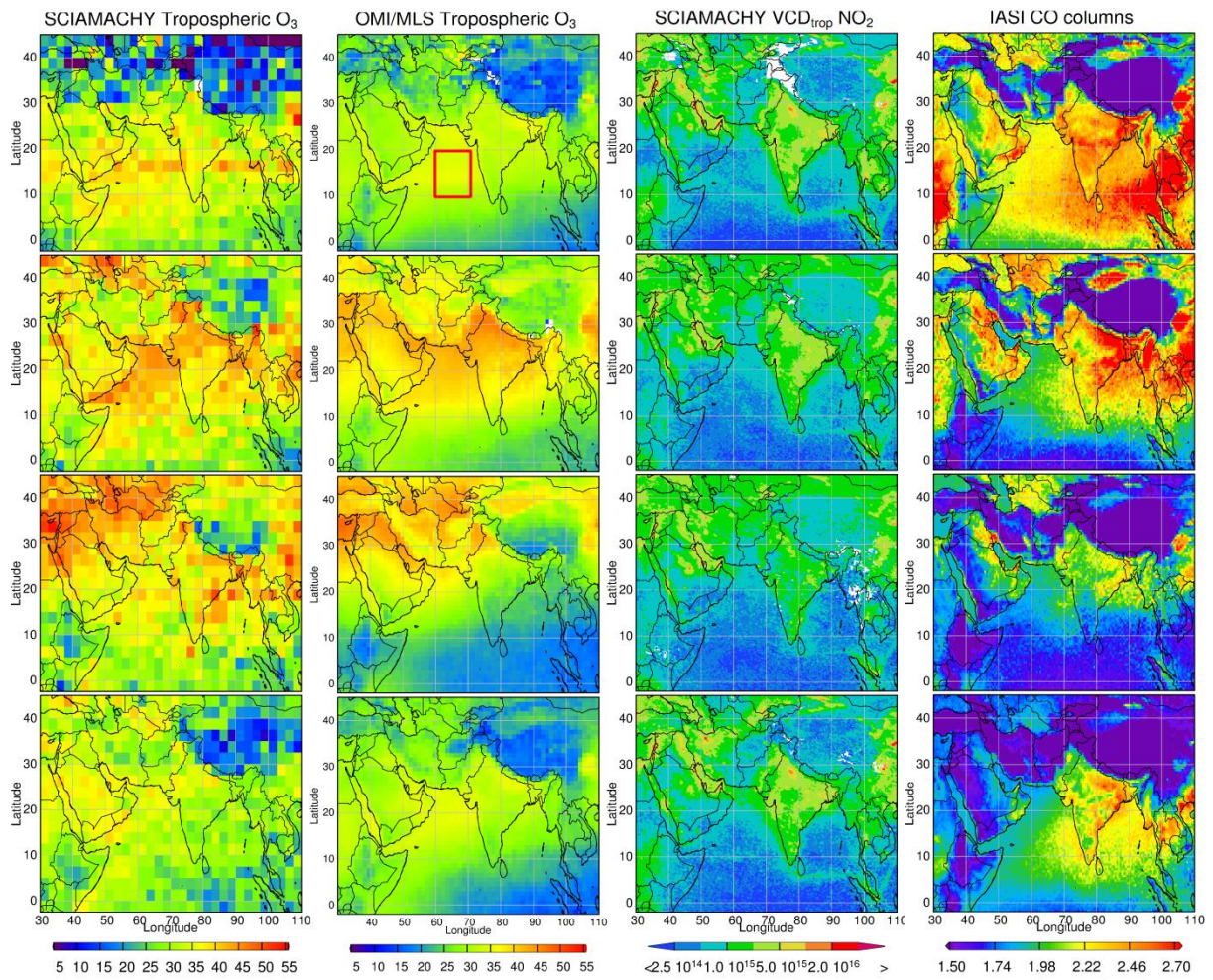
### 8 **3 Observation of a pre-monsoon enhancement in TOC data products**

9 Satellite retrieved TOCs have a better spatial and temporal coverage compared to ozonesonde measurements.  
10 However in situ measurements of ozone from ozonesondes are considered more accurate. Combining the two  
11 types of measurements provides an opportunity to investigate data-sparse regions such as the AS. In comparison  
12 with the studies using ozonesonde and ship measurements, the analysis of the satellite observations of TOCs  
13 regarding AS region is still a gap in the current state. In this section, the satellite observations and the model  
14 results are presented.

15 Figure 2 shows the regional distribution of the TOC and two of its photochemical precursors: NO<sub>2</sub> and CO. Sea-  
16 sonal cycles of TOC, CO and NO<sub>2</sub> over the AS are shown in Fig. 3. A seasonal pattern of TOC is observed in  
17 both OMI/MLS and TES. An offset of ~5 DU exists between the two investigated TOC data products. A maxi-  
18 mum of TOC over AS is observed (~42/47 DU) in every April during the years 2005–2012, followed by mon-  
19 soon/summer minima of ~20 DU. TOC recovers to ~35 DU in the post monsoon autumn but drops down slight-  
20 ly during the winter monsoon. This seasonal pattern is consistent with the results from the sonde station Ahmed-  
21 abad (Fig. 6 in Lal et al., 2014) and depends on the meteorological conditions (Sect. 3.1). [The spring TOC are](#)  
22 [higher over western AS than over eastern AS \(Fig.2\). This distribution is further discussed in Sect. 4.2.](#) The  
23 ozone precursors, CO and NO<sub>2</sub>, show a different behaviour than ozone. As NO<sub>2</sub> has a short lifetime (2-8 hours,  
24 Beirle et al., 2011), the tropospheric NO<sub>2</sub> data products, retrieved from observations of SCIAMACHY or other  
25 related instrumentation in space, show high values over anthropogenic sources and relatively low values, often  
26 below the detection limit, over the remote regions. Over the AS, tropospheric NO<sub>2</sub> columns are small being  
27 around 10<sup>14</sup> molec/cm<sup>2</sup>. This small concentration originates from ship emissions and continental outflow (Rich-  
28 ter et al., 2004). Higher values can be observed during the winter monsoon from transport off the Asian coast.  
29 CO has a longer life time than ozone (~2 months in average for CO and ~23 days for tropospheric ozone, Novel-  
30 li et al., 1998; Young et al., 2013). Due to the relatively long lifetime of CO and ozone, both trace gases show a  
31 similar transport pattern. For instance, the biomass burning plume originating from Southern Africa in boreal  
32 autumn in the Southern Hemisphere can be observed as well for CO as for ozone. However, in comparison to  
33 ozone, which is produced due to the photochemical production, the spatial pattern of CO is known to be more  
34 driven by emissions than dynamical processes (Logan et al., 2008). Thus, the time series of the data products for  
35 tropospheric CO reveal a similar winter maximum as NO<sub>2</sub>, and it also shows a smaller peak in spring time as  
36 TOC. The spring peaks of CO are observed one month earlier than that those of TOC. This shift can be caused  
37 by the combustion emission of CO in Southern Asia (Fig. 6 in Duncan et al., 2003). [The different spatial distri-](#)

1 bution among ozone precursors and ozone indicate a dynamic origin for high TOC over AS from long range  
 2 transport of ozone.

3  
 4  
 5  
 6

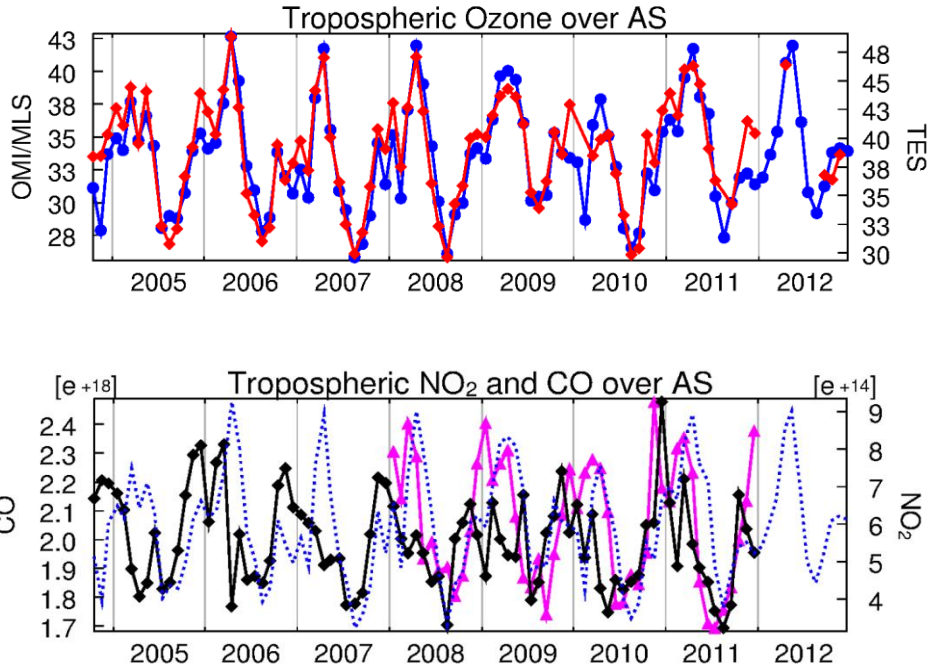


7  
 8 Figure 2. Plots of the TOC, NO<sub>2</sub> (Hilboll et al., 2013) and CO (x10<sup>18</sup>, George et al., 2009) as a function of sea-  
 9 son in 2008. The unit for TOC are DU and that for NO<sub>2</sub> and CO in molec/cm<sup>2</sup>. From top to bottom are DJF (De-  
 10 cember to February), MAM (March to May), JJA (June to August) and SON (September to November).

11  
 12 In this manuscript, MACC reanalysis data is used to provide vertical information of ozone. This choice is moti-  
 13 vated by the fact that OMI and MLS satellite ozone data were actively assimilated in the MACC reanalysis and  
 14 constrain tropospheric ozone (Inness et al., 2013). Figure 4 shows MACC results of ozone partial columns be-  
 15 tween 0 km and the TPH, determined from ECMWF retrieval (Ebojie et al., 2014), and between 0-8 km, respec-  
 16 tively. In a year with no ENSO (El Nino-Southern Oscillation) event in spring, for instance in 2006 (upper pan-  
 17 els of Fig. 4), the enhanced ozone during pre-monsoon is ~30 DU out of ~40 DU (~3/4) originating from the

1 lower troposphere (0-8 km). Because of this result, possible origins will be discussed in the following section  
2 (Sect. 3) by analysing 4 various altitude ranges: 0-4 km, 4-8 km, 8-12 km and 12-18 km.

3



4

5

6 Figure 3. Trace gas time series over AS (10-20°N, 60-70°E) from 2004 to 2012. The blue (solid and dotted)  
7 curves represents OMI/MLS ozone, red is TES ozone, magenta is IASI CO and black stands for SCIAMACHY  
8 NO<sub>2</sub>. The vertical columns are given in DU for ozone and molec/cm<sup>2</sup> for NO<sub>2</sub> and CO. The region used for this  
9 time series calculation is marked with red rectangle in Fig. 2. The time series of TOC from SCIAMACHY,  
10 MACC, OMI.MLS and TES in the year 2008 is presented in appendix Fig. A3.

11

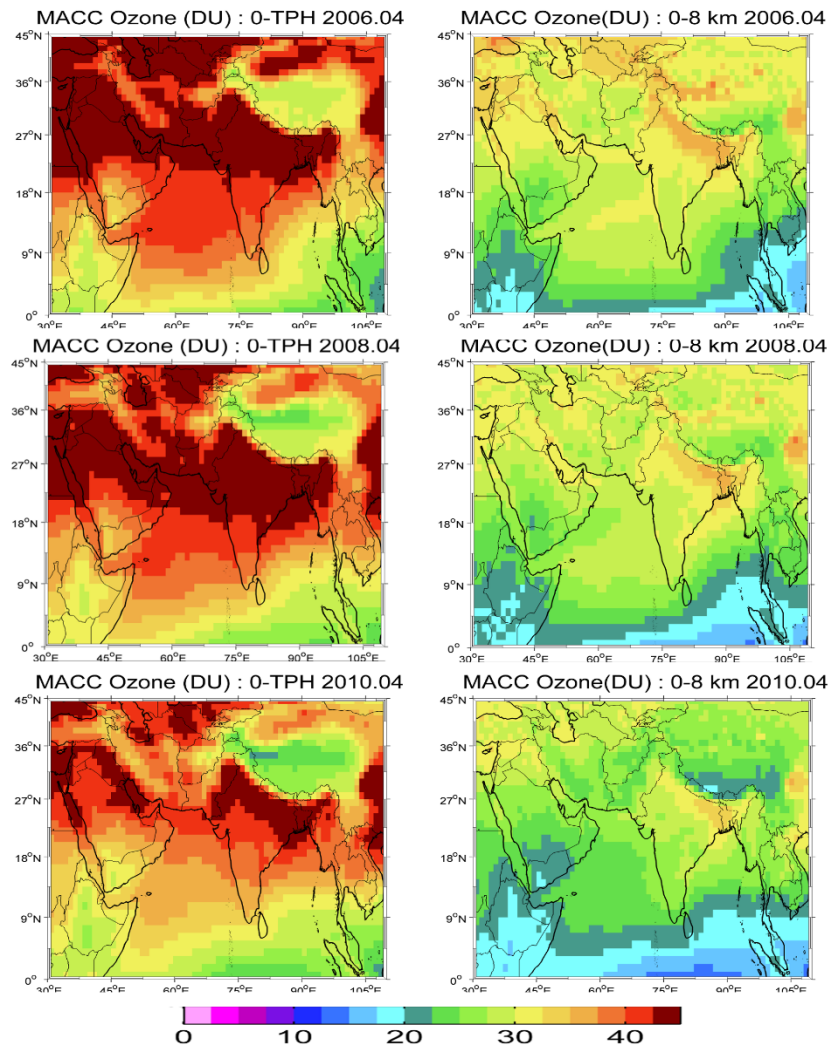
## 12 4 Potential origins of the AS pre-monsoon ozone pool

### 13 4.1 Influences of meteorology

14 The AS region is defined in this study as 10-20°N, 60-70°E on the west side of the sub-continental India. This  
15 location is influenced by the tropical/subtropical air mass exchanges and the sea breeze circulation (e.g., Law-  
16 rence and Lelieveld, 2010). The climate of AS can be divided into 4 different seasons, due to the seasonal varia-  
17 tion of the ITCZ: winter-spring monsoon (Dec-Feb), pre-monsoon transition (Mar-May), summer monsoon  
18 (Jun-Aug), and post-monsoon transition (Sep-Nov). In summer, the ITCZ is at its northernmost position. The  
19 wind appears to be westerly and strong due to the Somali jet (Fig. 5). This condition causes strong precipitation,  
20 higher cloud cover frequency and increased air humidity over AS (David and Nair, 2013). The wind and strong  
21 precipitation 'wash' the air masses and remove soluble pollutants. A summer monsoon minimum for the trace  
22 gases such as shown in Fig. 3 may be expected. The destruction of ozone by reactive halogens is another poten-

1 tial sink for the ozone in the marine boundary layer (Dickerson et al., 1999; Ali et al., 2009). During the pre-  
 2 monsoon transition, surface winds are westerly at the northern AS with an anticyclonic pattern centred over the  
 3 middle AS. At this time, the AS is most of the time cloud-free and dynamically steady. This cloud-free anticy-  
 4 clonic condition possibly causes subsidence of air masses and results in accumulation of pollutants (Sect. 3.2).

5  
6



7

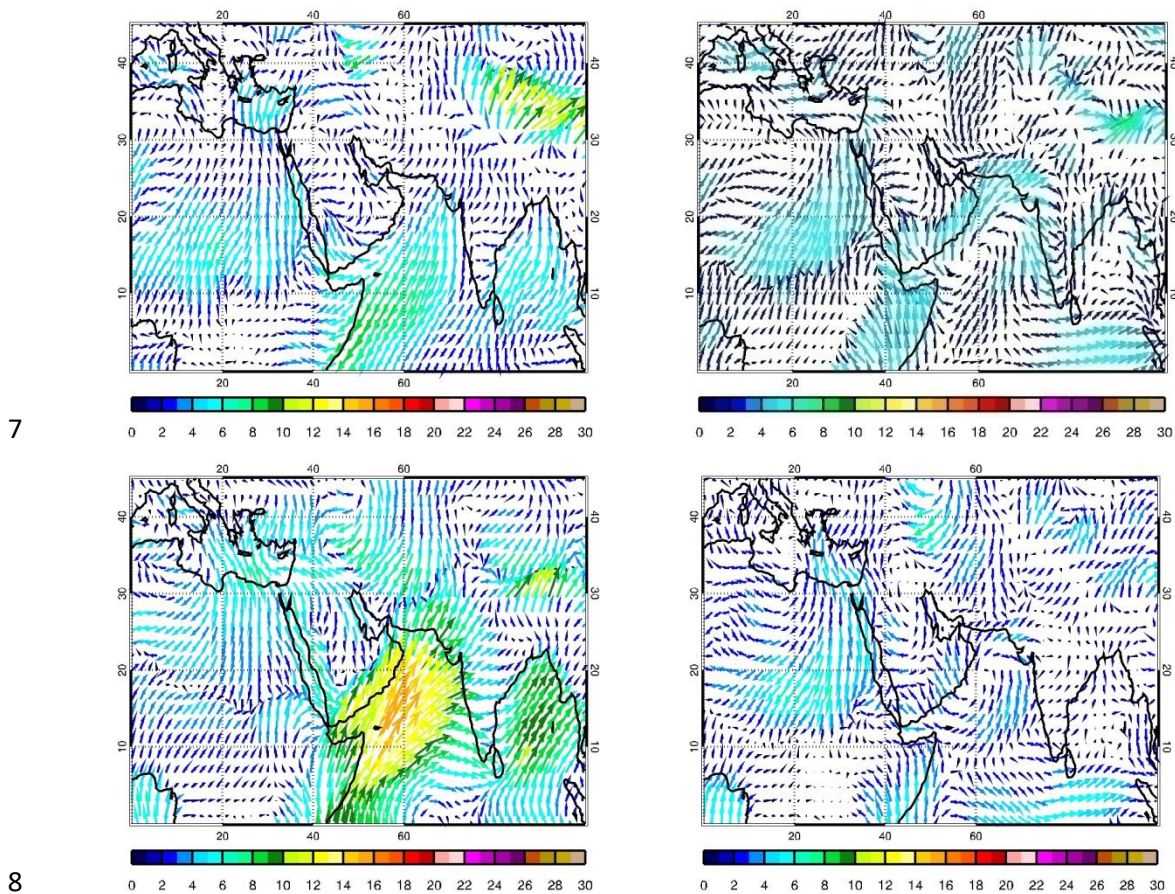
8 Figure 4. Ozone partial columns (TOC: 0km-TPH (~17 km over AS) column of tropospheric ozone in the left  
 9 panels and 0-8 km column of tropospheric ozone in the right panels) from MACC reanalysis model in April  
 10 2006 (upper panels), 2008 (middle panels) and 2010 (lower panels).

11

12 The ITCZ located at the southern part of the AS can become the 'border' that stops the pollutants (in this case,  
 13 tropospheric ozone) diffusing to the Indian ocean with ozone depletion on the surface of cloud droplets in the  
 14 convective region (Lelieveld and Crutzen, 1990).

1 It is worth mentioning that the solar radiation over the AS, unlike in the middle/high latitudes where it is strong-  
2 est in summer, reaches its maximum during pre-monsoon (Weller et al., 1998; David and Nair, 2013). One  
3 could argue that a maximum solar radiation can cause stronger photochemical reactions and thus an increased  
4 ozone concentration. To answer this question, the contribution of the photochemical production will be investi-  
5 gated in Sect. 3.3.

6



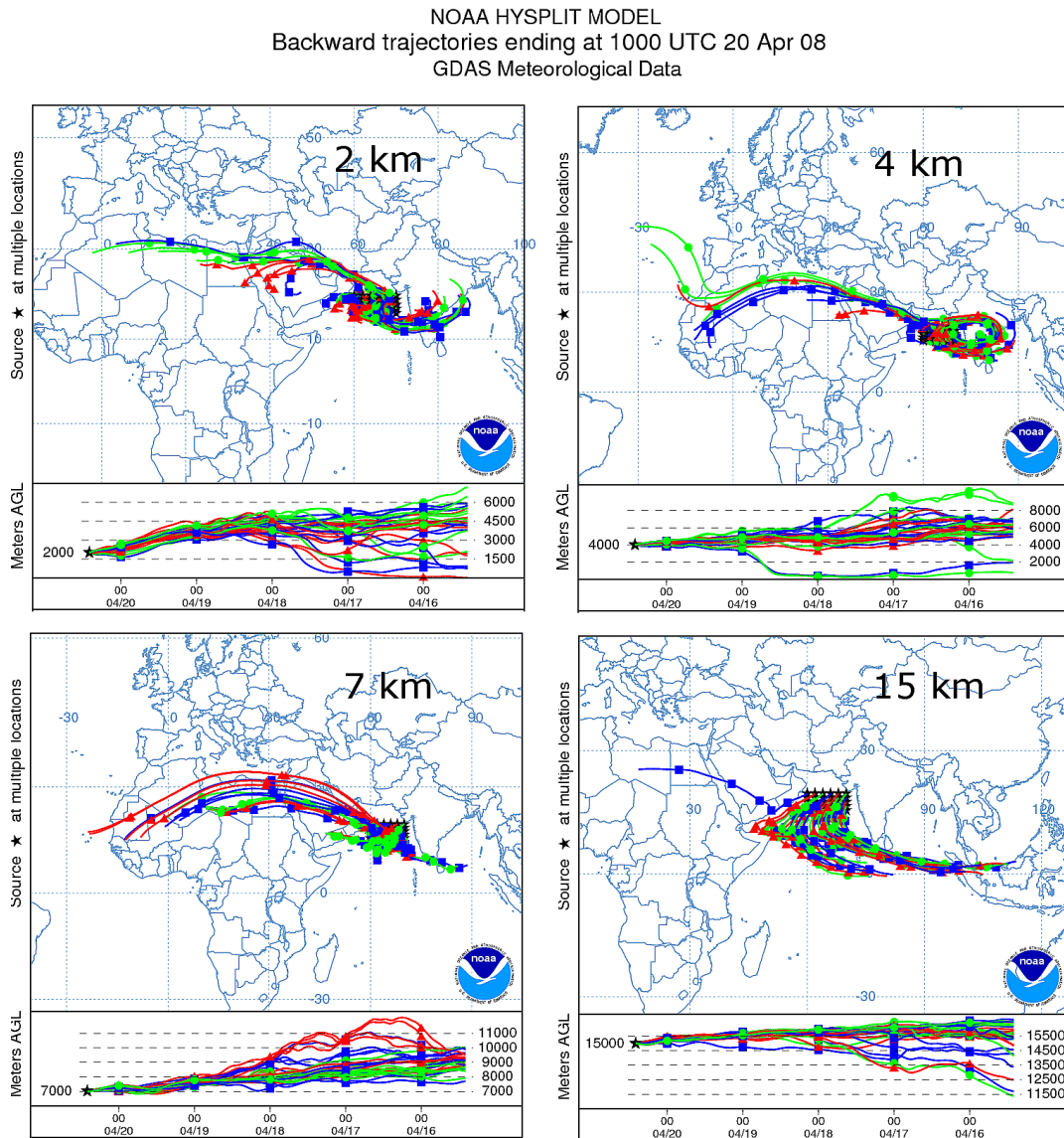
9 Figure 5. 10 meter sea surface wind on January (upper left), April (upper right), July (lower left) and October  
10 (lower right) over AS at 2008 from NCEP (National Center Environmental Prediction). Figure provided by  
11 Anne Blechschmidt from the University of Bremen.

12

#### 13 4.2 Long range transport mechanism and pollutant accumulation

14 It is established in the previous studies that LRT plays an important role in the AS pre-monsoon ozone pool (Lal  
15 and Lawrence, 2001; Chand et al, 2003; Srivastava et al., 2011, 2012; Lal et al., 2013, 2014). ~~For example, the~~  
16 ~~satellite data products for CO and TOC are highly correlated (Fig. 3).~~ Trajectory models are used to investigate  
17 the LRT pathways of the air parcels. Figures 6 and 7 show an example of the HYSPLIT backward and forward  
18 trajectory results for air masses over AS at 2, 4, 7 and 15 km in April 2008. In the lower troposphere (0-8 km),  
19 the sources are identified as the Middle East, India and North Africa, which are consistent with the previous

1 studies. The higher tropospheric ozone (12-18 km) is found in air which was uplifted and transported not only  
 2 from the North Africa, but also from the North Indian Ocean and Southeast Asia. The air masses in the lower  
 3 troposphere subside 4-5 km locally within a high pressure system within 10 days. This confirms the conclusion  
 4 on accumulation of pollutant which was derived from the wind field information in Sect. 3.1 (see Fig. 5). This  
 5 theory was also proved by Srivastava et al. (2011) from the TPSCF (Total Potential Source Contribution Func-  
 6 tion) results. One explanation for the larger TOC over the AS in comparison to surrounded regions is the lower  
 7 humidity which provides less favorable con-



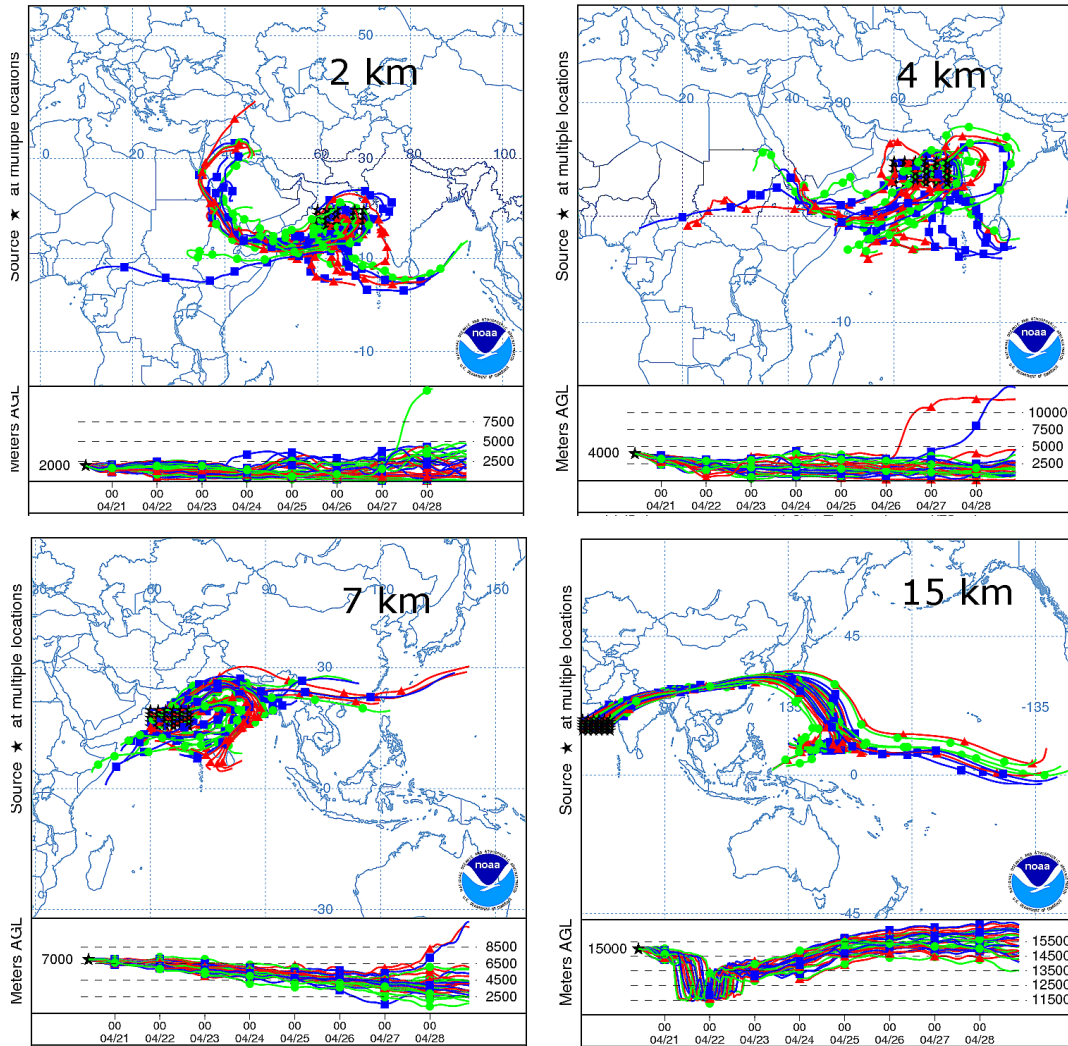
8  
 9 Figure 6. HYSPLIT trajectory 120 hr backward model results for air masses at AS with source location at 2, 4, 7  
 10 and 15 km.

11  
 12 dition for ozone depletion by Hydroxyl radicals (OH) (Fig. 12). This is further discussed in Sect. 3.3. In addition  
 13 to the sources, here we also investigate the areas that are influenced by the AS ozone pool (Fig. 7). The ozone-  
 14 rich air over the AS is transported back to India (lower left panel). HYSPLIT also simulates transport to the Red

1 Sea through the Gulf of Aden in the lower troposphere (upper panels), which is expected because of the moun-  
 2 tains aside acting as a barrier for pollution transport. The elevated tropospheric air masses are also transported  
 3 towards the Pacific Ocean via China (lower right panel).

4 To quantify contributions to LRT from different source locations, the tagged tracer simulation with MOZART-4

NOAA HYSPLIT MODEL  
 Forward trajectories starting at 1000 UTC 20 Apr 08  
 GDAS Meteorological Data

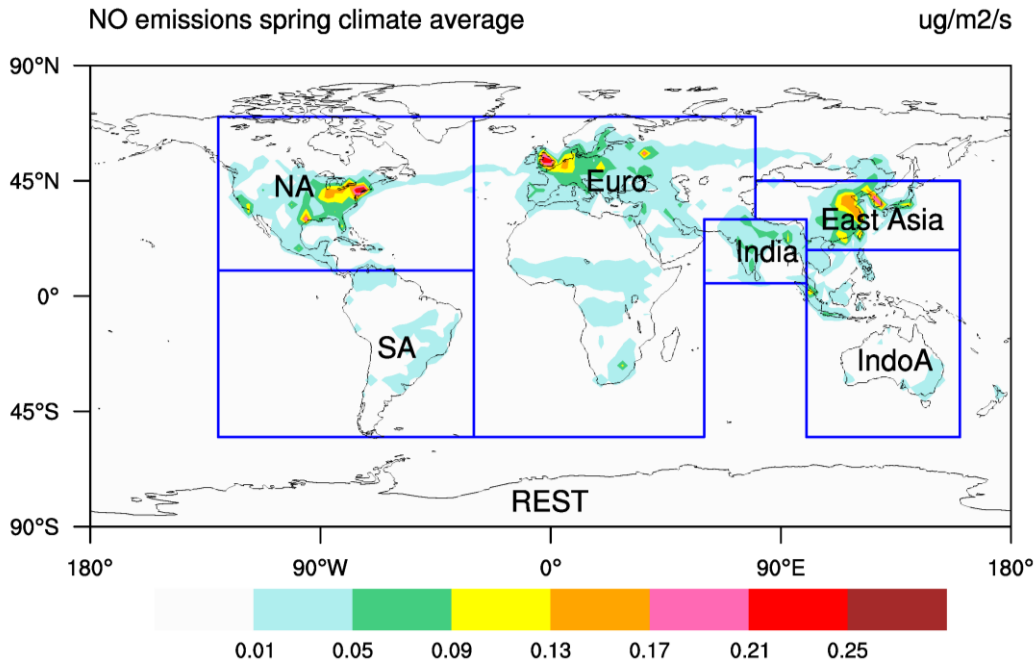


5  
 6 Figure 7. HYSPLIT trajectory 240 hr forward model results for air masses at AS with source location at 2, 4, 7  
 7 and 15 km.

8  
 9 CTM (Sudo and Akimoto, 2007; Hou et al., 2014) during 1997-2007 was used. Figure 8 shows the seven tagged  
 10 regions. Europe, Africa and the Middle East are combined into one hot spot as the closer western region (named  
 11 'Euro'). India, Bay of Bengal and AS are presented together as the closer eastern region (named 'India'). Note  
 12 that when evaluating the contribution from this region, the influence from pollutant accumulation over the AS  
 13 should always be considered. The Indian Ocean is included in the 'Rest' region. 'NA' and 'SA' represent North  
 14 America and South America respectively. The selected names are rather symbolic and do not pretend to be geo-



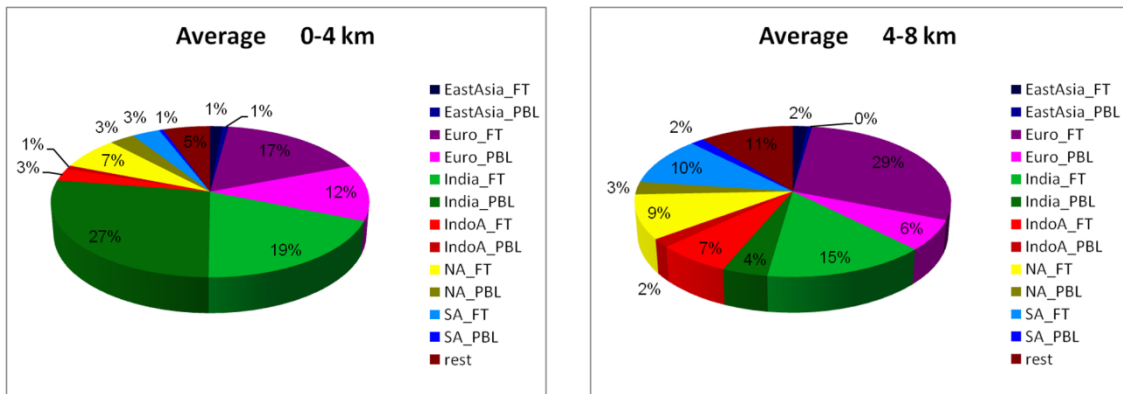
1 graphically fully correct. The regions are divided due to the time consumption of the model calculation. For  
2 further studies, another arrangement can be considered.  
3



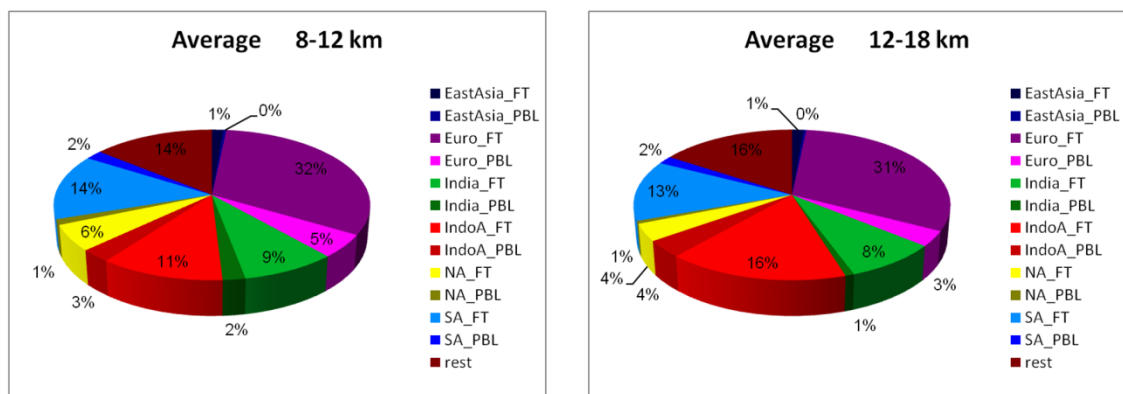
4  
5 Figure 8. Regional separation for tracer tagging with distributions of the spring mean emission rate ( $\mu\text{g}/\text{m}^2/\text{s}$ ) of  
6 NO (including anthropogenic, biomass burning, and soil emissions) at the surface used in the model simulations  
7 during 1997–2007.

8  
9 The source region distribution varies for different altitude ranges (Fig. 9). The percentage contributions from  
10 different regions are calculated by first estimating the ozone concentration (in ppbv) from a separated region  
11 using tagged tracer method (Sudo and Akimoto, 2007), then dividing this value by the sum of ozone concentra-  
12 tions. In the 0-4 km layer, ~30% of the transported ozone comes from the 'Euro' region. The 'India' region is the  
13 biggest source region that contributes 50%, of which 60% comes from the boundary layer. In the 4-8 km layer,  
14 the influences of the boundary layers are much smaller, while 'Euro\_FT' contributes ~10% more than to the 0-4  
15 km layer. The far-away source regions ('NA', 'SA' and 'IndoA') become non-negligible (~10% each). The contri-  
16 bution from 'IndoA' increases with height. Since the Indian Ocean is included, an increased contribution from  
17 'Rest' with altitude is expected. In conclusion, the main contributor to LRT is 'Euro\_FT' with 30% contribution  
18 in average, followed by the 'India' region with over 20% contribution. Since 'Euro\_FT' is the major source of  
19 TOC over AS, higher TOCs are observed over the western AS that is close to Southwest Asia, i.e., Oman, Yem-  
20 en, Pakistan, etc., instead of the eastern AS near west coast of India. The inputs from far-away source regions  
21 are similar, with ~10% each. The influence from East Asia is negligible. Note that the air masses in the higher  
22 altitudes are normally quickly removed by the strong advection (Fig. 10). The contributors in the lower altitudes  
23 (<12 km) have more influences on the ozone accumulation.

1



2



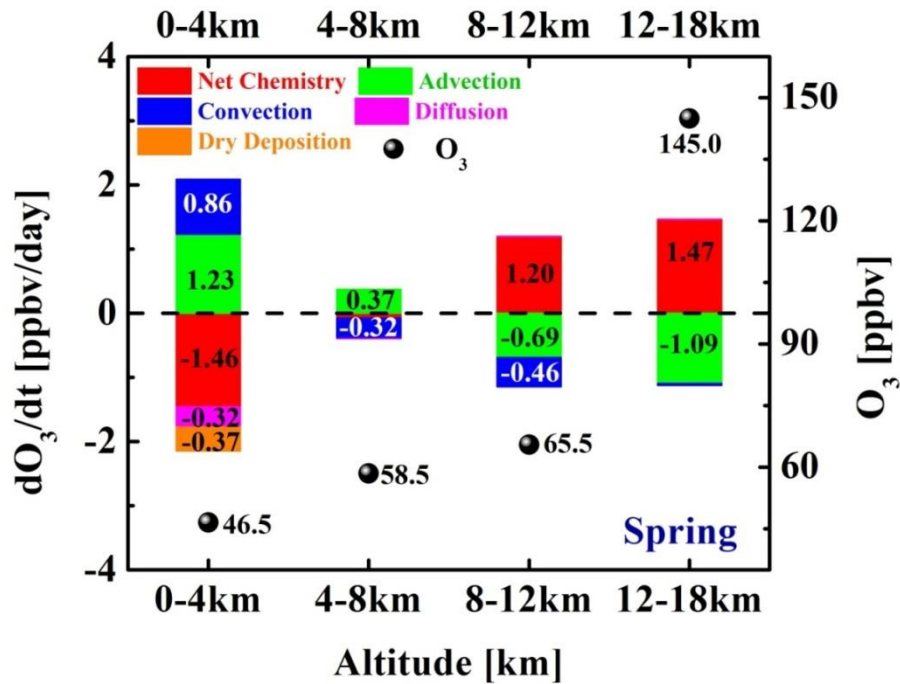
3

4 Figure 9. Averaged LRT contributions to the AS tropospheric ozone concentration from different source regions  
 5 to 4 atmospheric layers over the AS in April 1997-2007. PBL (planetary boundary layer) is defined as the region  
 6 from surface to the top of the boundary layer. FT (free troposphere) is defined as extending to the tropopause  
 7 above the BL.

### 8 4.3 Local chemistry

9 This section addresses two questions: (1), What is the role of the photochemistry for TOC above AS? (2), Is  
 10 more ozone been photochemically produced during the long accumulation time in the middle (4-8 km) or lower  
 11 (0-4 km) troposphere?

12 The ozone budget is calculated in the MOZART-4 model (Fig. 10) within the 1997-2007 time periods. Photo-  
 13 chemistry plays a very different role in the four altitude ranges. In the 0-4 km layer, water vapour acts as a  
 14 source of OH radicals and depletes ozone. Compared to the photochemical production, this depletion process  
 15 dominates (Nair et al., 2011). Thus a net outflow of ozone in chemistry was observed. In the higher layers (8-12  
 16 km, 12-18 km), photochemical production becomes a major source of ozone, while advection being the major



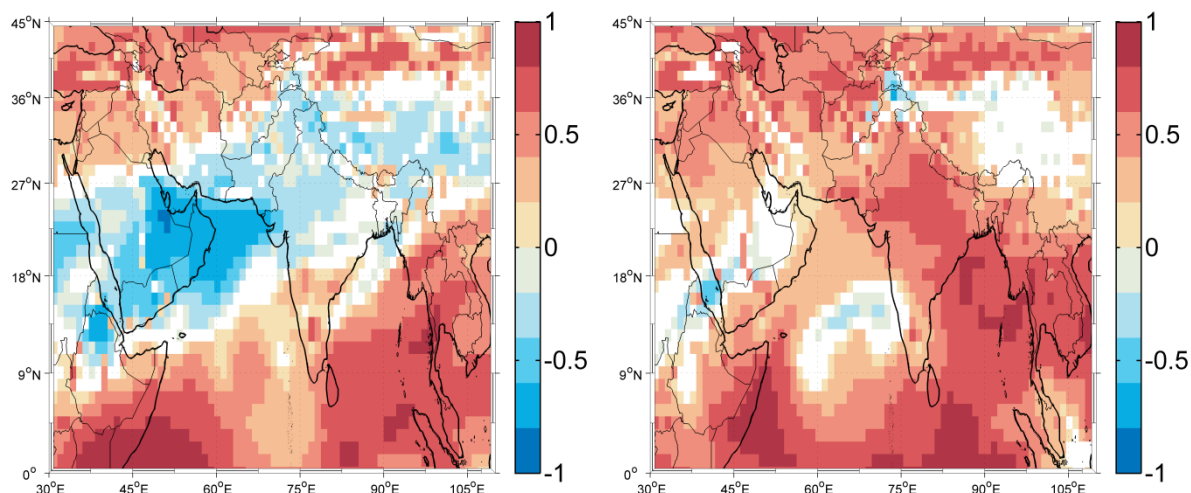
1

2 Figure 10. Averaged ozone budget in pre-monsoon from MOZART-4 at four layers over AS region. The ozone  
 3 partial column volumes (ppbv) calculated from MOZART-4 is presented as black dots.

4

5 sink. Zahn et al. (2002) estimated that the annual net ozone production rates over AS are  $17.6 \times 10^{10}$  molecules  
 6  $\text{cm}^{-2} \text{s}^{-1}$ , by using the CARIBIC (Civil Aircraft for the Regular Investigation of the atmosphere Based on an  
 7 Instrumented Container) aircraft data from 10-11 km altitude. However, Livesey et al. (2013) showed in MLS  
 8 data that such maximum of ozone amount around 215 hPa ( $\sim 11$  km) in pre-monsoon season is most likely a  
 9 zonal pattern. In the 4-8 km layer, the budget is rather small with a net inflow by advection. The net chemistry is  
 10 less than  $-0.1$  ppbv per day, indicating a negligible sink.

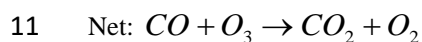
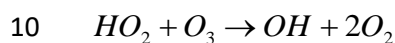
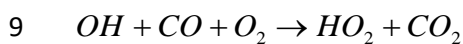
11 The O<sub>3</sub>-CO correlation has been broadly used to indicate tropospheric O<sub>3</sub> sources (Fishman and Seiler, 1983;  
 12 Kim et al., 2013; Inness et al., 2015). A positive O<sub>3</sub>-CO correlation denotes considerable chemical production of  
 13 O<sub>3</sub>. A negative correlation, on the other hand, can originate from chemical O<sub>3</sub> loss or deposition, or can suggest  
 14 that the air mass is either transported from the stratosphere, or moved by advection from the free troposphere.  
 15 Figure 11 shows the O<sub>3</sub>-CO correlation at 4-8 km in April using MACC data. The left panel is a typical correla-  
 16 tion result with strong negative correlations over AS (See also appendix Fig. A1). This correlation suggests that



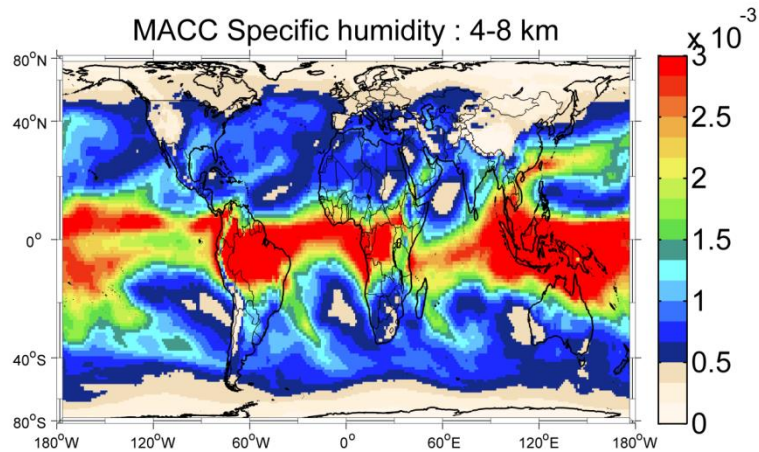
1  
 2 Figure 11.  $O_3$ -CO correlations calculated for 4-8 km column abundances with 3 hr temporal interval in April  
 3 2008 (left panel) and 2006 (right panel) from MACC reanalysis data.

4  
 5 a chemical production of ozone is most likely not the cause for the observed ozone enhancement. Some ozone  
 6 production is expected (e.g., year 2006 in the right panel), but this kind of situation is rare.

7 The averaged specific humidity in-between 4-8 km was used to investigate evidence for the impact of  $HO_x$  re-  
 8 moval on ozone in clean air conditions (Fig. 12):



12 Unlike the humid lowest troposphere, the air masses over the AS at 4-8 km are rather dry compared to the sur-  
 13 roundings. This can be explained by adiabatic lifting and expansion of marine boundary air followed by conden-  
 14 sation and removal for  $H_2O$ . The lifting is stronger over land than over ocean due to the temperature differences.  
 15 This is also one of the reasons that Southeast Asia has strongest convection. The dry air at 4-8 km can lead to a  
 16 smaller depletion contribution from OH radicals, thus it is more suitable for ozone accumulation. Hence, the AS  
 17 ozone columns in the 4-8 km altitude region are expected to be higher than its surroundings.

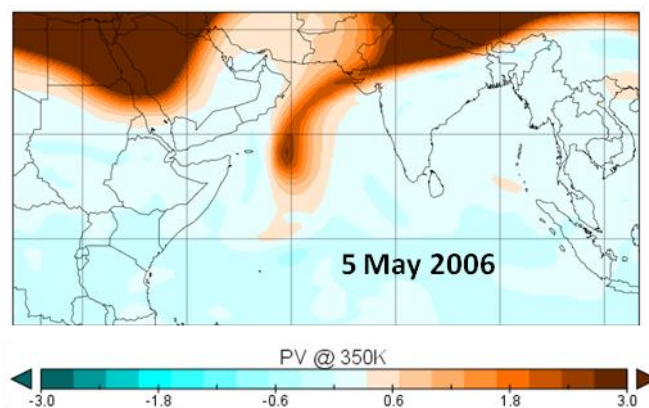


1  
2 Figure 12. Specific humidity (kg/kg) at 4-8 km in April 2006 from MACC reanalysis dataset.

### 3 4.4 Stratosphere-troposphere exchange

4 The STE is not the focus of this study, thus is only briefly mentioned here. The ozone concentrations in the ex-  
 5 tra-tropical lower stratosphere show a maximum in late winter/early spring as driven by the Brewer-Dobson  
 6 circulation (e.g., Fortuin and Kelder, 1998; IPCC/TEAP, 2005). Fadnavis et al (2010) indicated ozone strato-  
 7 spheric intrusion during winter and pre-monsoon season over the Indian region (5-40°N, 65-100°E) by using  
 8 both satellite and model data. One stratospheric intrusion was observed over AS during the ICARB campaign  
 9 (Lal et al., 2013) in 5 May 2006 (Fig. 13). However, it is not clear yet how much and how deep the influence  
 10 can be. In our study, the STE contribution simulated by MOZART-4 tagged tracer method is comparable with  
 11 the ones transported from 'Euro\_FT' in most each altitude ranges (STE to 'Euro\_FT' contributions are 0.955 at 0-  
 12 4 km, 0.861 at 4-8 km, 0.997 at 8-12 km, and 16.858 at 12-18 km). The STE origin might be a reason for the  
 13 strong negative O<sub>3</sub>-CO correlation since the chemical loss and deposition are excluded (Sect. 3.3).

14



15  
16 Figure 13. Potential Vorticity from ECMWF.

17

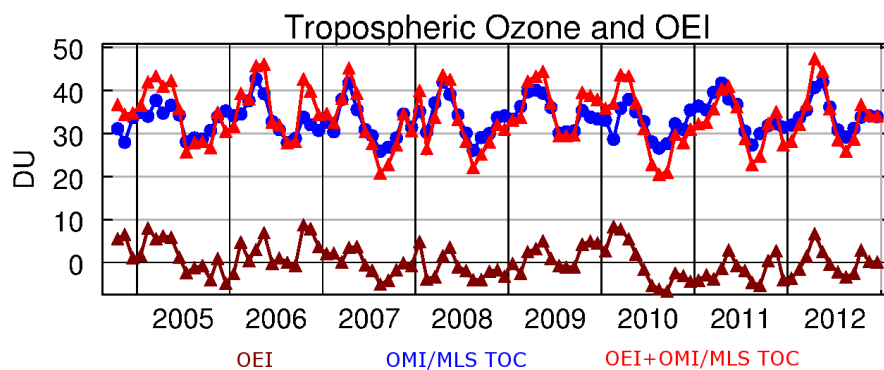
## 1 5 ENSO and Interannual variation

2 Two spring anomalies are depicted in 2005 and 2010 where ozone is ~5 DU lower compared to other years (up-  
3 per panel of Fig. 3). The decrease in 2010 is most likely to be the anomaly of the lower troposphere ozone as  
4 observed in Fig. 4. The two following facts suggest the anomaly to be dynamical: (1), the ozone reduced in a  
5 similar amount at continental surroundings; (2), similar to ozone, a lower CO maximum appeared in 2010 (low-  
6 er panel of Fig. 3).

7 The El Niño events, as driven by a reversal of the Walker Circulation, affect the temperature, humidity and bio-  
8 mass burning emissions, thus influence the trace gases including ozone. Particularly, the tropospheric ozone  
9 anomaly related to the El Niño event during the year 1997-1998 was intensively studied (e.g. Chandra et al.,  
10 1998; Sudo and Takahashi, 2001). The tropospheric ozone increased (up to 25 DU in the burning season) over  
11 the equatorial western Pacific due to a reduced convection and growing burning emissions, whereas decreased  
12 (4-8 DU) over the eastern Pacific because of the change in meteorological conditions. By using a model simula-  
13 tion, Zeng and Pyle (2005) reported that the tropospheric ozone concentration at specifically the equatorial re-  
14 gion 40-70°E decreases with similar amount as over the eastern Pacific during El Niño events. Ziemke et al.  
15 (2010) showed that the ENSO related response of tropospheric ozone over the western and eastern Pacific dom-  
16 inated interannual variability. An Ozone ENSO Index (OEI) was formed to represent the ENSO impact. The  
17 OEI was calculated by subtracting the eastern and central tropical Pacific region tropospheric ozone (15°S-15°N,  
18 110-180°W) from the western tropical Pacific-Indian Ocean region (15°S-15°N, 70-140°E) with the fact that the  
19 zonal variability of tropic stratospheric ozone is only ~1 DU.

20 Figure 14 shows the OEI index that is produced from OMI/MLS data for the related time period (dark red curve).  
21 A 'correction' of OMI/MLS TOCs over the AS by adding the OEI index is performed. The ozone spring maxima  
22 anomalies at pre-monsoon season in 2005 and 2010 (blue curve) can no more be seen after the 'correction'. This  
23 indicates that the El Niño induced dynamics might contribute to the interannual variability over pre-monsoon  
24 AS ozone. Since OEI contains both chemical (fire) and dynamical influences in the burning season, ozone peaks  
25 (in the red curve) can be observed in the winter of 2006 and 2009 when strong fires happened in Indonesia.

26



27

28 Figure 14. Time series of tropospheric ozone columns 'corrected' with OEI over AS (10-20°N, 60-70°E) from  
29 2004 to 2012. The blue curve represents OMI/MLS TOCs, dark red is OEI calculated from OMI/MLS and red  
30 stands for OMI/MLS TOCs with OEI 'correction'.

1

2 The dynamical influence of El Niño can be found in two aspects. El Niño can induce an increase of Sea Surface  
3 Temperature (SST) thus strengthens the water vapor upwelling to the middle troposphere, and then reduces the  
4 life time of ozone. It also possibly triggers changes in STE flux as mentioned by e.g. Neu et al. (2014). Moist  
5 air masses are observed from MACC reanalysis data in April 2010 (appendix Fig. A2). This confirms the as-  
6 sumption of the SST influence over AS. A STE flux variation can be caused by both El Niño and La Niña  
7 events. In this case La Niña events (in 2011) didn't contribute as much as El Niño events (in 2005 and 2010).  
8 The impact of El Niño is mainly expressed by the SST anomaly instead of the STE anomaly.

9

## 10 **6 Conclusions**

11 The 7 years composite averaged values for TOC presented over AS exhibit a seasonal pattern and have values  
12 similar to those in the Southern hemispheric biomass burning plume. A disciplined tropospheric ozone seasonal-  
13 ity with a ~42 DU maximum at the pre-monsoon season was shown in the satellite based OMI/MLS and TES  
14 observations as well as in the MACC reanalysis model. The seasonal feature is found to be strongly related to  
15 the meteorological conditions.

16 Previous studies illustrated the importance of LRT to the pre-monsoon ozone enhancement and confirmed the  
17 source locations to be the Middle East, West India, Africa, North America and Europe. Here various regional  
18 contributions to the AS pre-monsoon ozone through LRT were analysed by dividing the global range into 7 re-  
19 gions using the MOZART-4 tagging tracer simulation method. In the lowest 4 km, the sources from India con-  
20 tributed ~50% of the transported AS ozone amount. The free troposphere of the Middle East, Africa and Europe  
21 (so called 'Euro\_FT') started to play a major role from 4 km altitude and higher. The contribution is on average  
22 30%. The Indian region is still the second important source region at 4-8 km with ~20%. Its contribution is  
23 slowly replaced by the further-away source regions at higher altitude range. It is worth mentioning that South  
24 America plays a more important role compared to North America, yet there is no explanation for this result so  
25 far.

26 In addition, the vertical pollutant accumulation in the lower troposphere, especially at 4-8 km, is important to  
27 the AS spring ozone pool. The suitable meteorological conditions were discovered from wind field data from  
28 NECP and specific humidity data from MACC. First, the cloud-free anticyclonic condition that is observed from  
29 the wind field data can cause air to be transported upside down. This point is supported by the forward model  
30 results of HYSPLIT showing that at ~7/8 km or lower, the air circles down over the AS region for around 10  
31 days without diffusion. Second, at 4-8 km the air over AS is much dryer than the surroundings. This is most  
32 probably due to relatively lower temperature over the sea which caused that the moisture cannot be lifted up as  
33 high as over land. The dry conditions induce the accumulation of ozone with a longer life time thus cause the  
34 AS ozone to be outstanding from the sub continental regions.

35 The averaged spring ozone budget was calculated using MOZART-4 to improve our understanding of the addi-  
36 tional local chemical activity. Ozone is photochemically produced at high altitudes (8-18 km) and is removed by  
37 advection. In the lowest 4 km ozone is depleted by OH radicals. Positive ozone budgets from advection and  
38 convection can be observed, which supported the LRT and accumulation mechanisms. At 4-8 km, despite the

1 weak ozone destruction from OH radicals, the net chemical budget is negligible. This suggests a low photo-  
2 chemical production, which is also supported by the negative O<sub>3</sub>-CO correlation. According to the simulation  
3 results and the O<sub>3</sub>-CO correlation, a net contribution from STE can also influence the local ozone amount.

4 The two spring ozone interannual anomalies are believed to be influenced by the dynamical variations (SST  
5 anomaly) during the El Niño events. The climate interacts with the distribution of tropospheric ozone through  
6 temperature, humidity and dynamics.

7

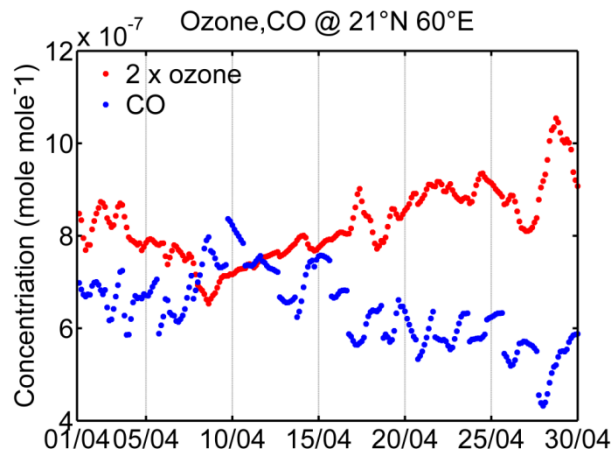
## 8 **Acknowledgements**

9 We would like to thank the SCIAMACHY LNM NO<sub>2</sub>, OMI/MLS, TES tropospheric ozone, IASI CO and teams  
10 for providing the data. We acknowledge the two working staffs on MACC reanalysis, NCEP, and MOZART-4.  
11 Jia Jia acknowledges funding by CSC (China Scholarship Council) and scientific support from ESSReS (Earth  
12 System Science Research School). We also acknowledge financial support provided by the University and State  
13 of Bremen. We would like to thank Anne-Marlene Blechschmidt for her help . Our gratitude goes to Prof. Chris-  
14 tian von Savigny for giving comments during the preparation of the manuscript. The authors acknowledge the  
15 North-German Supercomputing Alliance (HLRN) for providing HPC resources that have contributed to the re-  
16 search results reported in this paper.

17



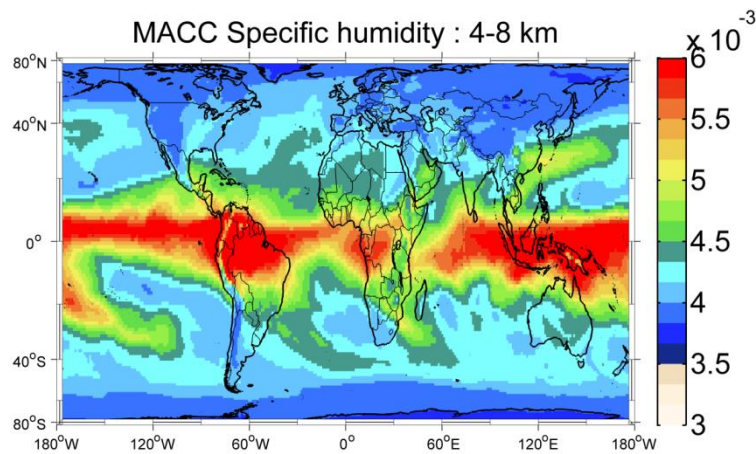
1 **Appendix**



2

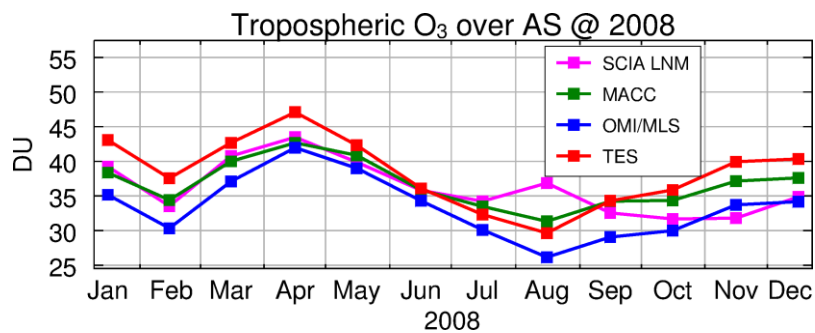
3 Figure A1. O<sub>3</sub> and CO partial column (4-8 km) time series at 21°N, 60°E over AS at April 2008 from MACC  
 4 reanalysis data. The plot is a 'point' example of Fig. 10.

5



6

7 Figure A2. Same as Fig. 12 but for the year 2010.



8

9 Figure A3. TOCs results over AS from SCIAMACHY Limb-Nadir-Matching, OMI/MLS, TES, and MACC  
 10 reanalysis data sets in 2008.

## 1 **References**

- 2 Ali, K., Beig, G., Chate, D. M., Momin, G. A., Sahu, S. K., and Safai, P. D.: Sink mechanism for significantly  
3 low level of ozone over the Arabian Sea during monsoon, *J. Geophys. Res.*, 114, D17306,  
4 doi:10.1029/2008JD011256, 2009.
- 5 Beer, R.: TES on the Aura mission: Scientific objectives, measurements, and analysis overview. *IEEE T. Geosci.*  
6 *Remote*, 44, 1102 – 1105. 20, 60, 2006.
- 7 Beirle, S., Boersma, K. F., Platt, U., Lawrence, M. G., and Wagner, T.: Megacity emissions and lifetimes of  
8 nitrogen oxides probed from space, *Science*, 333, 1737–1739, doi:10.1126/science.1207824, 2011.
- 9 Bovensmann, H., Burrows, J. P., Buchwitz, M., Frerick, J., Noël, S., Rozanov, V. V., Chance, K. V., and Goede,  
10 A. P. H.: SCIAMACHY: mission objectives and measurement modes. *J. Atmos. Sci.*, 56, 127–150, 1999.
- 11 Burrows, J. P., Hölzle, E., Goede, A., Visser, H., and Fricke, W.: SCIAMACHY – scanning imaging absorption  
12 spectrometer for atmospheric cartography, *Acta Astronaut.*, 35, 445–451, 1995.
- 13 Chand, D., Lal, S., and Naja, M.: Variations of ozone in the marine boundary layer over the Arabian Sea and the  
14 Indian Ocean during the 1998 and 1999 INDOEX campaigns, *J. Geophys. Res.*, 108, 4190,  
15 doi:10.1029/2001JD001589, 2003.
- 16 Chandra, S., Ziemke, J. R., Min, W., and Read, W. G.: Effects of 1997–1998 El Niño on tropospheric ozone.  
17 *Geophys. Res. Lett.*, 25, 3867–3870, 1998.
- 18 David, L. M. and Nair, P. R.: Tropospheric column O<sub>3</sub> and NO<sub>2</sub> over the Indian region observed by Ozone Mon-  
19 itoring Instrument (OMI): seasonal changes and long-term trends, *Atmos. Environ.*, 65, 25–39,  
20 doi:10.1016/j.atmosenv.2012.09.033, 2013.
- 21 Dickerson, R. R., Rhoads, K. P., Carsey, T. P., Oltmans, S. J., Burrows, J. P., and Crutzen, P. J.: Ozone in the  
22 remote marine boundary layer: a possible role for halogens, *J. Geophys. Res.*, 104, 21385–21395, 1999.
- 23 Duncan, B. N., Martin, R. V., Staudt, A. C., Yevich, R., and Logan, J. A.: Interannual and seasonal variability of  
24 biomass burning emissions constrained by satellite observations, *J. Geophys. Res.*, 108(D2), 4100,  
25 doi:10.1029/2002JD002378, 2003.
- 26 Ebojje, F., von Savigny, C., Ladstätter-Weißmayer, A., Rozanov, A., Weber, M., Eichmann, K.-U., Bötzel, S.,  
27 Rahpoe, N., Bovensmann, H., and Burrows, J. P.: Tropospheric column amount of ozone retrieved from SCI-  
28 AMACHY limb–nadir-matching observations, *Atmos. Meas. Tech.*, 7, 2073–2096, doi:10.5194/amt-7-2073-  
29 2014, 2014.
- 30 Emmons, L. K., Walters, S., Hess, P. G., Lamarque, J.-F., Pfister, G. G., Fillmore, D., Granier, C., Guenther, A.,  
31 Kinnison, D., Laepple, T., Orlando, J., Tie, X., Tyndall, G., Wiedinmyer, C., Baughcum, S. L., and Kloster, S.:  
32 Description and evaluation of the Model for Ozone and Related chemical Tracers, version 4 (MOZART-4), *Ge-*  
33 *osci. Model Dev.*, 3, 43–67, doi:10.5194/gmd-3-43-2010, 2010.
- 34 Fadnavis, S., Chakraborty, T., and Beig, G.: Seasonal stratospheric intrusion of ozone in the upper troposphere  
35 over India, *Ann. Geophys.*, 28, 2149–2159, doi:10.5194/angeo-28-2149-2010, 2010.

1 Fishman, J. and Seiler, W.: Correlative nature of ozone and carbon monoxide in the troposphere: Implications  
2 for the tropospheric ozone budget, *J. Geophys. Res.*, 88, 3662–3670, doi:10.1029/JC088iC06p03662, 1983.

3 Fishman, J., P. Minnis, and H. G. Reichle, Jr., The use of satellite data to study tropospheric ozone in the trop-  
4 ics, *J. Geophys. Res.*, 91, 14,451-14,465, 1986.

5 Fishman, J., Fakhruzzaman, K., Cros, B., and Nganga, D.: Identification of widespread pollution in the  
6 Southern Hemisphere deduced from satellite analyses, *Science*, 252, 1693–1696, 1991.

7 Fortuin, J. P. F., and Kelder, H.: An ozone climatology based on ozonesonde and satellite measurements, *J. Ge-  
8 ophys. Res.*, 103(D24), 31,709 – 31,734, 1998.

9 George, M., Clerbaux, C., Hurtmans, D., Turquety, S., Coheur, P.-F., Pommier, M., Hadji-Lazaro, J., Edwards,  
10 D.P., Worden, H., Luo, M., Rinsland, C., and McMillan, W.: Carbon monoxide distributions from the  
11 IASI/METOP mission: evaluation with other space-borne remote sensors, *Atmos. Chem. Phys.*, 9, 8317-8330,  
12 2009

13 Hilboll, A., Richter, A., and Burrows, J. P.: Long-term changes of tropospheric NO<sub>2</sub> over megacities derived  
14 from multiple satellite instruments, *Atmos. Chem. Phys.*, 13, 4145-4169, doi:10.5194/acp-13-4145-2013, 2013.

15 Holton, J.R., Haynes, P.H., McIntyre, M.E., Douglass, A.R., Rood, R.B., Pfister, L.: Stratosphere-troposphere  
16 exchange, *Reviews of Geophysics* 33, 403-439, 1995.

17 Hou, X., Zhu, B., Kang, H., and Gao, J.: Analysis of seasonal ozone budget and spring ozone latitudinal gradient  
18 variation in the boundary layer of the Asia-Pacific region, *Atmos. Environ.*, 94, 734–741,  
19 doi:10.1016/j.atmosenv.2014.06.006, 2014.

20 Inness, A., Baier, F., Benedetti, A., Bouarar, I., Chabrillat, S., Clark, H., Clerbaux, C., Coheur, P., Engelen, R. J.,  
21 Errera, Q., Flemming, J., George, M., Granier, C., Hadji-Lazaro, J., Huijnen, V., Hurtmans, D., Jones, L., Kaiser,  
22 J. W., Kapsomenakis, J., Lefever, K., Leitão, J., Razinger, M., Richter, A., Schultz, M. G., Simmons, A. J., Sut-  
23 tie, M., Stein, O., Thépaut, J.-N., Thouret, V., Vrekoussis, M., Zerefos, C., and the MACC team: The MACC  
24 reanalysis: an 8 yr data set of atmospheric composition, *Atmos. Chem. Phys.*, 13, 4073-4109, doi:10.5194/acp-  
25 13-4073-2013, 2013.

26 Inness, A., Benedetti, A., Flemming, J., Huijnen, V., Kaiser, J. W., Parrington, M., and Remy, S.: The ENSO  
27 signal in atmospheric composition fields: emission-driven versus dynamically induced changes, *Atmos. Chem.  
28 Phys.*, 15, 9083-9097, doi:10.5194/acp-15-9083-2015, 2015.

29 IPCC/TEAP, Bert Metz, Lambert Kuijpers, Susan Solomon, Stephen O. Andersen, Ogunlade Davidson, José  
30 Pons, David de Jager, Tahl Kestin, Martin Manning, and Leo Meyer (Eds), Cambridge University Press, UK. pp  
31 478, 2005.

32 Jia, J.: Improvement and interpretation of the tropospheric ozone columns retrieved based on SCIAMACHY  
33 Limb-Nadir Matching approach, PhD thesis, <http://nbn-resolving.de/urn:nbn:de:gbv:46-00105374-15>, Universi-  
34 ty of Bremen, Bremen, Germany, 2016.

1 Kim, P. S., Jacob, D. J., Liu, X., Warner, J. X., Yang, K., Chance, K., Thouret, V., and Nedelec, P.: Global  
2 ozone–CO correlations from OMI and AIRS: constraints on tropospheric ozone sources, *Atmos. Chem. Phys.*,  
3 13, 9321–9335, doi:10.5194/acp-13-9321-2013, 2013.

4 Lal, S., and Lawrence, M. G.: Elevated mixing ratios of surface ozone over the Arabian Sea, *Geophys. Res.  
5 Lett.*, 28(8), 1487–1490, doi:10.1029/2000GL011828, 2001.

6 Lal, S., Venkataramani, S., Srivastava, S., Gupta, S., Mallik, C., Naja, M., Sarangi, T., Acharya, Y. B., and Liu,  
7 X.: Transport effects on the vertical distribution of tropospheric ozone over the tropical marine regions sur-  
8 rounding India, *J. Geophys. Res. Atmos.*, 118, 1513–1524, doi:10.1002/jgrd.50180, 2013.

9 Lal, S., Venkataramani, S., Chandra, N., Cooper, O. R., Brioude, J., and Naja, M.: Transport effects on the ver-  
10 tical distribution of tropospheric ozone over western India, *J. Geophys. Res. Atmos.*, 119, 10012–10026,  
11 doi:10.1002/2014JD021854, 2014.

12 Lawrence, M. G. and Lelieveld, J.: Atmospheric pollutant outflow from southern Asia: a review, *Atmos. Chem.  
13 Phys.*, 10, 11017–11096, doi:10.5194/acp-10-11017-2010, 2010.

14 Lelieveld, J. and Crutzen, P. J.: Influences of cloud photochemical processes on tropospheric ozone, *Nature*, 343,  
15 227–233, 1990.

16 Levelt, P. F., van den Oord, G. H. J., Dobber, M. R., Mälkki, A., Visser, H., de Vries, J., Stammes, P., Lundell,  
17 J., and Saari, H.: The Ozone Monitoring Instrument (OMI). *IEEE T. Geosci. Remote*, 44(5), 1093–1101. 16, 20,  
18 2006.

19 Livesey, N. J., Logan, J. A., Santee, M. L., Waters, J. W., Doherty, R. M., Read, W. G., Froidevaux, L., and  
20 Jiang, J. H.: Interrelated variations of O<sub>3</sub>, CO and deep convection in the tropical/subtropical upper troposphere  
21 observed by the Aura Microwave Limb Sounder (MLS) during 2004–2011, *Atmos. Chem. Phys.*, 13, 579–598,  
22 doi:10.5194/acp-13-579-2013, 2013.

23 Logan, J. Megretskaia, A., Nassar, I., R., Murray, L. T., Zhang, L., Bowman, K. W., Worden, H. M., and Luo,  
24 M.: Effects of the 2006 El Niño on tropospheric composition as revealed by data from the Tropospheric Emis-  
25 sion Spectrometer (TES), *Geophys. Res. Lett.*, 35, L03816, doi:10.1029/2007GL031698, 2008.

26 Mills, G., Harmens, H., Wagg, S., Sharps, K., Hayes, F., Fowler, D., Sutton, M., and Davies, B.: Ozone impacts  
27 on vegetation in a nitrogen enriched and changing climate, *Environmental Pollution*, 208, 898–908, doi:  
28 10.1016/j.envpol.2015.09.038, 2016.

29 Monks, P. S.: A review of the observations and origins of the spring ozone maximum, *Atmos. Environ.*, 34,  
30 3545–3561, 2000.

31 Monks, P. S., Archibald, A. T., Colette, A., Cooper, O., Coyle, M., Derwent, R., Fowler, D., Granier, C., Law,  
32 K. S., Mills, G. E., Stevenson, D. S., Tarasova, O., Thouret, V., von Schneidmesser, E., Sommariva, R., Wild,  
33 O., and Williams, M. L.: Tropospheric ozone and its precursors from the urban to the global scale from air  
34 quality to short-lived climate forcer, *Atmos. Chem. Phys.*, 15, 8889–8973, doi:10.5194/acp-15-8889-2015, 2015.

35 Nair, P.R., David, L.M., Girach, I.A., and George, S.K.: Ozone in the marine boundary layer of Bay of Bengal  
36 during post-winter period: spatial pattern and role of meteorology, *Atmos. Environ.*, 45, 4671e4681, 2011.

1 Nassar, R., Logan, J. A., Worden, H. M., Megretskaia, I. A., Bowman, K. W., Osterman, G. B., Thompson, A.  
2 M., Tarasick, D. W., Austin, S., Claude, H., Dubey, M. K., Hocking, W. K., Johnson, B. J., Joseph, E., Merrill,  
3 J., Morris, G. A., Newchurch, M., Oltmans, S. J., Posny, F., Schmidlin, F. J., Vömel, H., Whiteman, D. N., and  
4 Witte, J. C.: Validation of Tropospheric Emission Spectrometer (TES) nadir ozone profiles using ozonesonde  
5 measurements, *J. Geophys. Res.*, 113, D15S17, doi:10.1029/2007JD008819, 2008.

6 Neu, J. L., Flury, T., Manney, G. L., Santee, M. L., Livesey, N. J., and Worden, J.: Tropospheric ozone varia-  
7 tions governed by changes in stratospheric circulation, *Nat. Geosci.*, 7, 340–344, doi:10.1038/ngeo2138, 2014.

8 Novelli, P. C., Masarie, K. A., and Lang, P. M.: Distributions and recent changes of carbon monoxide in the  
9 lower troposphere, *J. Geophys. Res.-Atmos.*, 103, 19015–19033, 1998.

10 Penkett, S.A., Reeves, C.E., Bandy, B.J., Kent, J.M., Richer, H.R.: Comparison of calculated and measured per-  
11 oxide data collected in marine air to investigate prominent features of the annual cycle of ozone in the tropo-  
12 sphere, *J. Geophys. Res.*, 103, 13377-13388, 1998.

13 Richter, A., Eyring, V., Burrows, J. P., Bovensmann, H., Lauer, A., Sierk, B., and Crutzen, P. J.: Satellite meas-  
14 urements of NO<sub>2</sub> from international shipping emissions, *Geophys. Res. Lett.*, 31, L23110,  
15 doi:10.1029/2004GL020822, 2004.

16 Srivastava, S., Lal, S., Venkataramani, S., Gupta, S., and Acharya, Y. B.: Vertical distribution of ozone in the  
17 lower troposphere over the Bay of Bengal and the Arabian Sea during ICARB-2006: Effects of continental out-  
18 flow, *J. Geophys. Res.*, 116, D13301, doi:10.1029/2010JD015298, 2011.

19 Srivastava, S., Lal, S., Naja, M., Venkataramani, S., and Gupta, S.: Influence of regional pollution and long  
20 range transport over Western India: analysis of ozonesonde data, *Atmos. Environ.*, 47 (2012), pp. 174–182,  
21 2012.

22 Sudo, K. and Akimoto, H.: Global source attribution of tropospheric ozone: Long-range transport from various  
23 source regions, *J. Geophys. Res.*, 112, D12302, doi:10.1029/2006JD007992, 2007.

24 Sudo, K., and Takahashi, M.: Simulation of tropospheric ozone changes during 1997–1998 El Niño: Meteor-  
25 ological impact on tropospheric photochemistry, *Geophys. Res. Lett.*, 28, 4091–4094, 2001.

26 Van Dingenen, R., Dentener, F. J., Raes, F., Krol, M. C., Emberson, L., and Cofala, J.: The global impact  
27 of ozone on agricultural crop yields under current and future air quality legislation, *Atmos. Envi-  
28 ron.*, 43, 604–618, doi:10.1016/j.atmosenv.2008.10.033, 2009.

29 Wang, Y., Jacob, D.J., Logan, J.A.: Global simulation of tropospheric O<sub>3</sub>-NO<sub>x</sub>-hydrocarbon chemistry: 3.  
30 Origin of tropospheric ozone and effects of nonmethane hydrocarbons, *Journal of Geophysical Research* 103,  
31 10757-10767, 1998.

32 Waters, J. W., Froidevaux, L., Harwood, R. S., Jarnot, R. F., Pickett, H. M., Read, W. G., Siegel, P. H., Cofield,  
33 R. E., Filipiak, M. J., Flower, D. A., Holden, J. R., Lau, G. K. K., Livesey, N. J., Manney, G. L., Pumphrey, H.  
34 C., Santee, M. L., Wu, D. L., Cuddy, D. T., Lay, R. R., Loo, M. S., Perun, V. S., Schwartz, M. J., Stek, P. C.,  
35 Thurstans, R. P., Boyles, M. A., Chandra, K. M., Chavez, M. C., Chen, G. S., Chudasama, B. V., Dodge, R.,  
36 Fuller, R. A., Girard, M. A., Jiang, J. H., Jiang, Y. B., Knosp, B. W., LaBelle, R. C., Lam, J. C., Lee, K. A., Mil-

1 ler, D., Oswald, J. E., Patel, N. C., Pukala, D. M., Quintero, O., Scaff, D. M., Van Snyder, W., Tope, M. C.,  
2 Wagner, P. A., and Walch, M. J.: The Earth Observing System Microwave Limb Sounder (EOS MLS) on the  
3 Aura satellite, *IEEE Trans. Geosci. Remote Sens.*, 44 (5), 1075–1092, doi:10.1109/TGRS.2006.873771, 2006.

4 Weller, R. A., Baumgartner, M. F., Josey, S. A., Fischer, A. S., and Kindle, J. C.: Atmospheric Forcing in the  
5 Arabian Sea during 1994–1995: Observations and Comparisons with Climatology and Models, *Deep Sea*  
6 *Research Part II: Topical Studies in Oceanography* 45: 1961–1999. doi:10.1016/S0967-0645(98)00060-5, 1998.

7 Young, P. J., Archibald, A. T., Bowman, K. W., Lamarque, J.-F., Naik, V., Stevenson, D. S., Tilmes,  
8 S., Voulgarakis, A., Wild, O., Bergmann, D., Cameron-Smith, P., Cionni, I., Collins, W. J., Dalsøren, S.  
9 B., Doherty, R. M., Eyring, V., Faluvegi, G., Horowitz, L. W., Josse, B., Lee, Y. H., MacKenzie, I. A., Na-  
10 gashima, T., Plummer, D. A., Righi, M., Rumbold, S. T., Skeie, R. B., Shindell, D. T., Strode, S. A., Sudo,  
11 K., Szopa, S., and Zeng, G.: Pre-industrial to end 21st century projections of tropospheric ozone from the  
12 Atmospheric Chemistry and Climate Model Intercomparison Project (ACCMIP), *Atmos. Chem. Phys.*, 13,  
13 2063–2090, doi:10.5194/acp-13-2063-2013, 2013.

14 Zahn, A., Brenninkmeijer, C. A. M., Asman, W. A. H., Crutzen, P. J., Heinrich, G., Fischer, H., Cuijpers, J. W.  
15 M., and van Velthoven, P. F. J.: Budgets of O<sub>3</sub> and CO in the upper troposphere: CARIBIC passenger aircraft  
16 results 1997–2001, *J. Geophys. Res.*, 107(D17), 4337, doi:10.1029/2001JD001529, 2002.

17 Zanis, P., Hadjinicolaou, P., Pozzer, A., Tyrllis, E., Dafka, S., Mihalopoulos, N., and Lelieveld, J.: Summertime  
18 free-tropospheric ozone pool over the eastern Mediterranean/Middle East, *Atmos. Chem. Phys.*, 14, 115–132,  
19 doi:10.5194/acp-14-115-2014, 2014.

20 Zeng, G. and Pyle, J. A.: Influence of El Niño Southern Oscillation on stratosphere/troposphere exchange and  
21 the global tropospheric ozone budget, *Geophys. Res. Lett.*, 32, L01814, doi:10.1029/2004GL021353, 2005.

22 Zhu, B., Hou, X., and Kang, H.: Analysis of the seasonal ozone budget and the impact of the summer monsoon  
23 on the northeastern Qinghai-Tibetan Plateau, *J. Geophys. Res. Atmos.*, 121, 2029–2042,  
24 doi:10.1002/2015JD023857, 2016.

25 Ziemke, J. R., Chandra, S., Duncan, B. N., Froidevaux, L., Bhartia, P. K., Levelt, P. F., and Waters, J. W.:  
26 Tropospheric ozone determined from Aura OMI and MLS: Evaluation of measurements and comparison with  
27 the Global Modeling Initiative’s Chemical Transport Model, *J. Geophys. Res.*, 111, D19303,  
28 doi:10.1029/2006JD007089, 2006.

29 Ziemke, J. R., Chandra, S., Labow, G. J., Bhartia, P. K., Froidevaux, L., and Witte, J. C.: A global climatology  
30 of tropospheric and stratospheric ozone derived from Aura OMI and MLS measurements, *Atmos. Chem. Phys.*,  
31 11, 9237–9251, doi:10.5194/acp-11-9237-2011, 2011.

32 Ziemke, J. R., Chandra, S., Oman, L. D., and Bhartia, P. K.: A new ENSO index derived from satellite meas-  
33 urements of column ozone, *Atmos. Chem. Phys.*, 10, 3711–3721, doi:10.5194/acp-10-3711-2010, 2010.